SCUOLA DI DOTTORATO
UNIVERSITÀ DEGLI STUDI DI MILANO-BICOCCA

**School of Medicine and Surgery**

PhD program Translational and Molecular Medicine – DIMET

Cycle XXXIII

# Development of novel cell based therapeutic approaches to correct primary and secondary bone defects

Penna Sara

Matricola 739014

Tutor: Dr. Marta Serafini

Co-tutor: Dr. Anna Villa

Coordinator: Prof. Andrea Biondi

**Anno accademico 2019/2020**

## SUMMARY

# Chapter 1

## 1. Introduction

### *1.1 Principles of bone biology*

Bone is a complex, highly specialized living tissue conferring support and protection to the organs in all high vertebrates. The extracellular matrix of bones is characterized by an inorganic portion, the mineralized matrix that guarantees rigidity and strength to the skeleton and simultaneously maintains some degree of elasticity [1]. Importantly, the extracellular matrix is a major source of inorganic ions, actively participating in calcium homeostasis in the body. The organic counterpart of the bone is composed of organic matrix, in particular, 95% by type I collagen and the remaining 5% by proteoglycans and numerous non-collagenous proteins. Moreover, the matrix contains deposits of calcium and phosphate in the form of hydroxyapatite, controlled by bone cells [2].

The process of bone formation is driven by osteoblasts that firstly depose organic matrix, secreting collagen proteins and other non-collagen protein like osteocalcin (OCN), osteonectin, bone SialoProteins I (BSPI), osteopontin and proteoglycans such as decorin and biglycan, comprehensively composing the osteoid. Then, while the matrix is not completely mineralized, osteoblasts and chondrocytes start to synthesize hydroxyapatite crystals within the matrix vesicles, requiring the activity of bone SialoProteins II (BSPII) and calbindin D9k, the calcium-binding phospholipids and

the calcium channel-forming annexin regulating the calcium uptake [3]. In parallel, phosphate intake is driven by the type III Na/Pi co-transporter [4] and the PHOSPHO1 phosphatase [5]. Once the concentration of calcium and phosphate is sufficient to overcome the point of solubility, the hydroxylation of $Ca_3(PO_4)_2$ (tricalcium phosphate) crystals starts and the hydroxyapatite is ready to be released into the extracellular space where it fills the gaps between the fibrils of collagen, forming the critical nucleus that gradually increases in size, giving rise to a secondary nucleation [4].

Morphologically, the skeleton is composed by cortical bone that provides mechanical and protective functions (80%) and trabecular bone (20%) metabolically active. Cortical bone is dense and composed of a branching network of cylindrical osteons called Haversian systems [6]. The outer cortical surface of bone is covered by periosteum and the inner surface is covered by endosteum. Periosteum is a fibrous connective tissue, whereas the endosteum is a membranous structure, both containing blood vessels, osteoblasts, and osteoclasts. Trabecular bone is organized as a honeycomb-like network of trabecular plates and rods surrounding the bone marrow compartment including adipocytes and hematopoietic cells [7].

Despite its inert appearance bone is defined as living tissue; it hosts four different cell types (Figure 1) and it is continuously remodelled by osteoclasts, giant multinucleated bone resorbing cells, osteoblasts that continuously create new bone tissue, osteocytes that permeate the mineralized bone, acting as

mechanosensors and orchestrators of this bone remodelling process and bone lining cells on bone surfaces, that seem to play a role in coupling bone resorption to bone formation, having a still unclarified function [1, 6, 8]. Osteoblasts, osteocytes, and bone-lining cells originate from local osteoprogenitor cells, whereas osteoclasts arise from the fusion of mononuclear precursors, which originate from the hematopoietic counterpart [2]. A description of each type of bone cells and their function will be detailed in the following paragraph.

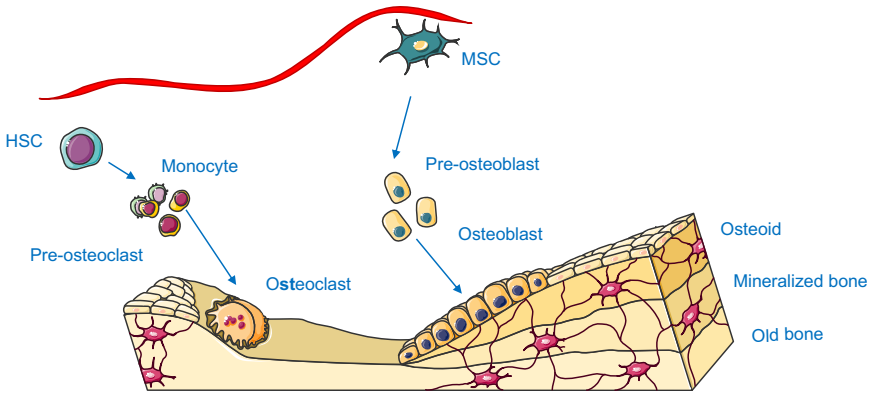


**Figure 1.** The origins and locations of bone cells .

### *1.2 Cells of bone*

Bone is a mineralized connective tissue composed by four types of cells: osteoblasts, bone lining cells, osteocytes and osteoclasts. The process of bone remodelling in which old bone is continuously replaced by new bone is the result of the coordinate actions of bone cells, which together form a temporary anatomical structure called "basic multicellular unit". Interestingly, the activities of bone cells

are variable over the human life: in particular, from 0 to 20 years of age bone cells operate in the development of the skeleton, a process called “bone modelling” in which bone formation is more active and exceed bone resorption. During the next three decades the skeleton is maintained by an equal turnover of bone resorption and bone formation. Remodelling process starts with a localized resorption that is succeeded by an equal bone deposition at the same site [9]. After fifty years of age, sometimes bone formation process fails and is surpassed by the bone resorptive activity of osteoclasts, with consequent impairment of skeletal mass, including the decrease of connectivity of trabecular bone. Depending on the imbalanced bone formation and bone resorption activities, the skeletal strength is reduced and the risk of fractures is progressively higher, increasing the susceptibility of old people to develop osteoporosis [2].

### *1.2.1 Osteoblasts*

As already mentioned, the major players in bone turnover are osteoblasts and osteoclasts; osteoblasts account for the 4–6% of total resident cells in the bone, mainly known for their bone forming function. Osteoblasts originate from a common pluripotent mesenchymal stem cell (MSC), that follows timely programmed steps of differentiation, guided by the expression of specific genes, which in turn are controlled by pro-osteogenic pathways. In this contest, bone morphogenetic proteins (BMPs) and Wnt pathways are crucial, especially for the early steps of osteoblast differentiation, in which MSCs are committed towards

an osteo/chondroprogenitor expressing Runt-related transcription factor 2 (Runx2), Distal-less homeobox 5 (Dlx5) and Osterix (Osx), the latter being a downstream target of Runx2 together with collagen type I (ColIA1) [10]. Following the multistep process of osteoblast differentiation (Figure 2a), after the establishment of a pool of osteoblast progenitors expressing Runx2 and collagen type I, a proliferation phase starts and osteoblast progenitors acquire Alkaline Phosphatase (ALP) activity, that provides high concentrations of phosphate at the mineral deposition site. Moreover, during bone remodelling, osteoblast precursors are recruited from the bone marrow to the bone surface by cytokines and growth factors like transforming growth factor-β (TGF-β) and insulin-like growth factor, which are released from the bone matrix during resorption phase [11]. Consequently, these cells become pre-osteoblasts, undergo morphological changes increasing their size and acquiring a cuboidal shape, they boost the expression of ALP and become very active in bone matrix protein secretion [12]. During their differentiation process, osteoblasts firstly attain a polarized phenotype [11], then, in the late stages, they are characterized by a higher expression of the bone matrix proteins like OCN [13], BSP I and II, and of collagen type I. Mature osteoblasts show morphological features of protein synthetizing cells, including abundant rough endoplasmic reticulum and prominent Golgi apparatus and various secretory vesicles [10, 14]. At the final step of their differentiation, osteoblasts that have encircled themselves with the just deposed and mineralized bone matrix, can differentiate into osteocytes (Figure 2b); on the other

hand, osteoblasts that remain on the bone surface, facing the periosteum, can undergo apoptosis or become bone-lining cells (Figure 2b)[10, 15].

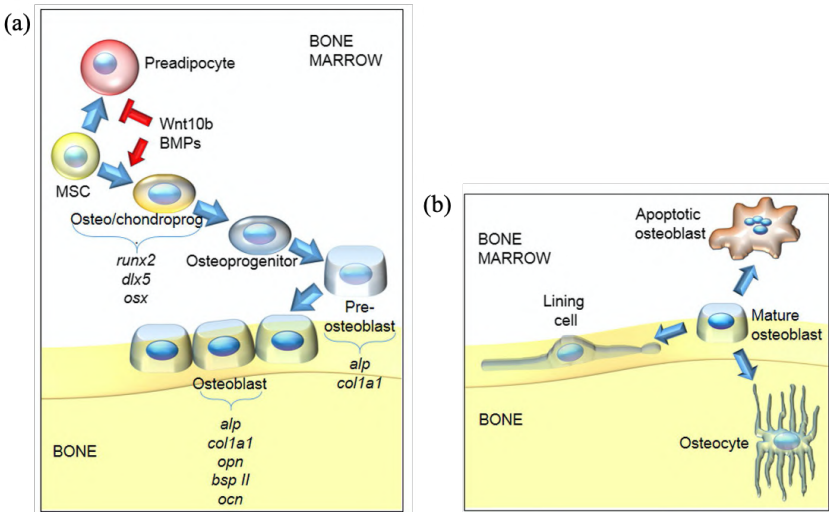


**Figure 2.** Osteoblast differentiation, morphology and fate. (a) Schematic representation of the multistep process of osteoblast differentiation (MSC = mesenchymal stem cell). (b) Schematic representation of the possible fate of a mature osteoblast. Readapted from Capulli, Paone, and Rucci 2014.

The role of bone forming cells has been already dissect in the 1.1 section; additionally, recent evidence highlighted the role of osteoblasts in influencing and regulating osteoclast differentiation and consequently the bone resorption process. This process is the result of a crosstalk between osteoblasts and osteoclasts, handled in three different modalities: in a paracrine manner via cytokines diffusion, through direct cell-cell contact or contacting each other

forming gap junctions allowing passage of small water-soluble molecules between the two cell types [16].

Osteoblasts regulate osteoclasts differentiation producing macrophage-colony stimulating factor (M-CSF) as a secreted or a transmembrane cytokine that interacts with its receptor c-Fms on the pre-osteoblast surface, promoting osteoclasts differentiation or proliferation [17]. Moreover, ostoclastogenesis is regulated via a cell-cell direct contact between osteoblasts and pre-osteoclasts, involving RANKL/RANK pathway. Receptor Activator of Nuclear kappa B Ligand (RANKL) is mainly produced by stromal cells in bone, in normal conditions, and primarily by osteocytes [18, 19]. RANKL is mostly expressed as membrane-bound and can be also released as soluble protein; the former is sufficient for most of the functions, while the latter contributes to physiological bone remodelling, as recently demonstrated in mice expressing a sheddase-resistant form of RANKL [20].

RANKL, binding its receptor RANK, expressed by osteoclast precursors, activates the fusion of pre-osteoclasts allowing the generation of multinucleated mature osteoclasts through the initiation of a downstream pathway that involved the nuclear translocation of Nuclear Factor-kappa B (NFkB) and the activation of NFATc1 pathway [21]. Osteoblasts are also able to negatively regulate osteoclastogenesis and limit bone resorption. To this end osteoblasts, produce osteoprotegerin (OPG) that binds RANKL preventing its interaction with RANK [22]. Regarding bone turnover regulation mediated by osteoblast-lineage cells, the literature reports a range of cytokines acting in a paracrine manner,

including interleukin 11, interleukin 1 beta, interleukin 6, tumour necrosis factor alpha (TNF-α), prostaglandin E2 (PGE2), parathyroid hormone-related protein (PTHrP) and oncostatin M that stimulate osteoblastic expression of RANKL, consequently stimulating osteoclasts differentiation and resorption [10, 21, 23]. In 2012 Karsenty's group described the bone tissue as an endocrine site able to contribute to other organ physiology with the production of specific hormones by osteoblasts [24]. In this study, authors dissected the role of OCN as a hormone specifically secreted by osteoblasts and odontoblasts. OCN is an osteoblast-specific protein that is secreted in large amount in the bone extracellular matrix, and the gene encoding for this protein starts to be expressed during development, when bone mineralization starts. OCN is produced as a pro/pre-molecule that needs to be cleaved before to be secreted in the extracellular matrix. In its mature undercarboxylated form, OCN can act as an hormone [25]. In particular OCN is able to influence pancreatic glucose metabolism, regulating insulin level that in turn negatively regulates osteoblast OPG expression, promoting osteoclastogenesis and bone resorption [24]. Recent literature report that OCN is also involved in testosterone synthesis and consequently in fertility acting on male gonadal function [26]. Lastly OCN has been reported to be able to cross the blood–brain barrier and binds to neurons of brainstem, midbrain and hippocampus, leading to an improvement in memory and in the prevention of depression; it is also able to cross blood-placenta barrier, thus protecting neurons from apoptosis before the embryo can produce OCN itself [27].

Zhang et al. in their study in 2003 dilucidated another important aspect of osteoblasts function, corroborating the hypothesis that a particular subset of osteoblasts, named spindle-shaped N-cadherin$^{+}$/CD45$^{-}$ osteoblasts (SNO) could play a key role in maintaining hematopoietic stem cell (HSC) in the bone niche in close proximity to endosteal surface [28]. Contemporary Calvi et al., taking advantage of a new murine model expressing a constitutively active parathyroid hormone receptor (caPTH1R) in osteoblastic cells, demonstrated an increase in bone mass, increased number of osteoblastic cells and a concurrent increase in phenotypic and functional HSCs [29]. However, the function of osteoblastic cell in HSC maintenance is still debated; as a matter of fact, osteocytes are caPTH1R expressing cells and they can activate PTH signalling resulting in osteoblastic expansion and activation leading to an increase in bone mass, but not influencing the number of HSC [30]. Moreover, regarding SNO, previously proposed as critical member of the HSC niche, conditional deletion of N-Cadherin from osteoblastic cells does not alter bone marrow support for HSCs [31].

In conclusion, while the activation of osteoblasts involving PTH receptor signalling, can increase the number of HSCs, and loss of osteoblastic cells can decrease HSC function [32], homeostatic HSC maintenance is not directly supported by osteoblasts, but is likely due to the activities of additional cell populations in the bone marrow, including the osteoblastic precursors MSCs and osteocytes [33].

### *1.2.2 Osteocytes*

Osteocytes are the most abundant bone cells in the adult skeleton (90-95%) and they have a long lifespan of 25 years. Osteocytes are star-shaped cells buried in the mineralized bone matrix, originated from MSCs lineage through osteoblast differentiation; in particular, when the osteoid matrix is completely mineralized, osteoblasts get embedded into the new mineralized bone and differentiate into osteocytes [34].

They are localized in the mineral lacunae, surrounded by bone fluid that confers them the possibility to receive nutrients and oxygen and maintain the equilibrium of calcium and phosphate [35]. Every single osteocyte is characterized by 40-100 cilia and cytoplasmatic processes that are impregnated by bone fluid growing through the calcified canaliculi towards the periosteal and endosteal surfaces, in order to reach hormones and signals in the bloodstream like inorganic phosphorous, PTH, estrogens or 125(OH)2 D3 vitamin [34]. Osteocytes interconnections compose a lacuno-canalicular system that allows their own communication, the contact with osteoblasts and bone lining cells, osteoclasts, bone marrow cells and also with blood vessels [35, 36]. Osteocyte processes contact each other and osteoblasts via gap junction composed by a hexameric arrays of connexin monomers that permit the diffusion of ions, metabolites and small signalling molecules in a PTH and pH-regulated manner [37, 38].

As already mentioned, osteocytogenesis is the active process of osteoblast transformation into osteocyte. During their transformation osteoblasts rearrange their cytoskeleton,

reorganizing proteins related to the establishment of the process morphology such as actin, actin-binding proteins (fimbrin, filamin, α-actinin), tubulin or vimentin [39]. Osteocyte maturation starts in the early phases of bone mineralization, and it is controlled by the E11 protein, the first specific marker expressed by the osteocyte, while the canaliculi formation depends on the expression of matrix metalloproteinase-14 (MMP-14), that regulates extracellular matrix degradation [40].

Osteocytes are involved in a wide range of functions, not limited to the bone. Current literature supports the role of osteocytes as mechanosensing cells translating mechanical stimuli into biochemical signals; in particular they influence bone formation and bone resorption acting on osteoblast and osteoclast differentiation and function [10]. The role of osteocytes in the regulation of osteoblast differentiation is still controversial, however Winkler et al. demonstrated that osteocytes act on osteoblast differentiation and function via sclerostin (SOST), a secreted glycoprotein that antagonizes the canonical Wnt pathway [41]. Osteocytes are also reported to be key regulators of bone resorption influencing osteoclast activity, in particular when a bone crack occurs, since osteocyte density is elevated due to their abundance, micro damages within the bone matrix would disrupt the canaliculi, causing osteocytes apoptosis. Apoptotic osteocytes directly produce RANKL or induce stromal and osteoblastic cells to produce RANKL stimulating osteoclastogenesis followed by osteoclast invasion to the fracture site [40].

In the past century, few pioneeristic studies hypothesized that osteocytes could play a key role in mineral homeostasis maintenance by a process named periosteocytic osteolysis, highlighting the presence of irregular borders, sign of bone resorption in the osteocyte lacunae [42, 43]. Belanger et al. introduced the term "osteocytic osteolysis" to describe this phenomenon [44] and later literature reported that this process account for the 90% of total calcium release through the acidification of osteocyte lacuna [45]. A recent report highlights an important role of osteocyte in supplying minerals in physiological condition like lactation, hibernation, and mechanical loading due to a bone resorptive activity, similarly to osteoclasts [46]. Roblin and Bonewald broadly reviewed the role of osteocytes in bone and described that they can regulate plasma calcium by releasing mineral from their surrounding matrix, especially in response to PTH and PTHrP due to the process of osteocytic osteolysis [47]. Osteocytes embedded in bone can secrete factors that can target distant organs. Indeed, they can regulate phosphate metabolism sending signals to the kidney, via the fibroblast growth factor 23 (FGF23) where it decreases the expression of NPT2, a sodium-phosphate cotransporter in the proximal tubule, decreasing the reabsorption and increasing excretion of phosphate [47, 48].

### *1.2.3 Bone lining cells*

Bone lining cells are flat, elongated, inactive cells that cover bone surfaces that are not undergoing neither bone formation nor resorption. These cells are quiescent and have few cytoplasmic

organelles [2], some of them extending into canaliculi and gap junctions connecting to each other and to osteocytes. Bone lining cell functions are not completely clarified, however, it has been reported that these cells mediate the interaction between osteoclasts and bone matrix to block bone resorption when it is not needed, and also influence osteoclastogenesis by the production of OPG and RANKL [1]. In 2002 Everts et al. demonstrated for the first time that bone lining cells activities are fundamental for bone remodelling; once osteoclasts terminate their resorption activity in a resorption pit and move further, bone lining cells enter the lacuna and eliminate bone matrix leftovers, in particular the unmineralized collagen protrusion digested by matrix metalloproteinases (MMP). This cleaning procedure guarantees the subsequent deposition of a first layer of collagenous proteins in the resorption pits [8]. Moreover, in the same study authors described bone lining cells as modulators of osteoclast activity expressing ICAM-1, known regulator of osteoclastogenesis [8, 49].

### *1.2.4 Osteoclasts*

Osteoclasts are multinucleated giant cells derived from hematopoietic lineage, however, the original precursor of these cells is still unknown. A common myeloid progenitor (CMP) with a still unclarified identity is shared between osteoclasts and other monocytic cells like macrophages (MΦ) and dendritic cells (DC); this progenitor has been recently identified downstream of the granulocyte/macrophage progenitor (GMp) through the myeloid differentiation pathway (Figure 3). In human bone marrow, this

unidentified progenitor has been described to express $CD11b^{-}$ $CD34^{+}$ c-$KIT^{+}$ $FLT3^{+}$ IL-$3R\alpha^{low}$ markers; moreover, it progressively lose its pluripotency, changing the pattern of expression and becoming committed to the various cell type downstream, in particular, it has been reported that osteoclast potential resides in the $B220^{-}$ fraction of the $CD11b^{low/neg}$ c-$Kit1^{+}$ c-$Fms1^{+}$ population [50]. Within this population other markers, CD27 and Flt3 discriminate the fate of the precursor, in particular Xiao et al. described a subset of oligopotent progenitors for macrophages/osteoclast/dendritic cells expressing $CD27^{+}Flt3^{+}$ and bipotent progenitors for macrophages/osteoclast expressing $CD27^{low/-}$ $Flt3^{-}$[50].

In mouse, $CD11b^{low/neg}$ c-$kit^{+}$ $CD115^{+}$ fraction contains osteoclast progenitor, and during osteoclast differentiation it down regulates c-kit and maintains CD115, ligand of M-CSF that increases the expression of RANKL and consequently stimulates osteoclatogenesis [51].

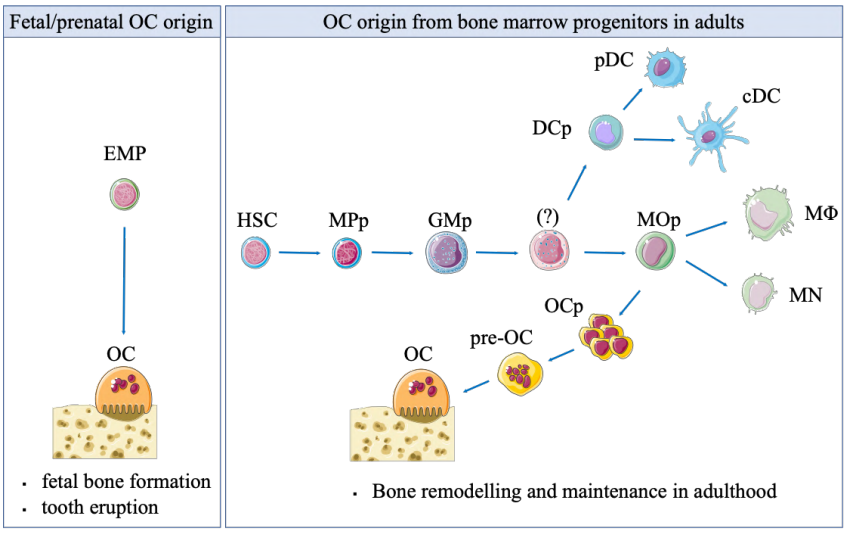


**Figure 3.** Osteoclast origin from fetal progenitors and bone marrow progenitors in adults. Erythro-myeloid progenitors (EMP), hematopoietic stem cells (HSC), multipotent progenitor (MPp), granulocyte/monocyte progenitor (GMp), common unidentified progenitor (?), dendritic cell progenitor (DCp), conventional/classical dendritic cells (cDCs) and plasmacytoid DCs (pDCs), monocyte/osteoclast progenitor (MOp), monocytes (MN), macrophages (MΦ), osteoclast progenitor (OCp), pre-osteoclast (pre-OC), osteoclast (OC).

Interestingly, osteoclasts originating from HSCs in the bone marrow and downstream progenitors seem to have a role in bone maintenance restricted to adulthood. This evidence emerges from the elegant study of Jacome-Galarza et al. in which they depleted RANK or CD115 expression in the bone marrow-HSC progenitors (using *Csf1r*$^{cre}$ mice) or in bone marrow-HSC and in embryonic erythro-myeloid progenitors (EMP) (using *Flt3*$^{cre}$ mice). The authors demonstrated that osteoclasts originating from EMP are necessary for normal bone development, and in the absence of

EMP-derived osteoclasts, transfusion of monocytes can partially rescue early onset osteopetrosis without bone marrow transplantation. Conversely, osteoclasts originated from bone marrow HSC progenitors are essential for bone turnover in adulthood [52]. These findings have relevant implications for gene transfer approach and suggest that both sources of progenitors might be required to modulate osteoclast activity and bone remodelling.

Since 80's osteoclasts have been morphologically described as multinucleated giant cells able to polarize and organize a unique plasma membrane complex of proteins allowing a huge digestive extracellular activity *in situ* [53]. This particular complex is in contact with the bone and comprises an outer circular domain containing adhesion structures defined as sealing membrane and its nearby cytoplasmic area is called clear zone in which the presence of organelles is rare, altogether forming the sealing zone [54, 55]. The sealing zone surrounds the ruffled border, an intricate array of membrane protrusions that faces the bone area to be resorbed. Osteoclasts are also in contact with the vascular compartment through the basolateral membrane presenting with important asymmetric distribution of ion transporters [53, 56] (Figure 4).

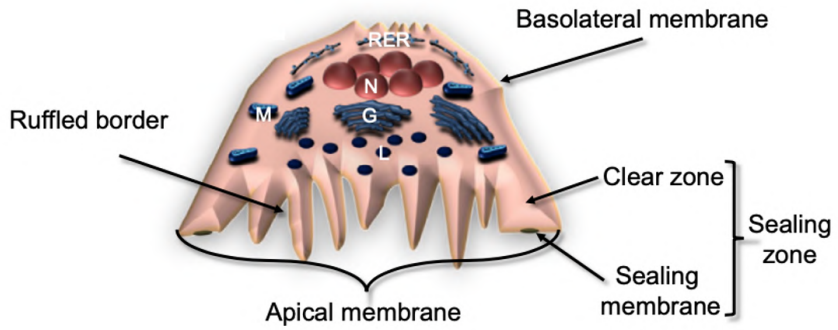


**Figure 4.** Osteoclast morphology: cartoon illustrating the plasma membrane domains of an osteoclast and the organelle distribution inside the cell. N: nucleus; M: mitochondrion; G: Golgi stack; L: lysosome; RER: Rough endoplasmic reticulum. Readapted from Cappariello et al., 2014.

Focusing on the sealing zone details, the sealing membrane is enriched of complex peculiar adhesions called podosomes that allow close attachment of osteoclasts to the bone matrix. Podosomes have a foot-like structure and they start forming singularly, becoming a cluster and moving to the outer area of the cell creating a belt-like structure. The main components of podosomes are actin microfilaments, actin-binding proteins, adhesion proteins, adapter proteins, signalling proteins, tyrosine kinases and integrin receptors. Once the belt-like structure of podosomes is completely formed, the osteoclast is ready to resorb the bone and the new formed podosome structure is defined as actin ring [57].

The osteoclast ruffled border has been recently defined as hyper-specialized subdomains composed of a fusion zone, the external part, and the inner uptake zone: the fusion zone acquires vesicles

prevalently from the endo/lysosomal compartment. It is also implicated in the uptake of ion transporters into the ruffled border and in the discharge of lysosomal enzymes. The uptake zone is involved in the degradation of products derived from bone resorption, that are delivered from the resorbed area to the vascular stream through a functional secretory domain of the basolateral membrane due to a transcytosis system that involves small guanosine triphosphate GTP-binding proteins [58] and microtubules [59]. The two subdomains are also implicated in membrane recycling, re-uptake of lysosomal enzymes, and vesicular trafficking [54].

The organelles organization of osteoclast is reported in Figure 4, in particular, nuclei count is higher or equal to three, they are located in proximity of the vascular side, surrounded by endoplasmic reticulum, closed to Golgi's apparatus and organized in multiple centres [60]. Mitochondria, located in proximity of the bone together with lysosomes and vacuoles, are present in a great number and they have a peculiar elongated shape. From the centre of the cell to the periphery, microfilaments create the podosomal cores and consequently form the actin ring; next to the nuclei region, microtubules branch from their centre to the periphery taking part to the membrane trafficking to the ruffled border [61].

When the fusion of mononuclear osteoclast precursors is complete osteoclasts increase their size becoming giant multinucleated mature cells. Mature osteoclast polarize onto the bone surface and the sealing membrane tightly and dynamically sets the resorption lacuna apart, segregating the underneath extracellular space from

the rest of the extracellular bone marrow space [62]. A complex machinery composed by the vacuolar $H^+$-ATPase (proton pump), the ClC7 $2Cl^-/1H^+$ antiporter (chloride channel type 7) and the acidic hydrolases released into the resorption lacuna microenvironment, is setup through exocytosis of lysosomes at the most peripheral area of the ruffled border; in particular, the fusion of the lysosomal membranes allows the insertion of all the bone resorption players in the into this plasma membrane domain and guarantee the adequate environment for bone resorption process, that is characterized by low pH, high calcium concentration and abundance of acidic hydrolyses [51]. Additionally, the d2 subunit of the vacuolar $H^+$-ATPase seems to play a role in osteoclast precursors fusion [63], while the $2Cl^-/1H^+$ antiporter is located to the ruffled border by its β-subunit, called osteopetrosis-associated transmembrane protein 1 (OSTM1) [64]. The process of acidification of the bone resorption lacunae is essential to initiate the bone resorption activity of osteoclasts; as reported in Figure 5, this process is driven by many players: the carbonic anhydrase type II (CA-II) that accelerates the hydration of $CO_2$ in $H_2CO_3$, which represents the intracellular source of protons, the anion $Cl^-/HCO_3^-$ exchanger located in the basolateral membrane that has the role to prevent cytoplasmic alkalinisation and influxes $Cl^-$ for subsequent release in the resorption lacuna [65], the still poorly investigated PLEHKM1 protein [66, 67], which is likely to contribute to vesicular trafficking to the ruffled border together with OSTM1 [64], and lastly, the SNX10 protein which drives the insertion of the vacuolar $H^+$-ATPase proton pump on the plasma membrane

[68, 69]. Mutation in genes encoding for the proteins involved in the acidification of the bone resorption lacunae and in the vesicular trafficking dramatically impair osteoclast functions and consequently induce the pathogenesis of a class of inherited bone disorders named osteoclast-rich osteopetrosis, characterized by inefficient bone resorption that leads to poorly remodelled bone, persistence of primary trabeculae, bone fragility, abnormal tooth eruption, fibrosis of bone marrow, infections and primary or secondary neural alterations [70, 71].

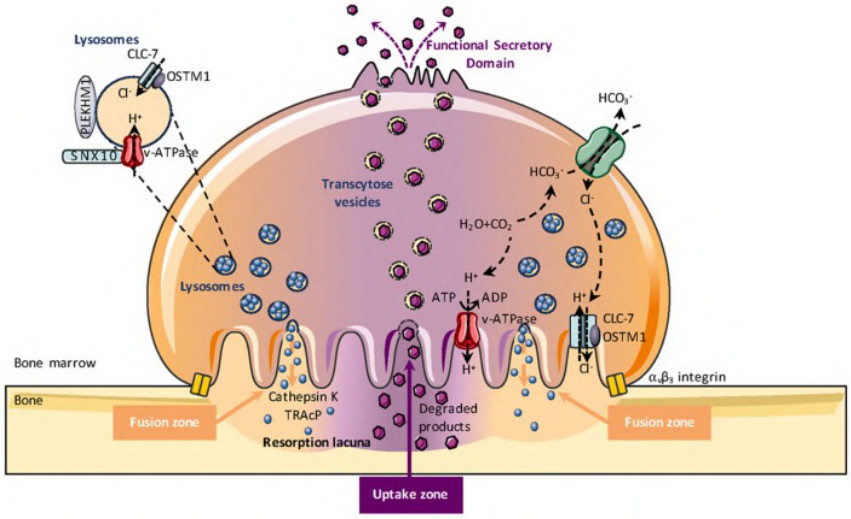


**Figure 5.** Osteoclast bone resorption machinery (Madel et al., 2019).

The process of acidification is necessary for the demineralization of the bone surface that osteoclast are resorbing; additionally, it is also important to expose the organic components of bone matrix, composed for 95% of type I collagen, that is degraded by cathepsin K [72]. Bone degradation requires the extracellular secretion of another lysosomal enzyme, the Tartrate-resistant acid phosphatase

(TRAcP) that is known to be converted into a ATP-ase by the cleavage activity of trypsin or cathepsin and to have substrates like transforming growth factor β (TGF β) and receptor-interacting protein (TRIP-1) [73].

Osteoclasts are reported to express matrix metalloproteinases (MMP) not directly implicated in bone resorption process, but necessary to guarantee the function of the osteoclast resorption machinery. In particular, MMP-2 plays a role in osteoclast differentiation [74]. MMP-9 is known to be involved in osteoclasts migration [75] together with cathepsin K and MMP-13. MPP-13, involved in type I collagen degradation, although is expressed by osteoblasts, it has been detected on the bone surface underneath the ruffled border and at sealing membrane [76].

Recently, osteoclasts have been identified not only as bone resorbing cell, but also as promoter of bone formation through the release of specific cytokines, defined as clastokines that attract osteoblast precursors, inducing their differentiation and promoting bone matrix deposition and mineralization [77]. In particular, the clastokines involved in the bone formation are the following: TRAcP, sphingosine-1-phospahte (S1P), bone morphogenetic protein (BMP6), wingless-type 10b (Wnt10b), hepatocyte growth factor (HGF) and collagen triple helix repeat-containing protein 1 (CTHRC1) [78]. Bone resorption and remodelling have always been identified as the principal activities of osteoclasts, ensuring the regulation of calcemia and phosphatemia; however, these two pathways belong to the intricate endocrine network that comprises sex hormones, calcium, vitamin D3 and PTH that control osteoclast

functions systemically [60]. Recently, researchers are attributing to osteoclasts a key role in the extensive endocrine network which regulates calcium absorption in the gut, bone turnover, kidney excretion of calcium and phosphate and 1α hydroxylation of 25-OH vitamin D3 [79]. Osteoclasts are directly sensors of increase of extracellular calcium even at supraphysiological level, and through this mechanism are able to regulate their resorption activity. On the contrary, they do not express receptors for vitamin D3 and PTH and these hormones seem to have an indirect influence on osteoclast activity, probably mediated by osteoclastogenic cytokines produced by other cell types, especially osteoblasts [80]. Additionally, bone resorption can be enhanced due to inflammatory conditions under the impulse of non-physiological stimuli that activate osteoclasts [81]. Thus, osteoclasts not only differentiate from bone marrow progenitors, but can also originate from cells already engaged in the monocytic or dendritic cells lineage, in presence of pathological conditions and acute inflammation [51]. During inflammatory conditions, many pro-inflammatory cytokines, chemokines, transcription factors, membrane receptors and co-stimulatory molecules are able to stimulate osteoclastogenesis supporting the close link between the skeletal and immune system. Both innate and adaptive immunity can provide osteoclast regulators such as RANKL and M-CSF, and also inflammatory cytokines like TNFα, IL-1 and IL-6, and other recently discovered players such as the S1P, regulator of lymphocyte chemotaxis [82]. $CD4^+$ T cells, specifically T helper cells produce IL-17 (Th17), during inflammatory conditions,

become activated and produce interleukins such as RANKL, TNFα, and IL-17 that are able to influence osteoclast precursors commitment enhancing osteoclast differentiation [83]. Th17 cells are also able to increase the expression of monocyte-attractant chemokines such as MCP1 and MIP1α in osteoblasts that consequently induce the recruitment of osteoclast monocytic progenitors in the bone marrow [84]. Conversely, in literature other stimuli, emerging from the immune system, able to negatively regulate osteoclast activity have been reported. In particular, other T cell-derived cytokines such as IFNγ, IL-4, IL-10, IL-12, and IL-18 as well as regulatory T cells were reported to have a negative effect on osteoclastogenesis [83]. As a further proof of osteoclast multi-functionality and their involvement in the immune response, it has been recently proposed that they may act as antigen presenting cells being able to regulate and control T cell activation as well as to initiate T cell responses in an antigen-dependent manner [51, 85].

Bone hosts HSC in its internal canals, where specialized endosteal osteoblasts contribute to the maintenance of the niche able to keep long-term hematopoiesis and myeloid repopulation [86]. Recently, not only osteoblasts but also osteoclasts have been reported as crucial regulators of HSC niche. They can exploit their role directly, increasing HSC mobilization due to the production of enzymes like cathepsin K, and MMP9 which cleaves stromal cell-derived factor 1, osteopontin, stem cell factor (SCF) and VCAM abrogating the connection between HSC and their bone niche [87].

Once the contact with the niche is abrogated, HSC are able to mobilize losing their quiescence [88, 89].

Lastly, osteoclasts sustain blood vessels construction, that is essential for physiological bone growth and remodelling. During their maturation osteoclasts upregulate endothelial vascular endothelial growth factor (VEGF) as a clastokine, through the typical NF-kB and hypoxia inducible factor a (HIF-1a) pathways that stimulates angiogenesis [90]. Additionally, osteoclasts can regulate angiogenesis producing heparinase, an enzyme that disrupts heparin sulphate proteoglycans, releasing heparin-binding growth factors. Moreover, bFGF, another potent angiogenic factor, is also reported to contribute to autocrine osteoclast activation and paracrine stimulation of osteoblast activity, highlighting the important crosstalk between osteoclast and osteoblast during bone remodelling [91].

### *1.3 Osteopetrosis as a model to study osteoclast-intrinsic defects: overview of the disease*

The term osteopetrosis or marble bone disease was firstly introduced by the German radiologist Albers Schönberg in 1904, describing a heritable disorder characterized by increased bone density on radiographs ranging in severity from benign to lethal in early childhood [92]. The disease originates from defective osteoclast differentiation and function and, consequently, failure in bone resorption resulting in high bone mass [71]. The overly dense bone architecture, typically described as “bone within bone” appearance, confers a structural brittleness that predisposes to

fracture [93]. Moreover, the impaired equilibrium of bone formation and bone remodelling give rise to skeletal deformities and dental abnormalities [94]. Patients are characterized by expansion of bone into marrow cavities that affect hematologic functions, causing severe anaemia, bleeding, frequent infections, and hepatosplenomegaly due to increased extramedullary hematopoiesis and encroachment of cranial nerve foramina that impairs neurologic function leading to blindness, deafness, and nerve palsies [94]. Basing on the pattern of inheritance, osteopetroses have been categorized into autosomal recessive (ARO), also defined as infantile malignant osteopetrosis due to the severity of symptoms affecting very young children [71], autosomal dominant osteopetrosis (ADO) usually considered an adult-onset more benign form [95] and the extremely rare X-linked osteopetrosis with only few unrelated patients reported [96-100]. Recently the spectrum of molecular defects causing osteopetrosis has been expanded taking advantage of new advanced technologies in genetic testing, clarifying the role of new mutations in the pathogenesis of the disease; however, about 10% of cases lack a molecular classification and need further genetic investigations [101].

### *1.3.1 Autosomal Recessive Osteopetrosis*

ARO has an incidence of 1:250000 live births and it is particularly frequent in specific geographic areas due to geographic isolation, high incidence of parental consanguinity or the presence of a founder effect. ARO is usually fatal within the first decade of life

without a prompt treatment, that so far is represented by hematopoietic stem cell transplantation (HSCT)[71]. Patients present with failure to thrive, skull abnormalities (macrocephaly, frontal bossing, choanal stenosis), hydrocephalus, hypocalcemia due to defective calcium mobilization activity of osteoclasts [94] and abnormal tooth eruption with frequent development of dental caries [102]. ARO is caused by mutations in different genes that are implicated in osteoclast functions (osteoclast-rich osteopetrosis) or differentiation (osteoclast-poor osteopetrosis) (Figure 6).

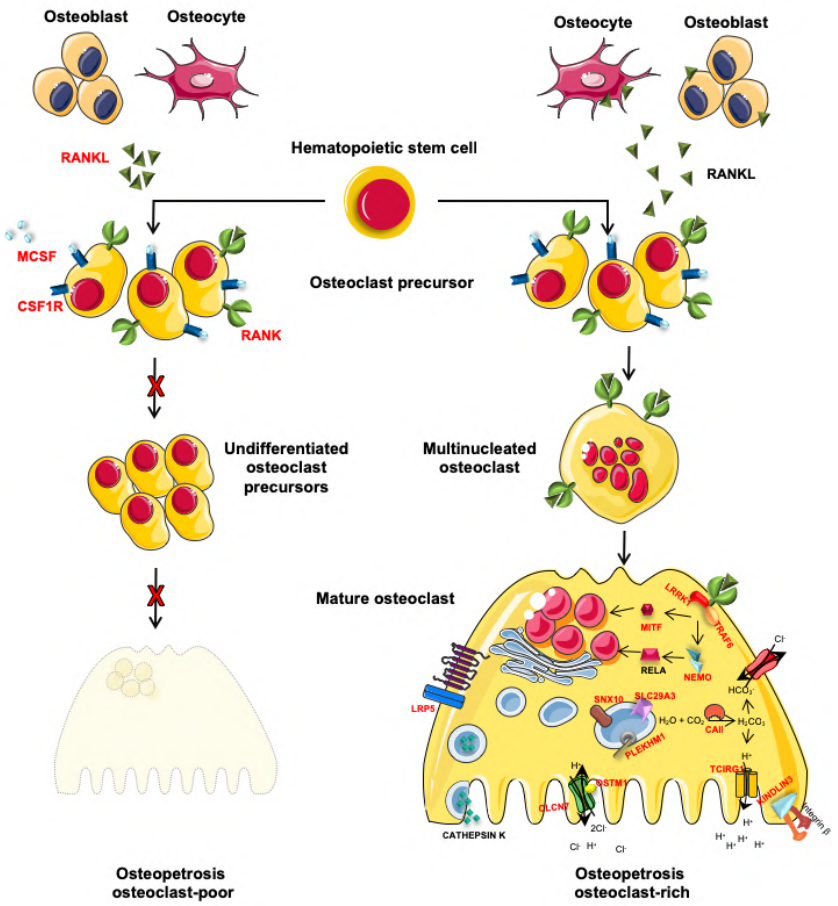


**Figure 6.** Schematic representation of genes involved in osteoclast-poor and osteoclast-rich osteopetrosis. In red are indicated genes involved in the pathogenesis of ARO. On the left of the figure are reported genetic mutations causing defective osteoclast differentiation. On the right are reported mutation affecting bone resorptive activity of osteoclasts (Penna et al., 2019).

### *1.3.2 Osteoclast-rich Osteopetrosis*

The most frequent form of ARO is caused by mutations in *TCIRG1* (T cell immune regulator 1) gene, accounting for more than 50%

of ARO cases. *TCIRG1* encodes for the a3 subunit of V0 complex of the V-ATPase proton pump, mainly expressed by osteoclasts and gastric parietal cells on apical membrane. The V-ATPase pump is responsible for the acidification of the bone resorption lacuna and for the dissolution of the hydroxyapatite crystals forming the bone mineral fraction, and the degradation of the matrix [103]. The a3 subunit is also involved in the interaction between actin cytoskeleton and microtubules, fundamental for the osteoclast ruffled border formation, mediating the tethering of lysosomes at the ruffled border before the fusion [71, 104]. Consequently, *TCIRG1*-mutated osteoclasts show defective ruffled border and markedly reduced or absent resorptive activity [104, 105]. The V-ATPase proton pump is important for the maintenance of low pH in the stomach, essential for the dietary $Ca^{2+}$ absorption; thus, ARO patients present rickets or osteomalacia due to defective calcium uptake [106]. The murine *oc/oc* model faithfully recapitulates the human *TCIRG1*-dependent ARO and for this reason it has been largely used to study the pathogenesis of osteopetrosis and novel therapeutic approaches, despite the strong severity of the phenotype of this model [107]. The *oc/oc* mouse carries a spontaneous deletion of 1.6 kb in the 5' of *Tcirg1* gene causing absence of ruffled border formation and defective bone resorption. Homozygous mice usually die within 3 weeks after birth due to severe bone marrow fibrosis. *oc/oc* mice are characterized by severe growth retardation, and exhibit the characteristic radiologic and histologic features of osteopetrosis such as increased skeletal density and absence of marrow cavities,

clubbed feet and circling behaviour due to cranial nerve compression and absent of or delayed eruption of the incisors [107]. Due to impairment of bone marrow niche, *oc/oc* mice are characterized by several hematological defects such as the high percentage of $CD11b^+$ cells and the increased number of myeloid progenitors revealing an augmented intra- and extramedullary myelopoiesis coupled with an increased number of non-functional osteoclasts. Moreover, B cell lymphopoiesis is also defective with a block of the progression from pro-B to pre-B cells caused by low level of expression of IL-7. Additionally, *oc/oc* mice have been reported to display an increase in the $CD11b^+CD11c^{low}$ dendritic population and impaired secretion of IFNγ by T cells [108].

17% of ARO cases represents the second most frequent form of osteopetrosis caused by a loss of function mutation in the *CLCN7* gene (chloride voltage-gated channel 7) [101, 109]. This gene codes a $2Cl^-/H^+$ antiporter expressed at the osteoclast ruffled border and on the membrane of late endosomes and lysosomes, regulated by voltage-gating mechanism [64]. This channel coupled with the V-ATPase proton pump is essential for the acid pH maintenance at the resorption lacunae; importantly it is also involved in vesicle trafficking in early and recycling endosomes, regulating the luminal $Cl^-$ concentration [110]. *CLCN7*-related osteopetrosis, depending on the type of mutation, is responsible for a large spectrum of clinical manifestations. In particular, the most severe cases of biallelic mutations are the cause of bone defects and hematological failure and they are associated in some patients with primary neurodegeneration, resembling lysosomal storage disease,

cerebral atrophy, spasticity, axial hypotonia and peripheral hypertonia [109, 111]. Intermediate forms of osteopetrosis caused by mutations in *TCIRG1* and *CLCN7* genes are characterized by milder clinical manifestations or later onset and slower progression of the disease [112-114].

*OSTM1* (osteopetrosis-associated transmembrane protein 1) mutations are reported in 5% of ARO cases [115, 116]. The protein has a highly glycosylated N-terminus that has been reported to stabilize CLCN7 protein and to be required, together with its transmembrane region, for CLCN7 $Cl^-/H^+$ transport activity [64]. OSTM1 acts also as an E3 ubiquitin ligase for the heterotrimeric G-protein Gαi3 and potentiates WNT canonical signalling by modulating β-catenin/Lef1 interaction [117, 118]. *OSTM1* mutations cause severe primary neurodegeneration, with a life expectancy shorter than 2 years [119].

*SNX10* gene, encoding for the sortin nexin 10 protein, one of the major interactors of the V-ATPase, able to target the proton pump from the Golgi network to the ruffled border [68, 120], has been reported in less than 5% of ARO cases [121]. SNX10 deficiency causes a reduction of osteoclasts count [122], that are bigger in size and pale at tartrate-resistant acid phosphatase (TRAP) staining [123]. The clinical manifestations are relatively variable in severity; the bone seems to be the only affected tissue and the defect can be almost completely rescued by hematopoietic stem cell transplantation [121].

Osteoclast-rich osteopetrosis is reported to be caused by very rare mutations in other genes like *CA-II* encoding for carbonic

anhydrase II, that affects less than one in a million live births and is associated with cerebral calcification and renal tubular acidosis [124]. This enzyme is involved in supplying protons to the vacuolar proton pump. Patients are characterized by renal defects, more severe than bone manifestations. Thus, this mutation is not usually considered a classical ARO [125].

Among very rare form of osteopetrosis, the loss-of-function mutations in the *PLEKHM1* (pleckstrin homology domain–containing family M member 1) gene has been reported [126]. *PLEKHM1* gene encodes for a cytosolic protein involved in lysosomal trafficking likely acting as an effector of Rab7 [127]. Mutations in this gene cause mild osteopetrosis in the *ia* (incisors absent) rat, as well as an intermediate form of osteopetrosis in humans due to inefficient bone resorption of osteoclasts that display altered morphology and abnormal podosome distribution [126].

Few cases of osteoclast-rich osteopetrosis originate from the mutations in *FERMT3* (fermitin family member 3) gene in association with leukocyte adhesion deficiency type III (LAD III), presenting with frequent bleeding and recurrent infections [128]. *FERMT3* gene is expressed by hematopoietic cells and encodes kindlin-3 protein, necessary for integrin signalling and platelet aggregation [129]. HSCT is reported to be curative for FERMT3 deficiency, with an early onset of the disease, although very few case have been described in literature so far [128].

Recently, a small cohort of cases has been described as carrier of the homozygous deletion of seven nucleotides in the last exon of

the *LRRK1* (leucine-rich repeat kinase 1) gene; patients present with osteosclerotic metaphyseal dysplasia, a form of osteopetrosis mainly affecting the metaphysis of long bones, the vertebral endplates, costal ends and margins of flat bones [130]. Moreover, *LRRK1* mutations have been reported as a mild form of osteopetrosis with a late onset as described by Howaldt in 2020 [131]. The role of LRRK1 needs to be fully elucidated however, recent studies described this protein as an interactor of the c-Src signalling pathway proteins, involved in cytoskeletal rearrangement and in ruffled border and podosome assembling [132].

Extremely rare cases of mutations causing osteoclast-rich osteopetrosis are attributed to *MITF* (microphtalmia-associated growth factor) gene, encoding for a transcription factor that acts downstream RANK/RANKL pathway [133], responsible for COMMAD (coloboma, osteopetrosis, microphthalmia, macrocephaly, albinism, and deafness) syndrome, suggesting a role of this protein in the regulation of various processes beside bone development and homeostasis [134].

### *1.3.3 Osteoclast-poor Osteopetrosis*

Mutations affecting osteoclast differentiation are responsible for the osteoclast-poor forms of osteopetrosis. In particular, mutations in the RANKL cytokine (2% of all ARO cases) or in its receptor RANK (4.5% of ARO forms) have been reported to cause osteoclast-poor ARO due to disruption of osteoclast differentiation

pathway and consequently the complete absence of mature differentiated osteoclasts in bone biopsies [135, 136].

*TNFSF11* and *TNFRSF11A* encode RANKL and its receptor RANK, respectively and they are essential for the activation of the downstream pathway that drives osteoclast precursors fusion and maturation [137]. RANKL deficiency presents with severe osteopetrosis, but in comparison with classical ARO, the disease progression is slower, leading to a delay in the diagnosis. Importantly, RANKL patients cannot benefit from HSCT since mutations in *TNFSF11* gene cause an osteoblast intrinsic defect. Besides bone defect, the absence of RANKL leads to impaired T cell proliferation and cytokines production [138]. Mutations in RANKL receptor encoded by the *TNFRSF11A* gene lead to a form of osteopetrosis characterized by absence of multinucleated osteoclasts. RANK-dependent osteopetrosis, is also associated with alteration in B cell memory subset and decreased immunoglobulin production. As opposed to *TNFSF11* deficiency, *TNFRSF11A*-deficient patients can benefit from HSCT [139].

Another group of mutations affecting osteoclast differentiation are those interesting *SLC29A3* (solute carrier family 29 member 3) gene encoding for a lysosomal nucleoside transporter highly expressed in myeloid cells [113, 140]. SLC29A3 deficiency, called dysosteosclerosis (DOS), is associated with red violet macular atrophy, platyspondyly and metaphyseal osteosclerosis. Moreover, a novel splice-site mutation in the intron 6 of *TNFRSF11A* has been recently described in one patient indicating *TNFRSF11A* as additional gene responsible for DOS [141].

A recent report described two affected siblings presenting osteopetrosis associated with severe combined immunodeficiency (SCID) caused by a large deletion on chromosome 11 encompassing *RAG1* and *RAG2* genes and the 5′ region of *TRAF6* (TNF receptor-associated factor 6 gene), the most important adaptor for the RANK/RANKL signalling pathway [142].
Lastly, a heterozygous truncating mutation in the *CSF1R* gene, which encodes for M-CSF receptor, was reported in the consanguineous parents of two deceased siblings, showing osteopetrosis and brain malformations [143].

### *1.3.4 Autosomal Dominant Osteopetrosis*

Autosomal Dominant Osteopetrosis (ADO) has an incidence of 1:20,000 live births with clinical onset typically in adolescence or adulthood [116] and some cases have been also diagnosed in paediatric age [112, 144]. ADO patients suffer from diffuse osteosclerosis, especially concerning the axial skeleton and symmetrical defects of the long bones. Two forms of ADO have been described. The ADO1 form, caused by mutations in the *LRP5* gene, leading to high bone mass syndrome characterized by clinical signs different from the classical form of osteopetrosis [145]. The ADO2 form is due to heterozygous missense mutations in the *CLCN7* gene. The mutant subunit is still able to dimerize but it impairs the function of the protein [146] Patients are characterized by a benign form of osteopetrosis, associated with frequent atraumatic fractures, osteonecrosis or osteomyelitis, vision and hearing impairment due to cranial nerve compression. In some

patients, bone defect may associate with bone marrow failure [144, 147].

### *1.3.5 X-Linked Osteopetrosis*

Few reports of mutations of the *IKBKG* (inhibitor of nuclear factor kappa B kinase subunit gamma) gene have been reported to cause osteopetrosis, occurring as a moderate complication of the OL-EDA-ID syndrome, lymphedema, anhidrotic ectodermal dysplasia and immunodeficiency (hence, the acronym) [148]. This gene is located on the X chromosome and encodes for NEMO, the regulatory subunit of IKK complex, fundamental for the activation of NF-kB transcription factor that induces osteoclastogenesis [96]. The evaluation of a bone biopsy from one patient revealed that osteoclasts were present in normal numbers and showed no morphological abnormalities [97], for this reason IKBKG deficiency is classified as an osteoclast-rich osteopetrosis [149].

## *1.4 Consensus guidelines for the treatment of osteopetrosis and new therapeutic approaches*

Hematopoietic stem cell transplantation (HSCT) is the therapy of choice for the cure of ARO osteopetrosis. However, in most of the cases, HSCT improves but does not fully rescue the disease. Despite fully engraftment in more than 50% of ARO transplanted patients, treated patients present progressive visual loss in the early post-transplant period [150]. The pharmacological treatment with corticosteroids, vitamin D/calcium supplementation, PTH or

gamma-interferon is supportive to HSCT, and not curative due to inefficient results with very few exceptions [94].

HSCT is not recommended for osteopetrosis associated with primary neuropathy, such as autosomal recessive forms caused by mutations in *CLCN7* and *OSTM1* genes and for osteopetrosis caused by absent osteoclasts due to mutation in *TNFSF11* gene [125].

Recently, successful transplants have been reported in intermediate forms of osteopetrosis providing a new therapeutic approach for these forms affecting adult individuals [151].

The treatment of ADO is usually driven by empiric approaches, that are generally aimed to cure the symptoms of the disease. To date, no guidelines for therapy are currently available. Patients that are not eligible for HSCT receive a conservative treatment based on multi-disciplinary approaches according to clinical manifestations of the single patients [152].

### *1.4.1 Hematopoietic stem cells transplantation for ARO patients: strengths and weaknesses*

If untreated, ARO is lethal in ~70% of cases in the first decade of life, primarily due to bone marrow failure and insufficient hematopoiesis. Since osteoclasts originate from hematopoietic precursors, intrinsic osteoclast defects can be treated by HSCT that results in improved bone remodelling and reversal of pancytopenia and extramedullary hematopoiesis [150]. Patients who can benefit from HSCT usually are younger than 1 year of age; after this age the risks related to the progression of the disease rapidly increase

overtime [94]. Moreover, increased frequency of transplant failure (rejection/graft failure and major toxic complications) has been reported in patients receiving HSCT after 10 months of age, particularly in haploidentical HSCT setting [152].

A retrospective study, reporting the international experience in outcomes after related and unrelated hematopoietic transplantation for infantile osteopetrosis in 193 patients, indicates the guidelines for the choice of HSCT donor, based on the analysis of overall survival with the longest follow up of 10 years after treatment (Figure 7) [150].

This comprehensive study suggested that the best match for HSCT would be an HLA-genoidentical family donor like a sibling or an HLA-matched donor with an overall survival at 10 years after transplant of 62%. When a matched donor is not available in a short period of time, transplantation using grafts from an HLA-mismatched relative, an adult unrelated donor or umbilical cord blood is a reasonable approach for an otherwise lethal disease, and the probability of survival reported in the longest follow up of 10 years is the 39%.

However, this analysis failed to show differences in survival after HLA-mismatched related, adult unrelated donor and umbilical cord blood transplantation, and this is probably a consequence of the difficulty in achieving engraftment in osteopetrosis, due to abnormalities in the marrow microenvironment and/or in the homing process of HSPC [150].

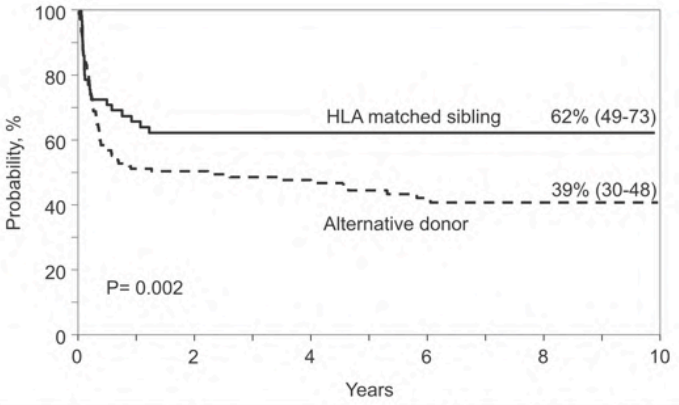


| Donor match | 100 days | 1 year | 5 years | 10 years |
|---|---|---|---|---|
| HLA- matched sibling (N = 65) | 72% | 65% | 62% | 62% |
| Alternative donor (N = 128) | 67% | 50% | 42% | 39% |

**Figure 7.** The upper graph summarizes the probability of overall survival based on the donor type and the table reports the percentage of survival in intermediate follow up (Orchard et al. 2015).

Other authors reported that the use of cord blood as donor source in a small cohort of patients with fluctuating success rates. However, frequent primary graft failures have been recorded, resulting in poor overall survival at 3 years [153-156]. Therefore, unrelated cord blood donors are no longer recommended. Another promising option for those patients without an HLA-genoidentical family donor, has been exploited in three patients receiving unrelated matched donor $CD34^+$ cells infused with TCR gamma/$delta^+$ and TCR alpha/$beta^+$ cells, that were initially depleted from the preparation and then repleted to a number not exceeding $25\times10^6$ cells/kg, together with a limited number of $CD19^+$ lymphocytes. This procedure allowed an acceptable long-

term donor cells engraftment and significatively limited the risk of graft versus host disease (GvHD) decreasing the risk of EBV-associated lymphoproliferative syndromes [157].

Moreover, poor donor stem cell engraftment has been observed because of the fibrosis of bone marrow cavity and absence of bone marrow niche, thus creating an inappropriate environment for donor cells engraftment [152]. Furthermore, poor outcome and side effects have been also associated with traditional myeloablative chemotherapy regimens, paving the way for the research of new approaches for the conditioning of osteopetrotic patients to ameliorate HSCT outcome [158].

New transplant strategies such as the Baltimore protocol of T replete haploidentical transplantation with cyclophosphamide post-transplant had been exploited for the treatment of children older than 10 months [159], being successful in several cases of re-transplantation after rejection or non-engraftment. Promising data have been recently obtained in osteopetrotic patients (younger than 6 years old), receiving transplant after reduced intensity conditioning regimen (RIC) based on fludarabine, treosulfan, thiotepa, and antithymocyte globulin, paving the way for the cure of patients older than 10 months of age [158].

RIC regimens have significantly improved the outcome of HSCT allowing to create sufficient space in the BM compartment, to achieve an acceptable levels of donor chimerism and to avoid side effects of myeloablative conditioning. In particular, fludarabine is associated with improved T-cell chimerism and treosulphan with a decreased risk of VOD [160]; RIC regimens usually include also

serotherapy as well as Cyclosporine A as prophylaxis for graft versus host disease (GvHD) [161].

Moreover, recent results of HLA-haploidentical transplant using a busulfan-fludarabine based conditioning regimen show limited toxicity and good efficacy resulting in a disease-free survival of 80% [152].

Despite improving in conditioning, severe side effects have been reported in transplanted patients. The risk of VOD [162], pulmonary hypertension (HTN), hypercalcemia still remains high [150, 152]. Moreover, poor donor stem cell engraftment has been observed because of the fibrosis of bone marrow cavity and absence of bone marrow niche thus creating an inappropriate environment for donor cells engraftment [152].

Other important complications to consider for the management of osteopetrotic patients are the risk of *Pneumocystic jirovecii* pneumonia infections due to the slow hematological and immunological reconstitution after HSCT, that can be prevent with antifungal and PCP prophylaxis.

The central nervous system (CNS) represents another target of transplant-related risks; malformations of cranial bones are reversible after HSCT, but these patients need a constant interdisciplinary monitoring to avoid or solve this severe condition. Additionally, hypocalcaemia and the risk of convulsions before the engraftment occur and can be attenuated by supplementation with calcium gluconate and 1-alpha vitamin D before HSCT; this treatment must be suspended after HSCT to avoid the opposite phenomenon of hypercalcemic crisis [152].

### *1.4.2 Innovative therapies for TCIRG1-dependent osteopetrosis*

In recent years, the outcome of HSCT has been strongly improved thanks to the promising data obtained from patients undergoing HSCT after RIC regimen. Despite improvement in conditioning, the availability of HLA-matched donors still remains an open issue particularly in patients older than 10 months. Because of the limited efficacy of HSCT due to the severity of the disease and the limited time window in which patients can be treated, alternative therapeutic strategies have been developed in the past. To prevent irreversible bone defect and bone marrow fibrosis, *in utero* transplantation of donor HSC was considered as additional therapeutic option.

A preclinical study in 2005 demonstrated the efficacy of allogeneic HSCT performed during fetal life in the *oc/oc* mouse model. Mutant embryos *in utero* transplanted at 14.5 days postcoitum showed restored osteoclasts resorption capacity and normalization of bone density. These data provided evidence that transplant has to be performed very early in life to avoid the development of secondary irreversible defects [163]. These results were further confirmed by a second study in which authors performed *in utero* injection of allogeneic fetal liver cells [164]. *In utero* experiments highlighted the need of a prenatal diagnosis and early intervention in ARO patients, showing promising results. In humans, *in utero* transplantation have been already performed in primary immunodeficiencies [165]. Additionally, considering the limitation of HSCT in non-compatible donor setting, autologous

transplantation of genetically modified $CD34^+$ cells remains a feasible and attractive alternative strategy [166]. To this end, preclinical model of gene therapy (GT) of *TCIRG1*-dependent osteopetrosis has been developed during these years to demonstrate the efficacy and safety of this therapeutic approach.

### *1.4.3 Gene therapy approaches to cure TCIRG1-dependent osteopetrosis*

In recent studies, lentiviral vectors (LVs) supplanted retroviral vectors in clinical trials of immunodeficiencies due to the proven clinical benefits in patients and the absent risk of leukemic side effects [167, 168]. In particular, a very important study in 2006 revealed the unique benefit that GT can achieve in comparison with HSCT in term of therapeutic protein expression in the hematopoietic progeny, leading to its increased bioavailability and widespread cross-correction in the central nervous system [169]. In this study a LV carrying the *ARSA* gene under the control of a PGK promoter have been used to achieve efficient gene transfer into HSPCs and long-term overexpression of the gene in their cellular progeny in the murine model of metachromatic leukodystrophy (MLD). Authors demonstrated that with GT they were able to revert the neurological deficits and neuropathological damage in affected mice, thus correcting the neurological symptoms [169]. Later, these results were confirmed in MLD patients transplanted with *ex-vivo* LV-transduced autologous HSCs, showing stable engraftment with high efficiency of transduction and without evidence of vector-induced genotoxicity [170].

Moreover, LVs with the elongation factor short (EFS) promoter are shown to have a significantly decreased risk of insertional mutagenesis and no evidence of clonal dominance was reported during clinical trials of GT for severe combined immunodeficiency X1 (SCID-X1) using the EFS promoter [171].

Taking advantage of these results a LV carrying *TCIRG1* gene under the control of the EFS promoter were able to improve bone defects and survival of *oc/oc* mice, despite the low number of successfully treated mice, due to the extremely severe phenotype of this model [172]. *oc/oc* c-kit$^{+}$ fetal liver cells transduced with EFS-hTCIRG1 were transplanted into sublethally irradiated *oc/oc* mice by temporal vein injection 1 day after birth. A total of 9 of 12 mice survived long term (19–25 weeks) and showing reversal of the osteopetrotic bone phenotype both *in vitro*, by osteoclast culture and *in vivo* through the quantification of CTX in the serum and histopathology analysis of the bones [172]. On the same line Richter's group previously demonstrated that this clinically applicable LV can also *ex-vivo* correct ARO circulating CD34$^{+}$ rescuing resorptive capacity of ARO patients-derived osteoclast *in vitro* [173]. Authors also demonstrated that transduced ARO CD34$^{+}$ cells are able to engraft in NSG mice with a rate similar to cord blood CD34$^{+}$ and that human CD34$^{+}$ isolated from bone marrow and spleen of NSG transplanted mice are able to differentiate in to bone resorbing osteoclast *in vitro* [173]. These results suggested that GT could be established as an innovative and personalized therapeutic approach for osteopetrotic patients lacking an HLA compatible donor.

### *1.4.4 Novel preclinical studies to cure other form of osteopetrosis*

ARO caused by osteoclast extrinsic deficiency, such as *TNFSF11* mutations, requires a different approach. RANKL replacement therapy has been explored at a preclinical level; this cytokine was administered to *Tnfsf11*$^{-/-}$ mice, rescuing bone defects and hematopoietic organ architecture [174].

Interestingly, mesenchymal stem cell (MSC) transplantation has been considered as alternative approach for osteoclast extrinsic osteopetrosis with the aim to restore the functionality of the osteoblastic counterpart; however, the clinical application of this method is still under debate, and far from a real clinical applicability [175].

Promising results have been obtained exploiting the use of biotechnological devices implanted subcutaneously, able to release soluble RANKL and allowing osteoclastogenesis in *Tnfsf11* $^{-/-}$ mice [176]. On the same line, a biomimetic scaffold, implanted subcutaneously in *Tnfsf11*$^{-/-}$ mice and carrying *Tnfsf11*$^{-/-}$ MSC, transduced with a lentiviral vector overexpressing human soluble RANKL, was demonstrated to drive the differentiation of TRAP positive osteoclasts [177].

For the treatment of ADO2 form of osteopetrosis new approaches came out recently, demonstrating the capacity of small interfering RNA (siRNA) to silence specifically the mutated *CLCN7* allele, restoring the resorption capacity of human osteoclast *in vitro* and improving osteopetrotic phenotype of the ADO2 mouse model *in vivo* [178].

Results of siRNA approach on ADO2 were promising and paved the way for the establishment of preclinical studies which can potentially introduce this innovative treatment to the clinic. Thus, Capulli et al. in 2018 demonstrated that Clcn7$^{G213R}$ siRNA is not only effective in pre-pubertal ADO2 male as shown in previous study, but can rescue the bone phenotype of aged mice, both males and females by intraperitoneal and subcutaneous administration. They also performed safety studies following prolonged chronic administration, identifying specific end-points of a clinical trials [179]. Later, they also demonstrated that the treatment with Clcn7$^{G213R}$ siRNA is able to improve the extra-skeletal alterations due to ADO2 disease [180].

### *1.5 Mucopolysaccharidosis: a lysosomal storage disease*

Mucopolysaccharidosis (MPS) belongs to lysosomal storage disorders (LSDs), a group of inherited metabolic diseases characterized by impaired lysosomal homeostasis caused by mutations in genes encoding for lysosomal hydrolases, membrane proteins and transporters involved in the degradation of molecules in different tissues and organs [181].

LSDs are multisystemic disorders characterized by chronic and progressive course, abnormalities in multiple tissues and organs comprising nervous system, bone, cartilage and viscera [182].

LSDs are extremely rare with a frequency of 1 in 8000 live births [183] and the majority of them have an autosomal recessive pattern of inheritance [184].

In MPS, lysosomes accumulate undegraded substrates called glycosaminoglycans (GAGs), polysaccharides characterized by high rate of sulphation able to link core proteins forming large complexes, known as proteoglycans [185]. GAGs accumulate due to the enzyme catabolic deficiency in lysosomes, acid organelles involved in the degradation of cellular substrates. The catabolic activity of lysosomes is possible due to their acid internal pH that guarantee the adequate environment for lysosomal enzymes, that are synthetized in the rough endoplasmic reticulum (RER) and modified in *cis* Golgi by the addition of mannose-6-phospate residue, acting as guide signal to segregate the enzyme to the lysosome [186]. The catabolic function of lysosome is exploited by a cascade of hydrolases that act in a consequential manner; thus, if one of the step of this cascade is blocked, the degradation process is interrupted resulting in the accumulation of materials, detrimental for the cellular homeostasis and consequently causing lysosomal dysfunctions [181]. The GAGs accumulation in lysosomes leads to multisystemic manifestations like hepatosplenomegaly, mental retardation, short stature, coarsened facial features, and a range of musculoskeletal deformities known as dysostosis multiplex. Abnormalities regarding the musculoskeletal apparatus are mainly caused by GAGs accumulation, in particular by dermatan sulphate (DS), in joint capsule ligaments tendons, in growth plate and in articular cartilage. The inflammatory response caused by DS accumulation is caused by the similarities of this molecule with bacterial lipopolysaccharides [187].

### *1.5.1 Mucopolysaccharidosis type I - Hurler syndrome as a model to study osteoclast extrinsic defects*

Mucopolysaccharidosis type I (MPS-I), is one of the most frequent form of LSDs, with an incidence of 1 on 100000 live births. It is a chronic and multisystemic disorder showing an autosomal recessive pattern of inheritance caused by the mutation in the gene encoding for the α-L-iduronidase (IDUA) enzyme [188]. IDUA is involved in the degradation of heparan sulphate (HS) and dermatan sulphate (DS) and the absence of its catabolic activity leads to GAGs accumulation into the lysosomes [189].

*IDUA* gene (19kb) localized on chromosome 4p16.3 encodes for a 74 kDa protein [190]. Although there is no correspondence between genotype and phenotype due to the spread heterogeneity of the disease, generally, patients with the most severe form are characterized by mutations in both alleles, causing the absence of IDUA enzyme or the impairment of its functionality [191].

MPSI is very heterogeneous in terms of clinical manifestations and based on the severity of the disease, three different clinical phenotypes can be identified. The most severe form of MPSI is the Hurler Syndrome (MPSIH) that has an early onset with symptoms appearance before one year of age and mental retardation before the age of three. The intermediate form called Hurler/Scheie (MPSIH/S), and the Scheie syndrome (MPSIS) that has a milder outcome with symptoms appearing at 5 years of age, although it does not impair the life-span and the mental capacities of affected individuals [192].

Most known cases belong to the severe form (MPSIH), which is our variant of interest for this project. Clinical manifestations of MPSIH start in the first year of life. They include upper airway obstruction due to mucosal and adenotonsillar hypertrophy and repeated infections, laryngeal and tracheal narrowing, hearing and visual deficit, gargoyle facies, organomegaly, abdominal hernia, valve disease and cardiomyopathy, skeletal deformities such as thoracolumbar gibbus and joint stiffness, and progressive neurological disease with severe cognitive delay [193].

Diagnosis of MPSI could be very challenging due to the heterogeneity of clinical features of patients; in fact, some cases could remain undiagnosed for years, especially in milder forms. The most common symptoms indicative of the disease are represented by respiratory infection in patients showing coarse facial features, enlarged tongue and hernias [194]. The diagnostic procedure is the quantification of urinary GAGs, that is sensitive but not highly specific, giving rise in some cases to false-negative responses [191]. Additionally, primary storage materials can be evaluated in serum, plasma and cerebral spinal fluid [195]. Regarding the evaluation of the enzymatic activity in MPSI patients, in the past, clinicians exploited the possibility to measure IDUA activity in culture of fibroblast and leucocytes and in biological fluids by biochemical analysis [196]. In recent years, these procedures have been replaced by the use of dried blood spot technique able to determine the definitive diagnosis for MPSI [191, 197].

The large number of single-occurrence mutations cause a huge heterogeneity of clinical phenotype and at the same time limit the predictive capacity of the *IDUA* gene sequencing for diagnostic purposes [191].

### *1.5.2 Current therapies and management of MPSI Hurler syndrome*

Enzyme replacement therapy (ERT) and allogeneic hematopoietic stem cell transplantation (HSCT) are the two available therapeutic approaches offered to cure MPSIH and considered as standard treatments.

ERT with human recombinant IDUA, a polymorphic form of the human enzyme, is the most diffuse treatment for MPSI patients and its safety and efficacy have been proven over the years. It is not recommended for the severe Hurler form because of the inability of the enzyme to cross the blood-brain barrier [198]. Additionally, the recombinant enzyme does not completely correct bone abnormalities, heart valvulopathy and corneal clouding [199]. However, more promising data of metabolic correction have been obtained after HSCT [200].

Therefore, HSCT became the gold standard for the treatment of severe form of MPSI [201] and then in patients diagnosed and treated before 2–2.5 years of age with developmental quotient (DQ) >70 at the time of HSCT [202]. Recently, due to the improved safety of this procedure, the therapeutic indication for HSCT has been extended to patients with severe Hurler-Scheie who are at risk of progressive neurocognitive impairment [203]. Regarding the

source of donor cells used in HSCT setting, bone marrow and peripheral blood HSC are the standard source of cells used historically; however, in recent reports umbilical cord blood (UCB) stem cells have been successfully used to transplant MPSI patients. UCB transplantation allowed a reduced incidence of GvHD and a high level of donor chimerism in *idua*$^{-/-}$ mouse model, becoming a promising alternative stem cell source for the treatment of these patients [204]. Moreover, in 2015 Yasuda et al. demonstrated that UCB comprises a small percentage of MSC that can differentiate into normal chondrocytes, restoring their physiological activity [205].

HSCT has been proven to delay the progression of cognitive retardation and the multiorgan damages due to GAGs accumulation [202]. Importantly, due to the increase knowledge of the pathogenesis of the disease and to the implementation of HSCT procedure, this approach has been fundamental to strongly increase the life-span and ameliorate the quality of life of these patients [206].

Despite the success of this approach, patients treated with HSCT may develop a significant burden of disease, especially heart valve disease, ocular involvement and osteo-articular complications requiring multiple surgical interventions. Additionally, transplant-related morbidity and mortality due to GvHD, infections and other complications need to be considered. In this regard, Boelens et al. reported 15% of mortality after HSCT with a poor engraftment in the 44% of MPSI patients [207].

Importantly, the severity of post-transplant cognitive impairment is usually related to age and/or psychomotor development at the time of transplantation and level of engraftment, suggesting that a prompt intervention and an early diagnosis can improve the outcome of the treatment [203, 208].

Thus, HSCT efficacy relies on the ability of hematopoietic donor cells producing IDUA to engraft and cross-correct the MPSI affected counterpart (MSCs) conferring a stable source of enzyme and restoring functionality of non-haematological organs [209].

On the other hand, it has been reported that the combination of ERT and HSCT does not impair engraftment nor promotes the development of GvHD [210]. Moreover, a recent 10-year follow-up highlighted a beneficial effect of peri-transplant ERT in which the IDUA recombinant enzyme has been administered at the point of diagnosis and continue through the period of donor selection and pre-transplant conditioning, until effective transplantation can be performed [211]. Nowadays, peri-transplant ERT is largely accepted and its used to be exploited during the period between diagnosis and HSCT, to improve the outcome of the transplant [206]. Moreover, the use of ERT in patients that underwent HSCT is currently under consideration based on the observation of a beneficial effect of post-transplant ERT, suggesting that a post-transplant support of recombinant IDUA could improve the outcome of HSCT [212].

The severity of the disease and the partial efficacy of HSCT in preventing neurodevelopmental and skeletal complications, make MPSI, among LSDs, a good candidate for GT. MPSI is a severe

monogenic disease and the genetic correction of IDUA defective hematopoietic lineage is sufficient to restore the production of the defective enzyme that can be uptaken by affected cells and improve the clinical status of the patient with a cross-corrective mechanism potentially overcoming the ERT periodic infusion [183, 213]. Moreover, transplantation of autologous *ex-vivo* modified HSCs showed supra-physiological levels of the lacking protein and strongly reduced the morbidities and mortality rate associated with GvHD observed in HSCT setting [214]. In recent years, as already mentioned, LVs are seen as safe and efficacious actors in *ex-vivo* GT approaches. Regarding MPSI, Visigalli et al. were able to achieve correction of neurologic and skeletal abnormalities in the preclinical model of MPSI mouse, applying an *ex-vivo* transduction protocol of BM HSCs [215]. Moreover, they validated the application of LV HSC GT in MPSI patients by biosafety studies, in term of toxicity and biodistribution [216].

In 2018 at San Raffaele Hospital in Milan, a phase I/II study (NCT03488394) has been established for the treatment of patients affected by MPSIH. The aim of this trial is to evaluate the safety and the efficacy of autologous hematopoietic stem and progenitor cells, genetically modified with a LV carrying *IDUA* gene. This trial is based on the *ex-vivo* transduction of MPSIH $CD34^+$ with the LV carrying the α-L-iduronidase cDNA and eight patients have been enrolled so far. Preliminary clinical results indicate that this strategy allows efficient HSPC transduction and patients showed rapid hematopoietic recovery, supraphysiologic IDUA levels in the

peripheral blood and metabolic correction of the IDUA enzyme deficiency in critical target tissues [217].

### *1.6 Scope of the thesis*

The scope of my PhD project was to develop a novel GT-based therapeutic approach to correct primary bone defects of Autosomal Recessive Osteopetrosis. In parallel, I contributed to analyse the results of pre/post GT clinical trial for Mucopolysaccharidosis type I, Hurler variant, investigating bone damage repair and the mechanisms of bone homeostasis.

**Chapter 2.** We developed a novel GT strategy based on clinically-optimized lentiviral vectors, driving *TCIRG1* expression. We tested our GT protocol on the *oc/oc* mouse model, closely resembling the human ARO obtaining an amelioration of the lifespan, improvement of the bone phenotype and clinical status.

**Chapter 3.** We isolated and characterized $CD34^+$ from the blood of ARO patients that were transduced and expanded, applying a protocol that allows stemness maintenance. We performed *in vitro* assays to evaluate resorption capacity of patient-derived osteoclasts and we evaluated the long-term multilineage repopulating potential of expanded $CD34^+$ cells by primary and secondary transplant into NSG mice.

**Chapter 4.** We investigated the impact of *ex-vivo* gene therapy on the bone damage in Mucopolysaccharidosis type I Hurler Syndrome and we dissected the pathophysiological mechanism undergoing bone cells crosstalk *in vitro*.

## References


1. Florencio-Silva, R., et al., *Biology of Bone Tissue: Structure, Function, and Factors That Influence Bone Cells.* BioMed research international, 2015. **2015**: p. 421746-421746.
2. Marks, S.C. and P.R. Odgren, *Chapter 1 - Structure and Development of the Skeleton*, in *Principles of Bone Biology (Second Edition)*, J.P. Bilezikian, L.G. Raisz, and G.A. Rodan, Editors. 2002, Academic Press: San Diego. p. 3-40.
3. Anderson, H.C., *Matrix vesicles and calcification.* Current Rheumatology Reports, 2003. **5**(3): p. 222-226.
4. Yoshiko, Y., et al., *Osteoblast Autonomous P<sub>i</sub> Regulation via Pit1 Plays a Role in Bone Mineralization.* Molecular and Cellular Biology, 2007. **27**(12): p. 4465.
5. Roberts, S., et al., *Functional Involvement of PHOSPHO1 in Matrix Vesicle–Mediated Skeletal Mineralization.* Journal of Bone and Mineral Research, 2007. **22**(4): p. 617-627.
6. Clarke, B., *Normal Bone Anatomy and Physiology.* Clinical Journal of the American Society of Nephrology, 2008. **3**(Supplement 3): p. S131.
7. Singh, S., T.J.P. Bray, and M.A. Hall-Craggs, *Quantifying bone structure, micro-architecture, and pathophysiology with MRI.* Clin Radiol, 2018. **73**(3): p. 221-230.
8. Everts, V., et al., *The Bone Lining Cell: Its Role in Cleaning Howship's Lacunae and Initiating Bone Formation.* Journal of Bone and Mineral Research, 2002. **17**(1): p. 77-90.
9. Parfitt, A.M., *Osteonal and hemi-osteonal remodeling: The spatial and temporal framework for signal traffic in adult human bone.* Journal of Cellular Biochemistry, 1994. **55**(3): p. 273-286.
10. Capulli, M., R. Paone, and N. Rucci, *Osteoblast and osteocyte: Games without frontiers.* Archives of Biochemistry and Biophysics, 2014. **561**: p. 3-12.
11. Dirckx, N., et al., *The role of osteoblasts in energy homeostasis.* Nat Rev Endocrinol, 2019. **15**(11): p. 651-665.
12. Bianco, P., et al., *Bone sialoprotein (BSP) secretion and osteoblast differentiation: relationship to bromodeoxyuridine incorporation, alkaline phosphatase, and matrix deposition.* Journal of Histochemistry & Cytochemistry, 1993. **41**(2): p. 183-191.

13. Lee, J.-S., J.-M. Lee, and G.-I. Im, *Electroporation-mediated transfer of Runx2 and Osterix genes to enhance osteogenesis of adipose stem cells.* Biomaterials, 2011. **32**(3): p. 760-768.
14. Marks, S.C. and S.N. Popoff, *Bone cell biology: the regulation of development, structure, and function in the skeleton.* Am J Anat, 1988. **183**(1): p. 1-44.
15. Rutkovskiy, A., K.-O. Stensløkken, and I.J. Vaage, *Osteoblast Differentiation at a Glance.* Medical science monitor basic research, 2016. **22**: p. 95-106.
16. Chen, X., et al., *Osteoblast-osteoclast interactions.* Connective tissue research, 2018. **59**(2): p. 99-107.
17. Felix, R., et al., *Impairment of macrophage colony-stimulating factor production and lack of resident bone marrow macrophages in the osteopetrotic op/op mouse.* J Bone Miner Res, 1990. **5**(7): p. 781-9.
18. Nakashima, T., et al., *Evidence for osteocyte regulation of bone homeostasis through RANKL expression.* Nat Med, 2011. **17**(10): p. 1231-4.
19. Fujiwara, Y., et al., *RANKL (Receptor Activator of NFκB Ligand) Produced by Osteocytes Is Required for the Increase in B Cells and Bone Loss Caused by Estrogen Deficiency in Mice.* J Biol Chem, 2016. **291**(48): p. 24838-24850.
20. Xiong, J., et al., *Soluble RANKL contributes to osteoclast formation in adult mice but not ovariectomy-induced bone loss.* Nature Communications, 2018. **9**(1): p. 2909.
21. Ono, T. and T. Nakashima, *Recent advances in osteoclast biology.* Histochemistry and cell biology., 2018. **149**(4): p. 325-341.
22. Simonet, W.S., et al., *Osteoprotegerin: A Novel Secreted Protein Involved in the Regulation of Bone Density.* Cell, 1997. **89**(2): p. 309-319.
23. Sims, N.A. and J.H. Gooi, *Bone remodeling: Multiple cellular interactions required for coupling of bone formation and resorption.* Seminars in Cell & Developmental Biology, 2008. **19**(5): p. 444-451.
24. Karsenty, G. and M. Ferron, *The contribution of bone to whole-organism physiology.* Nature., 2012. **481**(7381): p. 314-320.
25. Karsenty, G. and E.N. Olson, *Bone and Muscle Endocrine Functions: Unexpected Paradigms of Inter-organ Communication.* Cell, 2016. **164**(6): p. 1248-1256.

26. Oury, F., et al., *Endocrine regulation of male fertility by the skeleton.* Cell, 2011. **144**(5): p. 796-809.
27. Oury, F., et al., *Maternal and offspring pools of osteocalcin influence brain development and functions.* Cell, 2013. **155**(1): p. 228-41.
28. Zhang, J., et al., *Identification of the haematopoietic stem cell niche and control of the niche size.* Nature, 2003. **425**(6960): p. 836-41.
29. Calvi, L.M., et al., *Osteoblastic cells regulate the haematopoietic stem cell niche.* Nature, 2003. **425**(6960): p. 841-6.
30. Calvi, L.M., et al., *Osteoblastic expansion induced by parathyroid hormone receptor signaling in murine osteocytes is not sufficient to increase hematopoietic stem cells.* Blood, 2012. **119**(11): p. 2489-2499.
31. Bromberg, O., et al., *Osteoblastic N-cadherin is not required for microenvironmental support and regulation of hematopoietic stem and progenitor cells.* Blood, 2012. **120**(2): p. 303-313.
32. Bowers, M., et al., *Osteoblast ablation reduces normal long-term hematopoietic stem cell self-renewal but accelerates leukemia development.* Blood, 2015. **125**(17): p. 2678-2688.
33. Frisch, B.J., *The hematopoietic stem cell niche: What's so special about bone?* Bone, 2019. **119**: p. 8-12.
34. Tresguerres, F.G.F., et al., *The osteocyte: A multifunctional cell within the bone.* Annals of Anatomy - Anatomischer Anzeiger, 2020. **227**: p. 151422.
35. Bonewald, L.F., *The amazing osteocyte.* Journal of Bone and Mineral Research, 2011. **26**(2): p. 229-238.
36. Bellido, T., P.D. Pajevic, and L. Bonewald, *Chapter 14 - Osteocyte Biology*, in *Genetics of Bone Biology and Skeletal Disease (Second Edition)*, R.V. Thakker, et al., Editors. 2018, Academic Press. p. 227-240.
37. Civitelli, R., *Cell-cell communication in the osteoblast/osteocyte lineage.* Arch Biochem Biophys, 2008. **473**(2): p. 188-92.
38. Ishihara, Y., et al., *Hormonal, pH, and calcium regulation of connexin 43-mediated dye transfer in osteocytes in chick calvaria.* J Bone Miner Res, 2008. **23**(3): p. 350-60.
39. Dallas, S.L., M. Prideaux, and L.F. Bonewald, *The Osteocyte: An Endocrine Cell ... and More.* Endocrine Reviews, 2013. **34**(5): p. 658-690.

40. Bellido, T., *Osteocyte-Driven Bone Remodeling.* Calcified Tissue International, 2014. **94**(1): p. 25-34.
41. Winkler, D.G., et al., *Osteocyte control of bone formation via sclerostin, a novel BMP antagonist.* Embo j, 2003. **22**(23): p. 6267-76.
42. Baud, C.A., *MORPHOLOGIE ET STRUCTURE INFRAMICROSCOPIQUE DES OSTÉOCYTES.* Cells Tissues Organs, 1962. **51**(3): p. 209-225.
43. Teti, A. and A. Zallone, *Do osteocytes contribute to bone mineral homeostasis? Osteocytic osteolysis revisited.* Bone, 2009. **44**(1): p. 11-16.
44. Belanger, L.F., C. Belanger, and T. Semba, *Technical approaches leading to the concept of osteocytic osteolysis.* Clin Orthop Relat Res, 1967. **54**: p. 187-96.
45. Ramp, W.K. and W.F. Neuman, *Some factors affecting mineralization of bone in tissue culture.* Am J Physiol, 1971. **220**(1): p. 270-4.
46. Tsourdi, E., et al., *Physiological and pathological osteocytic osteolysis.* J Musculoskelet Neuronal Interact, 2018. **18**(3): p. 292-303.
47. Robling, A.G. and L.F. Bonewald, *The Osteocyte: New Insights.* Annu Rev Physiol, 2020. **82**: p. 485-506.
48. Jüppner, H., *Phosphate and FGF-23.* Kidney Int Suppl, 2011. **79**(121): p. S24-7.
49. Tanaka, Y., et al., *Intercellular adhesion molecule 1 discriminates functionally different populations of human osteoblasts: characteristic involvement of cell cycle regulators.* J Bone Miner Res, 2000. **15**(10): p. 1912-23.
50. Xiao, Y., et al., *Macrophages and osteoclasts stem from a bipotent progenitor downstream of a macrophage/osteoclast/dendritic cell progenitor.* Blood advances, 2017. **1**(23): p. 1993-2006.
51. Madel, M.B., et al., *Immune Function and Diversity of Osteoclasts in Normal and Pathological Conditions.* Front Immunol, 2019. **10**: p. 1408.
52. Jacome-Galarza, C.E., et al., *Developmental origin, functional maintenance and genetic rescue of osteoclasts.* Nature, 2019. **568**(7753): p. 541-545.
53. Baron, R., *Polarity and Membrane Transport in Osteoclasts.* Connective Tissue Research, 1989. **20**(1-4): p. 109-120.

54. Cappariello, A., et al., *Reprint of: The Great Beauty of the osteoclast.* Arch Biochem Biophys, 2014. **561**: p. 13-21.
55. Domon, T., et al., *Three-dimensional distribution of the clear zone of migrating osteoclasts on dentin slices in vitro.* Tissue and Cell, 2002. **34**(5): p. 326-336.
56. Supanchart, C. and U. Kornak, *Ion channels and transporters in osteoclasts.* Archives of Biochemistry and Biophysics, 2008. **473**(2): p. 161-165.
57. Schachtner, H., et al., *Podosomes in adhesion, migration, mechanosensing and matrix remodeling.* Cytoskeleton, 2013. **70**(10): p. 572-589.
58. Zhao, H., O. Ettala, and H.K. Väänänen, *Intracellular membrane trafficking pathways in bone-resorbing osteoclasts revealed by cloning and subcellular localization studies of small GTP-binding rab proteins.* Biochemical and Biophysical Research Communications, 2002. **293**(3): p. 1060-1065.
59. Ng, P.Y., et al., *Disruption of the dynein-dynactin complex unveils motor-specific functions in osteoclast formation and bone resorption.* Journal of Bone and Mineral Research, 2013. **28**(1): p. 119-134.
60. Peruzzi, B. and A. Teti, *The Physiology and Pathophysiology of the Osteoclast.* Clinical Reviews in Bone and Mineral Metabolism, 2012. **10**(2): p. 71-97.
61. Hirvonen, M.J., et al., *Novel perspectives on the transcytotic route in osteoclasts.* BoneKEy reports., 2013. **2**: p. 306.
62. Saltel, F., et al., *Actin cytoskeletal organisation in osteoclasts: a model to decipher transmigration and matrix degradation.* European journal of cell biology., 2008. **87**(8-9): p. 459-468.
63. Lee, S.-H., et al., *v-ATPase V0 subunit d2-deficient mice exhibit impaired osteoclast fusion and increased bone formation.* Nature medicine., 2006. **12**(12): p. 1403-1409.
64. Leisle, L., et al., *ClC-7 is a slowly voltage-gated 2Cl(-)/1H(+)-exchanger and requires Ostm1 for transport activity.* EMBO J, 2011. **30**(11): p. 2140-52.
65. Coury, F., et al., *SLC4A2-mediated Cl-/HCO3- exchange activity is essential for calpain-dependent regulation of the actin cytoskeleton in osteoclasts.* Proc Natl Acad Sci U S A, 2013. **110**(6): p. 2163-8.
66. Tabata, K., et al., *Rubicon and PLEKHM1 negatively regulate the endocytic/autophagic pathway via a novel Rab7-binding domain.* Mol Biol Cell, 2010. **21**(23): p. 4162-72.

67. Ye, S., et al., *LIS1 Regulates Osteoclast Formation and Function through Its Interactions with Dynein/Dynactin and Plekhm1.* PLOS ONE, 2011. **6**(11): p. e27285.
68. Worby, C.A. and J.E. Dixon, *Sorting out the cellular functions of sorting nexins.* Nat Rev Mol Cell Biol, 2002. **3**(12): p. 919-31.
69. Zhou, C., et al., *SNX10 Plays a Critical Role in MMP9 Secretion via JNK-p38-ERK Signaling Pathway.* J Cell Biochem, 2017. **118**(12): p. 4664-4671.
70. Penna, S., et al., *One Disease, Many Genes: Implications for the Treatment of Osteopetroses.* Front Endocrinol (Lausanne), 2019. **10**: p. 85.
71. Sobacchi, C., et al., *Osteopetrosis: genetics, treatment and new insights into osteoclast function.* Nat Rev Endocrinol, 2013. **9**(9): p. 522-36.
72. Lu, J., et al., *Advances in the discovery of cathepsin K inhibitors on bone resorption.* Journal of enzyme inhibition and medicinal chemistry., 2018. **33**(1): p. 890-904.
73. Patlaka, C., et al., *The growth factor-like adipokine tartrate-resistant acid phosphatase 5a interacts with the rod G3 domain of adipocyte-produced nidogen-2.* Biochem Biophys Res Commun, 2014. **454**(3): p. 446-52.
74. Mosig, R.A., et al., *Loss of MMP-2 disrupts skeletal and craniofacial development and results in decreased bone mineralization, joint erosion and defects in osteoblast and osteoclast growth.* Human Molecular Genetics, 2007. **16**(9): p. 1113-1123.
75. Okada, Y., et al., *Localization of matrix metalloproteinase 9 (92-kilodalton gelatinase/type IV collagenase = gelatinase B) in osteoclasts: implications for bone resorption.* Lab Invest, 1995. **72**(3): p. 311-22.
76. Nakamura, H., et al., *Immunolocalization of matrix metalloproteinase-13 on bone surface under osteoclasts in rat tibia.* Bone, 2004. **34**(1): p. 48-56.
77. Boyce, B.F., *Advances in the regulation of osteoclasts and osteoclast functions.* J Dent Res, 2013. **92**(10): p. 860-7.
78. Teti, A., *Mechanisms of osteoclast-dependent bone formation.* Bonekey Rep, 2013. **2**: p. 449.
79. Kovesdy, C.P. and L.D. Quarles, *Fibroblast growth factor-23: what we know, what we don't know, and what we need to know.*

Nephrology Dialysis Transplantation, 2013. **28**(9): p. 2228-2236.
80. Goltzman, D., M. Mannstadt, and C. Marcocci, *Physiology of the Calcium-Parathyroid Hormone-Vitamin D Axis.* Frontiers of Hormone Research, 2017. **50**: p. 1-13.
81. Danks, L. and H. Takayanagi, *Immunology and bone.* The Journal of Biochemistry, 2013. **154**(1): p. 29-39.
82. Nemeth, K., et al., *The role of osteoclast-associated receptor in osteoimmunology.* J Immunol, 2011. **186**(1): p. 13-8.
83. Sato, K., et al., *Th17 functions as an osteoclastogenic helper T cell subset that links T cell activation and bone destruction.* J Exp Med, 2006. **203**(12): p. 2673-82.
84. Ciucci, T., et al., *Bone marrow Th17 TNFα cells induce osteoclast differentiation, and link bone destruction to IBD.* Gut, 2015. **64**(7): p. 1072.
85. Li, H., et al., *Cross talk between the bone and immune systems: osteoclasts function as antigen-presenting cells and activate CD4+ and CD8+ T cells.* Blood, 2010. **116**(2): p. 210-217.
86. Porter, R.L. and L.M. Calvi, *Communications between bone cells and hematopoietic stem cells.* Archives of Biochemistry and Biophysics, 2008. **473**(2): p. 193-200.
87. Blin-Wakkach, C., M. Rouleau, and A. Wakkach, *Roles of osteoclasts in the control of medullary hematopoietic niches.* Arch Biochem Biophys, 2014. **561**: p. 29-37.
88. Ponzetti, M. and N. Rucci, *Updates on Osteoimmunology: What's New on the Cross-Talk Between Bone and Immune System.* Frontiers in Endocrinology, 2019. **10**(236).
89. Kollet, O., et al., *Osteoclasts degrade endosteal components and promote mobilization of hematopoietic progenitor cells.* Nature Medicine, 2006. **12**(6): p. 657-664.
90. Trebec-Reynolds, D.P., et al., *VEGF-A expression in osteoclasts is regulated by NF-kappaB induction of HIF-1alpha.* Journal of cellular biochemistry, 2010. **110**(2): p. 343-351.
91. Collin-Osdoby, P., et al., *Basic fibroblast growth factor stimulates osteoclast recruitment, development, and bone pit resorption in association with angiogenesis in vivo on the chick chorioallantoic membrane and activates isolated avian osteoclast resorption in vitro.* J Bone Miner Res, 2002. **17**(10): p. 1859-71.

92. Schönberg, A., *Rontgenbilder einer seltenen Knockener-krankung*, in *Munch Med Wochenschr*. 1904. p. 365-368.
93. Tolar, J., S.L. Teitelbaum, and P.J. Orchard, *Osteopetrosis.* N Engl J Med, 2004. **351**(27): p. 2839-49.
94. Wu, C.C., et al., *Diagnosis and Management of Osteopetrosis: Consensus Guidelines From the Osteopetrosis Working Group.* J Clin Endocrinol Metab, 2017. **102**(9): p. 3111-3123.
95. Sobacchi, C., et al., *CLCN7-Related Osteopetrosis*, M.P. Adam, et al., Editors. 1993, GeneReviews is a registered trademark of the University of Washington, Seattle. All rights reserved.
96. Döffinger, R., et al., *X-linked anhidrotic ectodermal dysplasia with immunodeficiency is caused by impaired NF-kappaB signaling.* Nat Genet, 2001. **27**(3): p. 277-85.
97. Dupuis-Girod, S., et al., *Osteopetrosis, lymphedema, anhidrotic ectodermal dysplasia, and immunodeficiency in a boy and incontinentia pigmenti in his mother.* Pediatrics, 2002. **109**(6): p. e97.
98. Roberts, C.M., et al., *A novel NEMO gene mutation causing osteopetrosis, lymphoedema, hypohidrotic ectodermal dysplasia and immunodeficiency (OL-HED-ID).* Eur J Pediatr, 2010. **169**(11): p. 1403-7.
99. Carlberg, V.M., et al., *Hypohidrotic ectodermal dysplasia, osteopetrosis, lymphedema, and immunodeficiency in an infant with multiple opportunistic infections.* Pediatr Dermatol, 2014. **31**(6): p. 716-21.
100. Miot, C., et al., *Hematopoietic stem cell transplantation in 29 patients hemizygous for hypomorphic IKBKG/NEMO mutations.* Blood, 2017. **130**(12): p. 1456-1467.
101. Palagano, E., et al., *Genetics of Osteopetrosis.* Curr Osteoporos Rep, 2018. **16**(1): p. 13-25.
102. Natsheh, J., et al., *Improved Outcomes of Hematopoietic Stem Cell Transplantation in Patients With Infantile Malignant Osteopetrosis Using Fludarabine-Based Conditioning.* Pediatr Blood Cancer, 2016. **63**(3): p. 535-40.
103. Frattini, A., et al., *Defects in TCIRG1 subunit of the vacuolar proton pump are responsible for a subset of human autosomal recessive osteopetrosis.* Nat Genet, 2000. **25**(3): p. 343-6.
104. Nakamura, I., et al., *Lack of vacuolar proton ATPase association with the cytoskeleton in osteoclasts of osteosclerotic (oc/oc) mice.* FEBS Letters, 1997. **401**(2-3): p. 207-212.

105. Del Fattore, A., et al., *Clinical, genetic, and cellular analysis of 49 osteopetrotic patients: implications for diagnosis and treatment.* J Med Genet, 2006. **43**(4): p. 315-25.
106. Schinke, T., et al., *Impaired gastric acidification negatively affects calcium homeostasis and bone mass.* Nat Med, 2009. **15**(6): p. 674-81.
107. Scimeca, J.C., et al., *The gene encoding the mouse homologue of the human osteoclast-specific 116-kDa V-ATPase subunit bears a deletion in osteosclerotic (oc/oc) mutants.* Bone : official journal of the international and mineral society, 2000. **26**(3): p. 207-213.
108. Blin-Wakkach, C., et al., *Hematological defects in the oc/oc mouse, a model of infantile malignant osteopetrosis.* Leukemia, 2004. **18**(9): p. 1505-11.
109. Kornak, U., et al., *Loss of the ClC-7 chloride channel leads to osteopetrosis in mice and man.* Cell, 2001. **104**(2): p. 205-15.
110. Novarino, G., et al., *Endosomal Chloride-Proton Exchange Rather Than Chloride Conductance Is Crucial for Renal Endocytosis.* Science, 2010. **328**(5984): p. 1398.
111. Sobacchi, C., et al., *CLCN7-Related Osteopetrosis*, in *GeneReviews(®)*, M.P. Adam, et al., Editors. 2007, University of Washington, Seattle

112. Pangrazio, A., et al., *Molecular and clinical heterogeneity in CLCN7-dependent osteopetrosis: report of 20 novel mutations.* Hum Mutat, 2010. **31**(1): p. E1071-80.
113. Howaldt, A., et al., *Sclerosing bone dysplasias with hallmarks of dysosteosclerosis in four patients carrying mutations in SLC29A3 and TCIRG1.* Bone, 2019. **120**: p. 495-503.
114. Sobacchi, C., et al., *As little as needed: the extraordinary case of a mild recessive osteopetrosis owing to a novel splicing hypomorphic mutation in the TCIRG1 gene.* J Bone Miner Res, 2014. **29**(7): p. 1646-50.
115. Lange, P.F., et al., *ClC-7 requires Ostm1 as a beta-subunit to support bone resorption and lysosomal function.* Nature, 2006. **440**(7081): p. 220-3.
116. Teti, A. and M.J. Econs, *Osteopetroses, emphasizing potential approaches to treatment.* Bone, 2017. **102**: p. 50-59.

117. Fischer, T., et al., *Promotion of Gαi3 subunit down-regulation by GIPN, a putative E3 ubiquitin ligase that interacts with RGS-GAIP.* Proceedings of the National Academy of Sciences, 2003. **100**(14): p. 8270.
118. Feigin, M.E. and C.C. Malbon, *OSTM1 regulates β-catenin/Lef1 interaction and is required for Wnt/β-catenin signaling.* Cellular Signalling, 2008. **20**(5): p. 949-957.
119. Ott, C.E., et al., *Severe neuronopathic autosomal recessive osteopetrosis due to homozygous deletions affecting OSTM1.* Bone, 2013. **55**(2): p. 292-7.
120. Zhu, C.H., L.R. Morse, and R.A. Battaglino, *SNX10 is required for osteoclast formation and resorption activity.* J Cell Biochem, 2012. **113**(5): p. 1608-15.
121. Pangrazio, A., et al., *SNX10 mutations define a subgroup of human autosomal recessive osteopetrosis with variable clinical severity.* J Bone Miner Res, 2013. **28**(5): p. 1041-9.
122. Aker, M., et al., *An SNX10 mutation causes malignant osteopetrosis of infancy.* J Med Genet, 2012. **49**(4): p. 221-6.
123. Stattin, E.L., et al., *SNX10 gene mutation leading to osteopetrosis with dysfunctional osteoclasts.* Sci Rep, 2017. **7**(1): p. 3012.
124. Alsharidi, A., M. Al-Hamed, and A. Alsuwaida, *Carbonic anhydrase II deficiency: report of a novel mutation.* CEN Case Rep, 2016. **5**(1): p. 108-112.
125. Stark, Z. and R. Savarirayan, *Osteopetrosis.* Orphanet J Rare Dis, 2009. **4**: p. 5.
126. Van Wesenbeeck, L., et al., *Involvement of PLEKHM1 in osteoclastic vesicular transport and osteopetrosis in incisors absent rats and humans.* J Clin Invest, 2007. **117**(4): p. 919-30.
127. Fujiwara, T., et al., *PLEKHM1/DEF8/RAB7 complex regulates lysosome positioning and bone homeostasis.* JCI Insight, 2016. **1**(17): p. e86330.
128. Palagano, E., et al., *Hematopoietic stem cell transplantation corrects osteopetrosis in a child carrying a novel homozygous mutation in the FERMT3 gene.* Bone, 2017. **97**: p. 126-129.
129. Moser, M., et al., *Kindlin-3 is essential for integrin activation and platelet aggregation.* Nat Med, 2008. **14**(3): p. 325-30.
130. Iida, A., et al., *Identification of biallelic LRRK1 mutations in osteosclerotic metaphyseal dysplasia and evidence for locus heterogeneity.* J Med Genet, 2016. **53**(8): p. 568-74.

131. Howaldt, A., et al., *Adult osteosclerotic metaphyseal dysplasia with progressive osteonecrosis of the jaws and abnormal bone resorption pattern due to a LRRK1 splice site mutation.* J Bone Miner Res, 2020.
132. Xing, W.R., et al., *Role and mechanism of action of leucine-rich repeat kinase 1 in bone.* Bone Res, 2017. **5**: p. 17003.
133. Lu, S.-Y., M. Li, and Y.-L. Lin, *Mitf regulates osteoclastogenesis by modulating NFATc1 activity.* Experimental Cell Research, 2014. **328**(1): p. 32-43.
134. George, A., et al., *Biallelic Mutations in MITF Cause Coloboma, Osteopetrosis, Microphthalmia, Macrocephaly, Albinism, and Deafness.* Am J Hum Genet, 2016. **99**(6): p. 1388-1394.
135. Pangrazio, A., et al., *RANK-dependent autosomal recessive osteopetrosis: characterization of five new cases with novel mutations.* J Bone Miner Res, 2012. **27**(2): p. 342-51.
136. Lo Iacono, N., et al., *RANKL cytokine: from pioneer of the osteoimmunology era to cure for a rare disease.* Clin Dev Immunol, 2013. **2013**: p. 412768.
137. Leibbrandt, A. and J.M. Penninger, *RANK/RANKL: Regulators of Immune Responses and Bone Physiology.* Annals of the New York Academy of Sciences, 2008. **1143**(1): p. 123-150.
138. Sobacchi, C., et al., *Osteoclast-poor human osteopetrosis due to mutations in the gene encoding RANKL.* Nat Genet, 2007. **39**(8): p. 960-2.
139. Guerrini, M.M., et al., *Human osteoclast-poor osteopetrosis with hypogammaglobulinemia due to TNFRSF11A (RANK) mutations.* Am J Hum Genet, 2008. **83**(1): p. 64-76.
140. Campeau, P.M., et al., *Whole-exome sequencing identifies mutations in the nucleoside transporter gene SLC29A3 in dysosteosclerosis, a form of osteopetrosis.* Hum Mol Genet, 2012. **21**(22): p. 4904-9.
141. Guo, L., et al., *Dysosteosclerosis is also caused by TNFRSF11A mutation.* J Hum Genet, 2018. **63**(6): p. 769-774.
142. Weisz Hubshman, M., et al., *Homozygous deletion of RAG1, RAG2 and 5' region TRAF6 causes severe immune suppression and atypical osteopetrosis.* Clin Genet, 2017. **91**(6): p. 902-907.
143. Monies, D., et al., *Autozygosity reveals recessive mutations and novel mechanisms in dominant genes: implications in variant interpretation.* Genet Med, 2017. **19**(10): p. 1144-1150.

144. Frattini, A., et al., *Chloride channel ClCN7 mutations are responsible for severe recessive, dominant, and intermediate osteopetrosis.* J Bone Miner Res, 2003. **18**(10): p. 1740-7.
145. Bollerslev, J., et al., *Autosomal dominant osteopetrosis revisited: lessons from recent studies.* Eur J Endocrinol, 2013. **169**(2): p. R39-57.
146. Pang, Q., et al., *Novel mutations of CLCN7 cause autosomal dominant osteopetrosis type II (ADO-II) and intermediate autosomal recessive osteopetrosis (IARO) in Chinese patients.* Osteoporos Int, 2016. **27**(3): p. 1047-1055.
147. Waguespack, S.G., et al., *Autosomal dominant osteopetrosis: clinical severity and natural history of 94 subjects with a chloride channel 7 gene mutation.* J Clin Endocrinol Metab, 2007. **92**(3): p. 771-8.
148. Carlberg, V.M., et al., *Hypohidrotic Ectodermal Dysplasia, Osteopetrosis, Lymphedema, and Immunodeficiency in an Infant with Multiple Opportunistic Infections.* Pediatric Dermatology, 2013. **31**(6): p. 716-721.
149. Steward, C.G., *Hematopoietic stem cell transplantation for osteopetrosis.* Pediatr Clin North Am, 2010. **57**(1): p. 171-80.
150. Orchard, P.J., et al., *Hematopoietic stem cell transplantation for infantile osteopetrosis.* Blood, 2015. **126**(2): p. 270-6.
151. Stepensky, P., et al., *Stem cell transplantation for osteopetrosis in patients beyond the age of 5 years.* Blood Adv, 2019. **3**(6): p. 862-868.
152. Schulz, A.S., et al., *Osteopetrosis. Consensus guidelines for diagnosis, therapy and follow-up*. 2015, ESID and the EBMT WP Inborn Errors.
153. Tsuji, Y., et al., *Successful nonmyeloablative cord blood transplantation for an infant with malignant infantile osteopetrosis.* J Pediatr Hematol Oncol, 2005. **27**(9): p. 495-8.
154. Jaing, T.H., et al., *Successful unrelated cord blood transplantation in a girl with malignant infantile osteopetrosis.* Chin Med J (Engl), 2008. **121**(13): p. 1245-6.
155. Chiesa, R., et al., *Outcomes after Unrelated Umbilical Cord Blood Transplantation for Children with Osteopetrosis.* Biol Blood Marrow Transplant, 2016. **22**(11): p. 1997-2002.
156. Behfar, M., et al., *Non-total body irradiation myeloablative conditioning with intravenous busulfan and cyclophosphamide in hematopoietic stem cell transplantation for malignant*

*infantile osteopetrosis.* Pediatr Transplant, 2015. **19**(4): p. 422-7.
157. Porta, F., et al., *Partial depletion of TCR alpha/beta(+)/ CD19(+) cells in matched unrelated transplantation of three patients with osteopetrosis.* Bone Marrow Transplant, 2015. **50**(12): p. 1583-5.
158. Shadur, B., et al., *Successful hematopoietic stem cell transplantation for osteopetrosis using reduced intensity conditioning.* Pediatr Blood Cancer, 2018. **65**(6): p. e27010.
159. Fuchs, E.J., *Human leukocyte antigen-haploidentical stem cell transplantation using T-cell-replete bone marrow grafts.* Current opinion in hematology, 2012. **19**(6): p. 440-447.
160. Slatter, M.A., et al., *Treosulfan-based conditioning regimens for hematopoietic stem cell transplantation in children with primary immunodeficiency: United Kingdom experience.* Blood, 2011. **117**(16): p. 4367-4375.
161. Veys, P., *Reduced intensity transplantation for primary immunodeficiency disorders.* Pediatr Rep, 2011. **3 Suppl 2**(Suppl 2): p. e11.
162. Corbacioglu, S., et al., *Stem cell transplantation in children with infantile osteopetrosis is associated with a high incidence of VOD, which could be prevented with defibrotide.* Bone Marrow Transplant, 2006. **38**(8): p. 547-53.
163. Frattini, A., et al., *Rescue of ATPa3-deficient murine malignant osteopetrosis by hematopoietic stem cell transplantation in utero.* Proc Natl Acad Sci U S A, 2005. **102**(41): p. 14629-34.
164. Tondelli, B., et al., *Fetal liver cells transplanted in utero rescue the osteopetrotic phenotype in the oc/oc mouse.* Am J Pathol, 2009. **174**(3): p. 727-35.
165. Magnani, A., et al., *Successful in utero stem cell transplantation in X-linked severe combined immunodeficiency.* Blood advances, 2019. **3**(3): p. 237-241.
166. Steward, C.G., et al., *High peripheral blood progenitor cell counts enable autologous backup before stem cell transplantation for malignant infantile osteopetrosis.* Biol Blood Marrow Transplant, 2005. **11**(2): p. 115-21.
167. Sessa, M., et al., *Lentiviral haemopoietic stem-cell gene therapy in early-onset metachromatic leukodystrophy: an ad-hoc analysis of a non-randomised, open-label, phase 1/2 trial.* The Lancet, 2016. **388**(10043): p. 476-487.

168. Thrasher, A.J. and D.A. Williams, *Evolving Gene Therapy in Primary Immunodeficiency.* Molecular Therapy, 2017. **25**(5): p. 1132-1141.
169. Biffi, A., et al., *Gene therapy of metachromatic leukodystrophy reverses neurological damage and deficits in mice.* J Clin Invest, 2006. **116**(11): p. 3070-82.
170. Biffi, A., et al., *Lentiviral hematopoietic stem cell gene therapy benefits metachromatic leukodystrophy.* Science, 2013. **341**(6148): p. 1233158.
171. Hacein-Bey-Abina, S., et al., *A modified γ-retrovirus vector for X-linked severe combined immunodeficiency.* The New England journal of medicine, 2014. **371**(15): p. 1407-1417.
172. Löfvall, H., et al., *Hematopoietic Stem Cell-Targeted Neonatal Gene Therapy with a Clinically Applicable Lentiviral Vector Corrects Osteopetrosis in.* Hum Gene Ther, 2019. **30**(11): p. 1395-1404.
173. Moscatelli, I., et al., *Targeting NSG Mice Engrafting Cells with a Clinically Applicable Lentiviral Vector Corrects Osteoclasts in Infantile Malignant Osteopetrosis.* Hum Gene Ther, 2018. **29**(8): p. 938-949.
174. Lo Iacono, N., et al., *Osteopetrosis rescue upon RANKL administration to Rankl(-/-) mice: a new therapy for human RANKL-dependent ARO.* J Bone Miner Res, 2012. **27**(12): p. 2501-10.
175. Bianco, P. and P.G. Robey, *39 - Skeletal Stem Cells*, in *Handbook of Stem Cells*, R. Lanza, et al., Editors. 2004, Academic Press: Burlington. p. 415-424.
176. Cappariello, A., et al., *Biotechnological approach for systemic delivery of membrane Receptor Activator of NF-κB Ligand (RANKL) active domain into the circulation.* Biomaterials, 2015. **46**: p. 58-69.
177. Menale, C., et al., *Mesenchymal Stromal Cell-Seeded Biomimetic Scaffolds as a Factory of Soluble RANKL in Rankl-Deficient Osteopetrosis.* Stem Cells Transl Med, 2019. **8**(1): p. 22-34.
178. Capulli, M., et al., *Effective Small Interfering RNA Therapy to Treat CLCN7-dependent Autosomal Dominant Osteopetrosis Type 2.* Mol Ther Nucleic Acids, 2015. **4**: p. e248.
179. Maurizi, A., et al., *RNA interference therapy for autosomal dominant osteopetrosis type 2. Towards the preclinical development.* Bone, 2018. **110**: p. 343-354.

180. Maurizi, A., et al., *Extra-skeletal manifestations in mice affected by.* Bone Res, 2019. **7**: p. 17.
181. Platt, F.M., B. Boland, and A.C. van der Spoel, *The cell biology of disease: lysosomal storage disorders: the cellular impact of lysosomal dysfunction.* J Cell Biol, 2012. **199**(5): p. 723-34.
182. Parenti, G., G. Andria, and A. Ballabio, *Lysosomal storage diseases: from pathophysiology to therapy.* Annu Rev Med, 2015. **66**: p. 471-86.
183. Parenti, G., et al., *New strategies for the treatment of lysosomal storage diseases (review).* Int J Mol Med, 2013. **31**(1): p. 11-20.
184. James, R.A., et al., *Lysosomal storage disorders: A review of the musculoskeletal features.* J Paediatr Child Health, 2016. **52**(3): p. 262-71.
185. Oussoren, E., et al., *Bone, joint and tooth development in mucopolysaccharidoses: relevance to therapeutic options.* Biochim Biophys Acta, 2011. **1812**(11): p. 1542-56.
186. Coutinho, M.F., M.J. Prata, and S. Alves, *Mannose-6-phosphate pathway: a review on its role in lysosomal function and dysfunction.* Mol Genet Metab, 2012. **105**(4): p. 542-50.
187. Aldenhoven, M., et al., *Musculoskeletal manifestations of lysosomal storage disorders.* Ann Rheum Dis, 2009. **68**(11): p. 1659-65.
188. Grosse, S.D., et al., *Cognitive outcomes and age of detection of severe mucopolysaccharidosis type 1.* Genet Med, 2017. **19**(9): p. 975-982.
189. de Ru, M.H., et al., *Capturing phenotypic heterogeneity in MPS I: results of an international consensus procedure.* Orphanet journal of rare diseases., 2012. **7**: p. 22.
190. Scott, H.S., et al., *Chromosomal localization of the human alpha-L-iduronidase gene (IDUA) to 4p16.3.* Am J Hum Genet, 1990. **47**(5): p. 802-7.
191. Muenzer, J., et al., *Mucopolysaccharidosis I: management and treatment guidelines.* Pediatrics, 2009. **123**(1): p. 19-29.
192. Terlato, N.J. and G.F. Cox, *Can mucopolysaccharidosis type I disease severity be predicted based on a patient's genotype? A comprehensive review of the literature.* Genet Med, 2003. **5**(4): p. 286-94.
193. Parini, R., et al., *Open issues in Mucopolysaccharidosis type I-Hurler.* Orphanet J Rare Dis, 2017. **12**(1): p. 112.

194. Tomatsu, S., et al., *Neonatal cellular and gene therapies for mucopolysaccharidoses: the earlier the better?* J Inherit Metab Dis, 2016. **39**(2): p. 189-202.
195. Clarke, L.A., et al., *Biomarkers for the mucopolysaccharidoses: discovery and clinical utility.* Mol Genet Metab, 2012. **106**(4): p. 395-402.
196. Ashton, L.J., et al., *Immunoquantification and enzyme kinetics of alpha-L-iduronidase in cultured fibroblasts from normal controls and mucopolysaccharidosis type I patients.* Am J Hum Genet, 1992. **50**(4): p. 787-94.
197. Verma, J., et al., *Inherited Metabolic Disorders: Efficacy of Enzyme Assays on Dried Blood Spots for the Diagnosis of Lysosomal Storage Disorders.* JIMD Rep, 2017. **31**: p. 15-27.
198. Boelens, J.J., P.J. Orchard, and R.F. Wynn, *Transplantation in inborn errors of metabolism: current considerations and future perspectives.* British Journal of Haematology, 2014. **167**(3): p. 293-303.
199. Muenzer, J., *Early initiation of enzyme replacement therapy for the mucopolysaccharidoses.* Mol Genet Metab, 2014. **111**(2): p. 63-72.
200. Wynn, R.F., et al., *Use of enzyme replacement therapy (Laronidase) before hematopoietic stem cell transplantation for mucopolysaccharidosis I: experience in 18 patients.* J Pediatr, 2009. **154**(1): p. 135-9.
201. Hobbs, J.R., et al., *Reversal of clinical features of Hurler's disease and biochemical improvement after treatment by bone-marrow transplantation.* Lancet, 1981. **2**(8249): p. 709-12.
202. de Ru, M.H., et al., *Enzyme replacement therapy and/or hematopoietic stem cell transplantation at diagnosis in patients with mucopolysaccharidosis type I: results of a European consensus procedure.* Orphanet J Rare Dis, 2011. **6**: p. 55.
203. Aldenhoven, M., et al., *Hematopoietic cell transplantation for mucopolysaccharidosis patients is safe and effective: results after implementation of international guidelines.* Biol Blood Marrow Transplant, 2015. **21**(6): p. 1106-9.
204. Azario, I., et al., *Neonatal umbilical cord blood transplantation halts skeletal disease progression in the murine model of MPS-I.* Sci Rep, 2017. **7**(1): p. 9473.
205. Yasuda, E., et al., *Long-term follow-up of post hematopoietic stem cell transplantation for Hurler syndrome: clinical,*

*biochemical, and pathological improvements.* Mol Genet Metab Rep, 2015. **2**: p. 65-76.
206. Valayannopoulos, V. and F.A. Wijburg, *Therapy for the mucopolysaccharidoses.* Rheumatology (Oxford), 2011. **50 Suppl 5**: p. v49-59.
207. Boelens, J.J., et al., *Outcomes of hematopoietic stem cell transplantation for Hurler's syndrome in Europe: a risk factor analysis for graft failure.* Bone Marrow Transplant, 2007. **40**(3): p. 225-33.
208. Aldenhoven, M., et al., *Long-term outcome of Hurler syndrome patients after hematopoietic cell transplantation: an international multicenter study.* Blood, 2015. **125**(13): p. 2164-72.
209. Prasad, V.K. and J. Kurtzberg, *Cord blood and bone marrow transplantation in inherited metabolic diseases: scientific basis, current status and future directions.* British Journal of Haematology, 2010. **148**(3): p. 356-372.
210. Tolar, J., et al., *Combination of enzyme replacement and hematopoietic stem cell transplantation as therapy for Hurler syndrome.* Bone Marrow Transplant, 2008. **41**(6): p. 531-5.
211. Ghosh, A., et al., *Enzyme replacement therapy prior to haematopoietic stem cell transplantation in Mucopolysaccharidosis Type I: 10 year combined experience of 2 centres.* Mol Genet Metab, 2016. **117**(3): p. 373-7.
212. Valayannopoulos, V., et al., *Laronidase for cardiopulmonary disease in Hurler syndrome 12 years after bone marrow transplantation.* Pediatrics, 2010. **126**(5): p. e1242-7.
213. Haskins, M., *Gene therapy for lysosomal storage diseases (LSDs) in large animal models.* Ilar j, 2009. **50**(2): p. 112-21.
214. Biffi, A., *Hematopoietic Stem Cell Gene Therapy for Storage Disease: Current and New Indications.* Mol Ther, 2017. **25**(5): p. 1155-1162.
215. Visigalli, I., et al., *Gene therapy augments the efficacy of hematopoietic cell transplantation and fully corrects mucopolysaccharidosis type I phenotype in the mouse model.* Blood, 2010. **116**(24): p. 5130-9.
216. Visigalli, I., et al., *Preclinical Testing of the Safety and Tolerability of Lentiviral Vector-Mediated Above-Normal Alpha-L-Iduronidase Expression in Murine and Human Hematopoietic Cells Using Toxicology and Biodistribution*

*Good Laboratory Practice Studies.* Hum Gene Ther, 2016. **27**(10): p. 813-829.
217. Gentner, B., et al., *Extensive Metabolic Correction of Hurler Disease By Hematopoietic Stem Cell-Based Gene Therapy: Preliminary Results from a Phase I/II Trial.* Blood, 2019. **134**(Supplement_1): p. 607-607.

## Chapter 2

# Development of lentiviral vector gene therapy for the treatment of Autosomal Recessive Osteopetrosis

Sara Penna[1,2], Valentina Capo[2,5], Elena Draghici[2]; Lucia Sergi Sergi[2], Eleonora Palagano[3,4], Stefano Mantero[3,5], Elena Fontana[3,5], Andrea Cappelleri[6], Francesca Ficara[3,5], Cristina Sobacchi[3,5], Eugenio Scanziani[6], Thorsten Schinke[7], Bernhard Gentner[2], Anna Villa[2,5]

[1]University of Milano-Bicocca, School of Medicine and Surgery, Monza, Italy.
[2]San Raffaele Telethon Institute for Gene Therapy (SR-Tiget), Division of Regenerative Medicine, Stem Cells and Gene Therapy, San Raffaele Scientific Institute, Milan, Italy
[3]Humanitas Clinical and Research Center, Rozzano, Milan, Italy.
[4]Department of Medical Biotechnologies and Translational Medicine, University of Milan, Milan, Italy.
[5]Milan Unit, Istituto di Ricerca Genetica e Biomedica, Consiglio Nazionale delle Ricerche, Milan, Italy.
[6]Mouse & Animal Pathology Lab, Fondazione Filarete, Milan, Italy; Department of Veterinary Medicine, University of Milan, Milan, Italy
[7]Institut für Osteologie und Biomechanik, Hamburg, Germany.

**Abstract**

The *oc/oc* mouse, carrying a spontaneous deletion in *Tcirg1* gene, is the model of choice to study bone damage due to osteoclast dysfunction in autosomal recessive osteopetrosis (ARO), a severe inherited bone disorder. In humans, mutations in *TCIRG1* gene are the most frequent causes of ARO (55%). This disease causes high bone density and fragility, neurological defects due to cranial nerves compression and abnormal tooth eruption, being lethal in the first decade of life. Hematopoietic stem cell transplantation (HSCT) is the only therapeutic option. However, HSCT presents hard limitations due to the high incidence of adverse outcomes and the low availability of compatible donors. To overcome these issues, we designed and tested a gene therapy (GT) strategy on *oc/oc* mice to find an alternative cure for ARO. To this purpose, we developed a clinically-optimized lentiviral vector, driving *TCIRG1* expression under the control of the phosphoglycerate kinase promoter. *oc/oc* lineage negative cells were transduced and injected intra-liver into irradiated *oc/oc* newborn mice at two days of life. Untreated *oc/oc* mice usually have a life expectancy of two weeks; conversely, 6 out of 14 *oc/oc* GT mice survived long-term and were sacrificed 4 months after treatment, showing an improved lifespan, absence of circling behaviour and, in few cases, the eruption of the incisors. Of note, GT mice presented amelioration of bone architecture and reduced parathyroid hormone level in the serum. In parallel, we investigated the efficacy of plerixafor-based hematopoietic stem cell (HSC) mobilization from the limited and

fibrotic bone marrow niche of *oc/oc* mice observing an increased number of circulating hematopoietic stem and progenitor cells in the blood of treated mice. In conclusion, we proved the efficacy of GT in rescuing the severe phenotype of *oc/oc* murine model and the feasibility of plerixafor-based HSC mobilization as alternative method to obtain an adequate source of cells for autologous transplantation in ARO condition.

## Introduction

Autosomal recessive osteopetrosis (ARO) is an inherited bone disorder, characterized by a general increase of bone density resulting from a defect in osteoclast (OC) differentiation or function. Mutations in *TCIRG1* gene are the most frequent (55%) and cause the most severe form of ARO in humans. ARO patients are characterized by dense and brittle bones with dramatic fibrosis of the bone marrow (BM) cavity, severe anaemia, hepatosplenomegaly, macrocephaly, progressive deafness and blindness due to cranial nerves compression [1, 2]. *TCIRG1* gene encodes for the a3 subunit of the V0 complex of the ATPase proton pump, necessary for the acidification of the bone resorption lacunae and consequently for bone resorptive function of OCs [3]. Sequencing of the 5' end of the *TCIRG1* gene of *oc/oc* osteopetrotic mice showed a 1.6-kb deletion on chromosome 19, including the translation start site, which abolishes the physiologic transcription of the ATPase proton pump subunit [4, 5]. In *oc/oc* mouse, this mutation leads to the absence of the enzyme in the apical membranes of OCs impeding the resorptive function of these cells [4]. Thus, this mouse model closely resembles the human disease and is characterized by a life expectancy of 3 weeks and symptoms like growth retardation, failure of eruption of the incisors, clubbed feet, circling behaviour, generalized increase in skeletal density with absence of bone marrow (BM) cavities, hypocalcaemia and hyperparathyroidism. Moreover, in literature

are reported microscopic examination of the spleen and liver revealing areas of extensive extramedullary hemopoiesis [4-6].

HSCT is currently the only therapeutic option for ARO patients. However, many patients do not have a compatible donor or are not eligible for this cure due to the pre-existing symptoms. Despite recent advances in conditioning protocols, the transplant-related morbidity is still high [7, 8]. The risk of these complications increases with the patient's age, highlighting the importance to obtain an early diagnosis and to treat ARO patients in a short window of time after birth [2, 9].

Due to HSCT related risks, Steward and colleagues reported the collection of an autologous backup of BM hematopoietic stem cells (HSC) before transplantation, to be reinfused in case of graft failure [10]. Notably, in ARO condition, BM harvest is precluded by the dense bone sclerosis of BM cavity. On the other hand, these patients present a high frequency of circulating $CD34^+$ cells in their blood and this source has been exploited for autologous backup. The use of G-CSF-based HSC mobilization has been reported in the past on two patients with atypical osteopetrosis having a poor $CD34^+$ cell count in peripheral blood, to guarantee an adequate autologous backup before transplantation [10]. However, mobilization of osteopetrotic patients remains a strongly debated and poorly investigated approach, especially in severely affected ARO children. AMD3100 is a selective antagonist of chemokine stromal cell derived factor-1 (also known as CXCL12), probably involved in HSPC retention in BM, largely used before HSCT, or in the GT setting to obtain an adequate amount of CD34+ as

autologous cell source. Importantly, AMD3100 is able to bind CXCL12 receptor, CXCR4, resulting in HSC mobilization both in mice and in humans [11, 12].

Early attempts to cure the *oc/oc* mouse with total BM or splenic cells were unsuccessful [13]. However, a partial rescue of the phenotype has been obtained in later studies, thanks to the optimization of the HSCT procedure in terms of timing, cell dose, and irradiation level in *oc/oc* neonates [14]. Based on these results, Johansson et al. demonstrated that *oc/oc* phenotype can be rescued by gene therapy (GT) using a gammaretroviral vector-mediated gene transfer of mouse *Tcirg1* gene into mouse HSCs [15]. However, gammaretroviral vectors have been reported to cause insertional mutagenesis at transcription start sites with the related risk of the development of leukemia [16]. Recently, lentiviral vectors (LVs) definitely supplanted gammaretroviral vectors, resulting safer in successful GT studies [17-21]. Based on these evidences, we developed a clinically-optimized *TCIRG1*-expressing LV driven by the phosphoglycerate kinase (*PGK1*) promoter (LV PGK.TCIRG1) able to restore resorptive function of ARO patients derived OCs *in vitro* [22]. Similar results have been obtained by Richter's group, who designed a self-inactivating LV, suitable for clinical application, carrying the human *TCIRG1* gene under the control of elongation factor 1α short (EFS) promoter [23]. They confirmed the efficacy of this LV on *oc/oc* neonates, improving long-term survival and bone phenotype of GT treated mice [24].

In this study, we tested the efficacy of GT approach *in vivo*, transplanting *oc/oc* neonates with lineage negative ($Lin^-$) cells transduced with LV PGK.TCIRG1, already described in Capo et al. [22]. We also investigated the effect plerixafor-based HSC mobilization in *oc/oc* mice, which represents an instrumental model to study transplantation issues in pathological BM niche.

## Results

### *LV in vitro correction of oc/oc derived OCs*

We developed a GT strategy taking advantage of a clinically-optimized LV carrying *TCIRG1* gene under the control of phosphoglycerate kinase (*PGK1*) promoter (LV PGK.TCIRG1) (Figure 8a), that has been shown to correct bone resorptive function of ARO patients derived OCs *in vitro* [22]. First, we set up a protocol for the *in vitro* differentiation and correction of murine OCs, starting from splenic Lin- cells (Figure 8b). Since *oc/oc* mice show a severe osteopetrotic phenotype with a life expectancy of 3 weeks, splenocytes of 12-day-old *oc/oc* mice were used as Lin- source and transduced overnight with LVs. In order to reduce the total culture period, we adapted the transduction protocol, using only 1 hit of LV transduction. Lin- cells were cultured in presence of a cytokine cocktail, driving myeloid commitment and then OC differentiation. Cultures were performed on tissue-culture treated 96-well plates to evaluate osteoclastogenesis or on dentine slices to study bone resorption. *oc/oc* OCs normally differentiated into multinucleated TRAP positive cells independently of the transduction and comparably to WT control (Figure 8c, upper panel). As opposite to untransduced (UT) *oc/oc* OCs, transduced *oc/oc* OCs displayed the rescue of resorptive function, with some variability according to the VCN of OC precursors in liquid culture (15.85 ± 6.874 SEM) (Figure 8c).

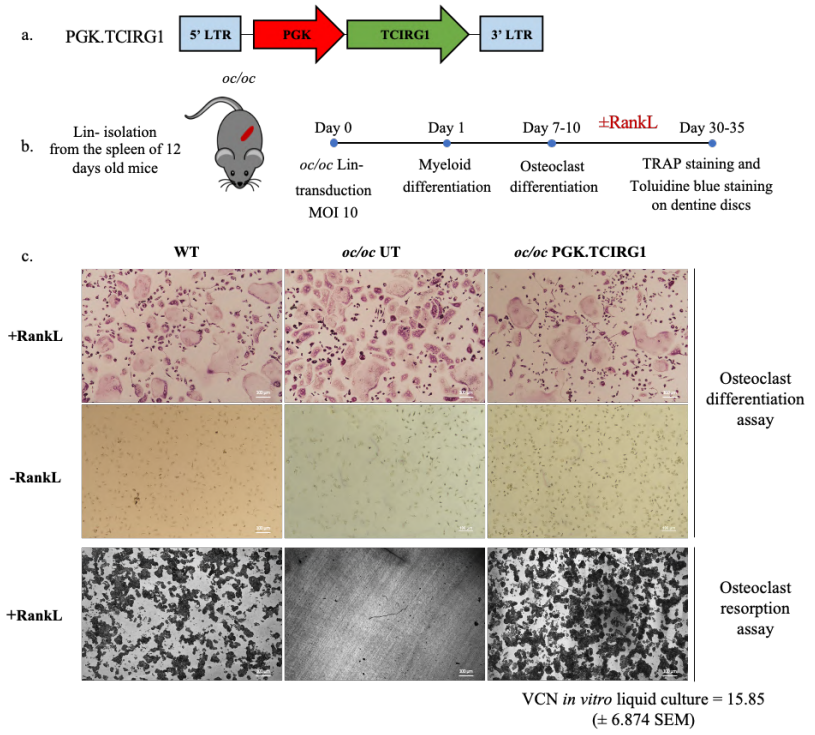


**Figure 8. LV *in vitro* correction of *oc/oc* derived OCs.** (a) The clinically-optimized LV PGK.TCIRG1 contains the human *TCIRG1* gene under the control of the phosphoglycerate kinase (PGK1) promoter, flanked by defective long terminal repeat elements (LTR). (b) The experimental strategy consists in the isolation of splenic lin- cells from 12 day-old pups, both *oc/oc* and WT as positive control. *oc/oc* lin- were transduced with LV PGK.TCIRG1 with a MOI of 10 and then differentiated toward myeloid lineage for 7-10 days. Once OC precursors were obtained, we started OC differentiation on plastic 96-well plates or on dentine slices to evaluate OC formation or bone resorption capacity respectively. (c) Representative picture of OC differentiated from WT, untransduced (UT) *oc/oc* and LV PGK.TCIRG1 transduced *oc/oc* Lin- cells, cultured in presence of RankL (upper row), essential cytokine for OC differentiation, or without RankL as negative control (middle row). OCs were stained for tartrate-resistant acid phosphatase (TRAP) activity.

The bottom of the panel shows representative picture of bone resorption assay performed on WT, UT *oc/oc* and LV PGK.TCIRG1 transduced *oc/oc* OCs cultured on dentine slices. Toluidine blue staining of dentine slices shows bone resorption pits in dark colour. The mean vector copy number (VCN) of transduced *oc/oc* myeloid precursors ± SEM is reported. Scale bar is reported in pictures. All images were acquired with Nikon ECLIPSE E600 microscope equipped with Nikon DS-Ri2 camera, using Plan Fluor 4x/0.13 objective and NIS-Elements F 4.30.01 software.

### *GT improves oc/oc mice survival and the osteopetrotic phenotype*

In order to improve the life expectancy and the clinical status of *oc/oc* mice, we tested our GT protocol *in vivo* on very young *oc/oc* pups (1-2 days old), since the timing of treatment is fundamental to restore bone phenotype, avoiding the occurrence of severe complications due to OC dysfunction that results in osteopetrosis already at 3-4 days of life (Figure 9).

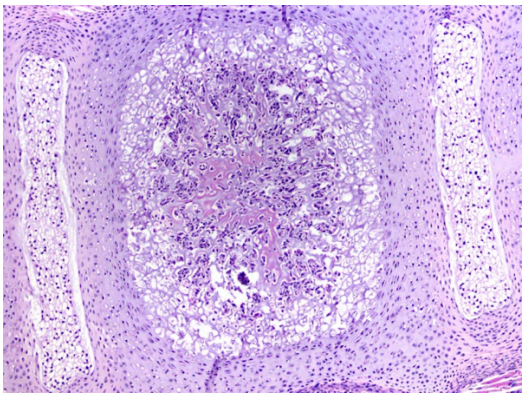

**Figure 9. Vertebral column histology of *oc/oc* pups.** Representative image of haematoxylin and eosin (H&E) staining of vertebral column section of 3 days old *oc/oc* newborn. Image was acquired with a magnification of 100X.

We decided to move to fetal liver as Lin- cell source, to obtain more *oc/oc* donors, avoiding perinatal loss which is especially frequent in *oc/oc* mice. Fetal liver Lin- cells are reported to be a good source of Lin- cells, comparable to BM derived cells [25]. Lin- cells were transduced with the 1-hit protocol, already tested in splenic Lin- cells for the *in vitro* studies. We transplanted transduced *oc/oc* Lin- cells, or WT Lin- cells as positive controls, by intrahepatic injection into irradiated *oc/oc* neonates (Figure 10a). GT mice were weaned at 18-20 days old and provided with fresh high calories gel food every two days to facilitate their autonomous feeding, in the absence of teeth. We followed GT mice overtime measuring the weight and observing their health status. Ten out of fourteen mice overcame the canonical period of mortality (3 weeks), and 6 of them reached the age of 4 months, which was set as the end point of the experiment (Figure 10b, Supplementary Table 1). In parallel, we transplanted untransduced WT Lin- cells in 15 *oc/oc* recipients, as positive control. Half of *oc/oc* mice transplanted with WT Lin- survived longer than 3 weeks, the expected lifespan of untreated *oc/oc* mice, and 4 mice were still alive 4 months after the transplant (Figure 10b). GT mice, comparably to WT Lin- transplanted mice, showed absence of circling behaviour and restored, though abnormal, eruption of the incisors (Figure 10c). However, they remained smaller than WT littermates and WT-transplanted controls in body weight and size (Figure 10c-e).

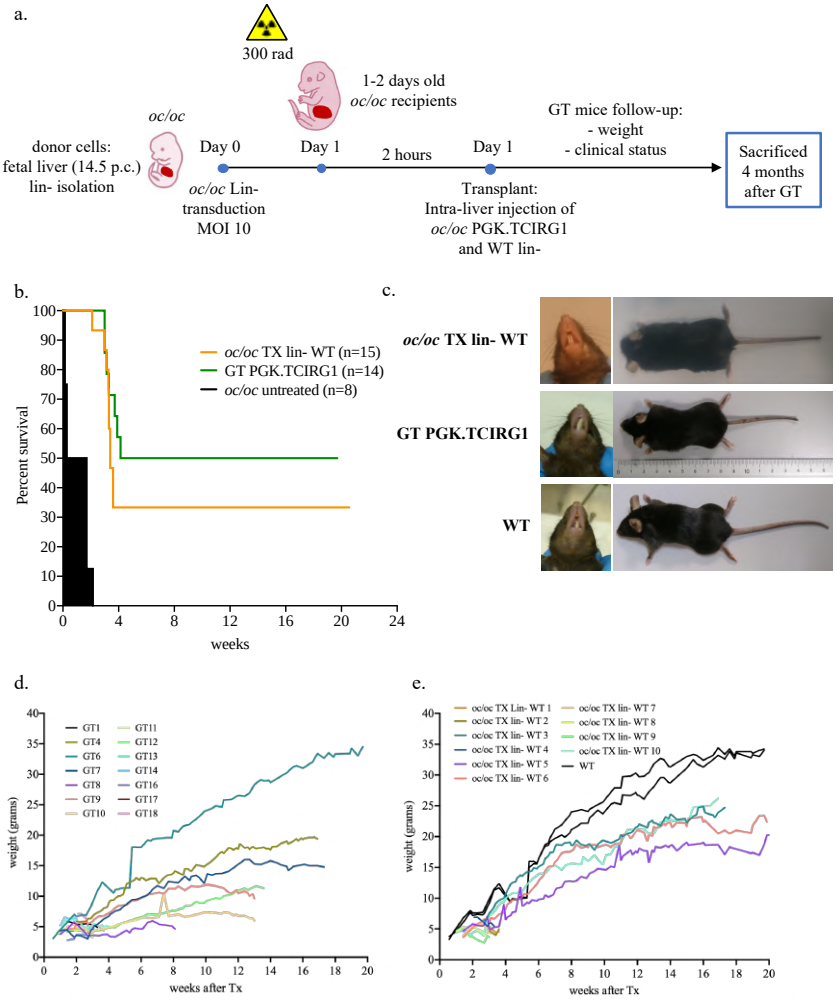


**Figure 10. *in vivo* GT of *oc/oc* mice.** (a) The GT protocol consists in the isolation of Lin- cells from 14.5 days post coitum *oc/oc* and WT fetal liver in parallel. *oc/oc* lin- were transduced with LV PGK.TCIRG1 with a MOI of 10 and then transplanted by intra-liver injection into 300 rad conditioned *oc/oc* recipients at 1 or 2 day of life. In parallel, we transplanted *oc/oc* neonates with WT Lin- cells as control group. Transplanted mice were followed overtime and daily weighed and controlled for their clinical status. For long-term surviving mice the sacrifice was set at 4 months after the transplant. (b) The Kaplan-Meier

curve shows the survival of GT mice (GT PGK.TCIRG1, n=14) compared to *oc/oc* transplanted with WT Lin- (*oc/oc* TX Lin- WT, n=15) and *oc/oc* UT mice (*oc/oc* untreated, n=8). (c) Representative pictures show tooth eruption and body size of GT mice compared to *oc/oc* transplanted with WT Lin- and WT littermates. (d) The graph shows the body weights of GT mice overtime. (e) The graph shows the body weights of *oc/oc* transplanted with WT Lin- and WT controls overtime (in black).

Despite the low VCN observed in all the analysed organs (BM, spleen and thymus) and in *ex vivo* methylcellulose cultures (Supplementary Table 1), we observed an increased cellularity of the BM of *oc/oc* GT mice similarly to WT littermates, as opposite to *oc/oc* UT mice in which BM cells are virtually absent due to bone fibrosis. Additionally, we observed lower spleen and thymus cells counts of GT mice than untreated WT controls (Figure 11a). These results were confirmed by the analysis of HSC colony-forming units grown in methylcellulose, in which we observed a normalization of BM colonies count in GT mice, comparable to WT controls. On the other hand, we observed a number of HSC colonies from the spleen of GT mice higher than colonies obtained from the spleens of WT transplanted mice or untreated WT controls thus suggesting the occurrence of extramedullary hematopoiesis, frequently observed in osteopetrosis (Figure 11b).

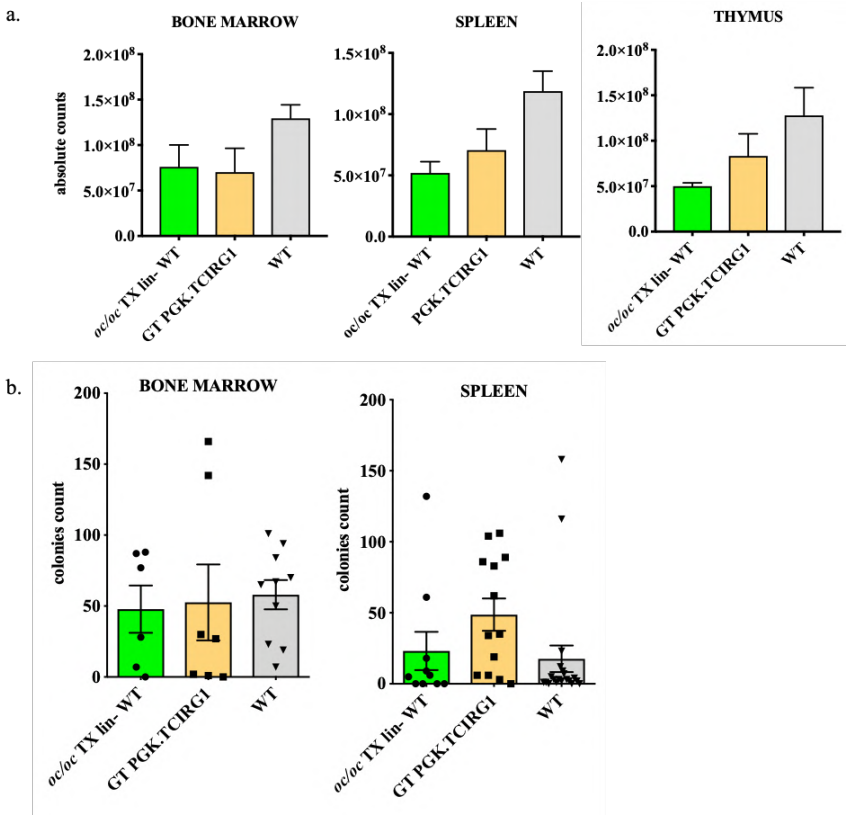


**Figure 11. BM, spleen and thymus cellularity and analysis of methylcellulose colony forming units.** (a) The graphs show absolute counts of BM (left), spleen (middle) and thymus (right) in GT mice (BM, n=7; spleen, n=9; thymus, n=8), *oc/oc* mice transplanted with WT Lin- (BM, n=10; spleen, n=10; thymus, n=3) and WT littermates (BM, n=11; spleen, n=11; thymus, n=7). (b) Graphs show absolute counts of total hematopoietic progenitor colonies obtained in methylcellulose cultures of the BM and spleen. Data show mean ± SEM.

Osteopetrotic phenotype includes metabolic defects related to calcium homeostasis, due to the absent bone resorptive activity of OCs. Parathyroid hormone (PTH), one of the major regulators of bone turnover, is dramatically increased in *oc/oc* mice due to a

compensatory mechanism aimed to increase free calcium concentration, boosting OCs bone resorption. Thus, in *oc/oc* mice hypocalcaemia is coupled with hyperparathyroidism [6]. To evaluate the correction of this symptom and to have an indirect indication of bone resorption *in vivo*, we measured level of PTH in the serum of GT mice by ELISA assay, and observed a decreased PTH concentration in the serum of GT4, GT6, GT7 compared to *oc/oc* UT, similarly to WT controls. However, GT8, GT9, GT10 and GT12 showed a high PTH concentration in the serum, despite their long survival and their good clinical status (Figure 12).

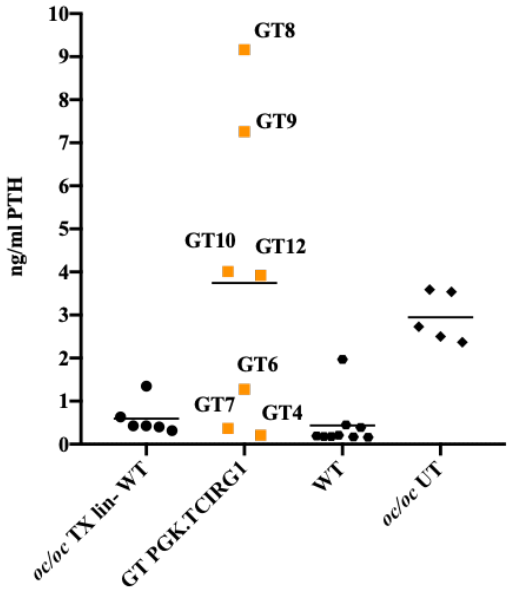


**Figure 12. Parathyroid hormone (PTH) level in the serum of GT mice.** PTH concentration (ng/ml) in the serum of indicated experimental groups. Each dot represents the mean of two technical replicates. oc/oc transplanted with WT Lin- (n=6), GT mice (n=7) and WT controls (n=9)

are adult mice (8-20 weeks of age). Serum samples of oc/oc UT controls (n=5) have been collected from mice of 2-3 weeks of age.

### *GT BM cells and splenocytes differentiate in functional OCs*

We harvested BM cells from WT, *oc/oc* mice transplanted with WT Lin- cells and GT mice at 8–20 weeks after transplantation. BM total cells were isolated by crashing bones and filtering cellular suspension. Then, cells were seeded and differentiated on tissue-culture treated 96-well plates to assess osteoclastogenesis by TRAP staining or on dentine slices to evaluate OCs function by toluidine blue staining. BM cells resulted inadequate for OC differentiation, probably due to the poor quality of cells suspension, rich of bone debris that preclude differentiation of OCs precursors (data not shown). Similarly, we could not observe OC differentiation from GT1 and GT8 BM cell suspension (Figure 13a). Toluidine blue staining of dentine slices revealed very few or absent resorption pits on most sample, except for GT4 and GT6 BM cells, that showed high number of OCs and resorption pits (Figure 13b).

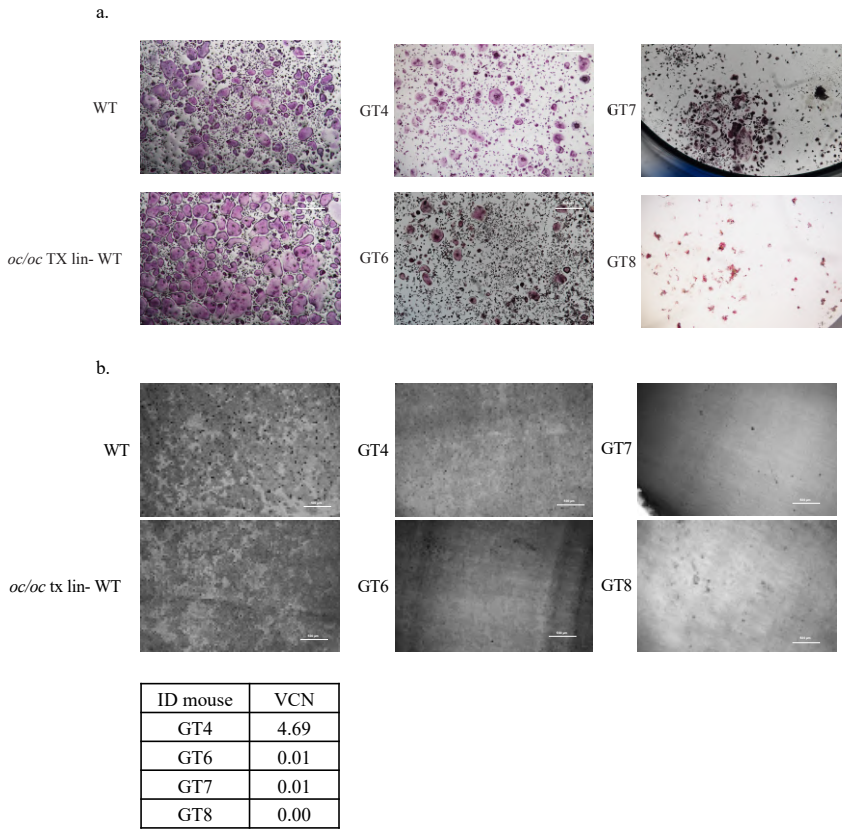


| ID mouse | VCN |
|---|---|
| GT4 | 4.69 |
| GT6 | 0.01 |
| GT7 | 0.01 |
| GT8 | 0.00 |

**Figure 13. Osteoclastogenesis and bone resorption assay of BM OCs precursors *ex vivo*.** (a) Representative pictures of tartrate-resistant acid phosphatase (TRAP) stained osteoclasts on plastic 96-well plates from the BM of GT mice, *oc/oc* mice transplanted with WT Lin- cells and and WT controls. (b) Representative pictures of resorption pits stained with toluidine blue, obtained after OC differentiation on dentine slice from the experimental groups indicated in panel a. Images were acquired with Nikon ECLIPSE E600 microscope equipped with Nikon DS-Ri2 camera, using Plan Fluor 4x/0.13 objective and NIS-Elements F 4.30.01 software. Table indicates vector copy numbers (VCN) of BM cells.

In parallel, we collected splenocytes that contain OC precursors and avoid the limitations of cell cultures due to the presence of bone debris. As expected, splenic OCs precursors isolated from *oc/oc* UT mice, normally differentiated into multinucleated TRAP positive OCs, comparably to all the other experimental groups (Figure 14a). As opposite, splenic *oc/oc* UT OCs were not able to resorb dentine slices, as shown by the absence of resorption pits (Figure 14b). Importantly, we observed resorption pits in OCs culture of GT4, GT6, GT8 and GT9, demonstrating the rescue of their OC function after GT. However, resorption pits were absent in GT7 and GT10 OC cultures, despite their long survival and good clinical status (Figure 14b).

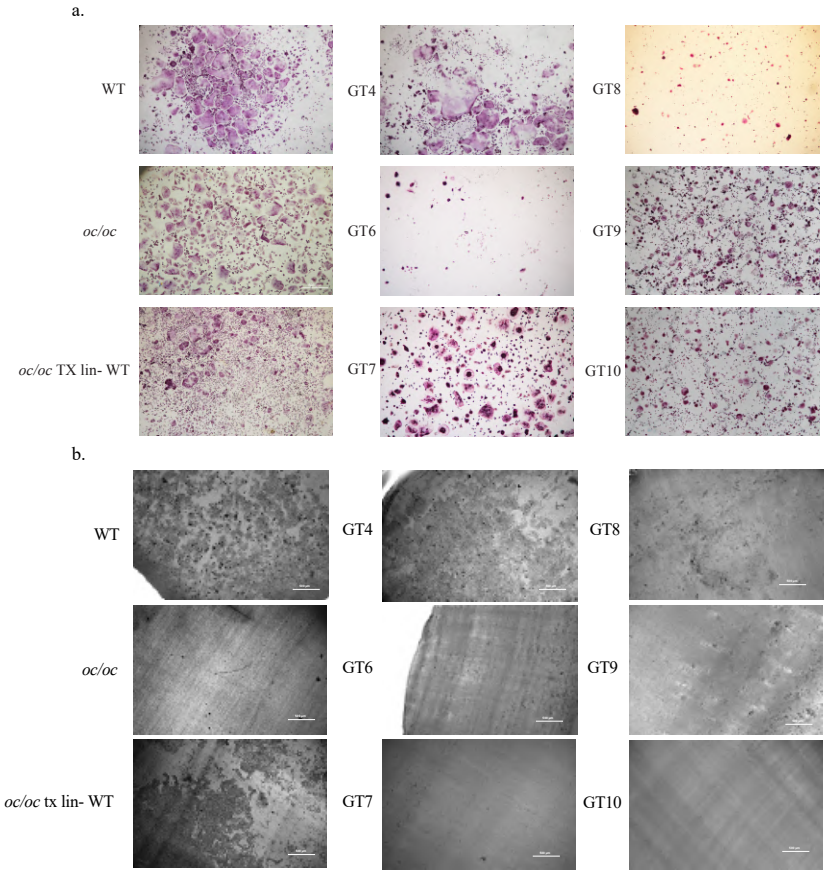


| ID mouse | VCN |
|---|---|
| GT4 | 4.11 |
| GT6 | 0.00 |
| GT7 | 0.01 |
| GT8 | 0.00 |
| GT9 | 0.00 |
| GT10 | 0.01 |

**Figure 14. Osteoclastogenesis and bone resorption assay of splenic OCs precursors *ex vivo*.** (a) Representative pictures of tartrate-resistant acid phosphatase (TRAP) stained osteoclasts (in purple) on plastic 96-well plates from the spleen of GT mice, *oc/oc* mice transplanted with WT Lin- cells and and WT controls. (b) Dentine slice, where splenic OC precursors were differentiated, stained with toluidine blue to highlight resorption pits (darker areas). Images were acquired with Nikon

ECLIPSE E600 microscope equipped with Nikon DS-Ri2 camera, using Plan Fluor 4x/0.13 objective and NIS-Elements F 4.30.01 software. Table indicates vector copy numbers (VCN) of total spleen cells.

### *GT ameliorates bone architecture of oc/oc treated mice*

Femurs and vertebral columns of GT mice were analysed by histology to evaluate the effect of GT on bone architecture. In particular, we performed haematoxylin and eosin staining of vertebral column sections of all experimental groups. *oc/oc* UT vertebrae were collected from 2-3 weeks old mice and appear completely fibrotic with no BM space. On the contrary, GT mice showed a variable reconstitution of physiological bone architecture, spanning from full rescue in GT4 and GT6 to dense bones and very small cluster of BM cells in GT1, GT7, GT9 and GT10 (Figure 15).

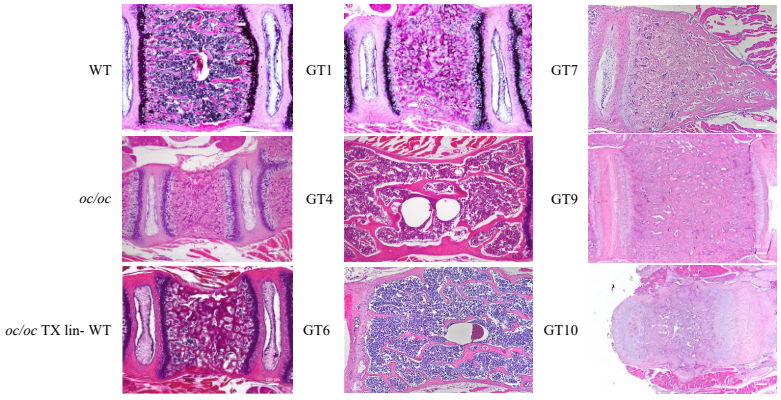


**Figure 15. Vertebral column histology.** Representative images of haematoxylin and eosin (H&E) staining of vertebral column section of GT, *oc/oc* UT, WT mice and *oc/oc* mice transplanted with WT Lin- cells. Samples of *oc/oc* transplanted with WT Lin- cells, GT mice and WT

controls have been obtained from adult mice (8-20 weeks of age), while *oc/oc* UT mice were 2-3 weeks old. Images were acquired with a 50X magnification.

To further dissect the bone architecture changes, femora sections were stained for TRAP. In particular, GT4 and GT6 mice showed TRAP positive bone-resorbing OCs in the growth plate, in cortical and trabecular bones, with absence of BM fibrosis. Conversely, GT1, GT7, GT9 and GT10 showed diffuse fibrosis of bones, which caused high non-specific TRAP signal (Figure 16).

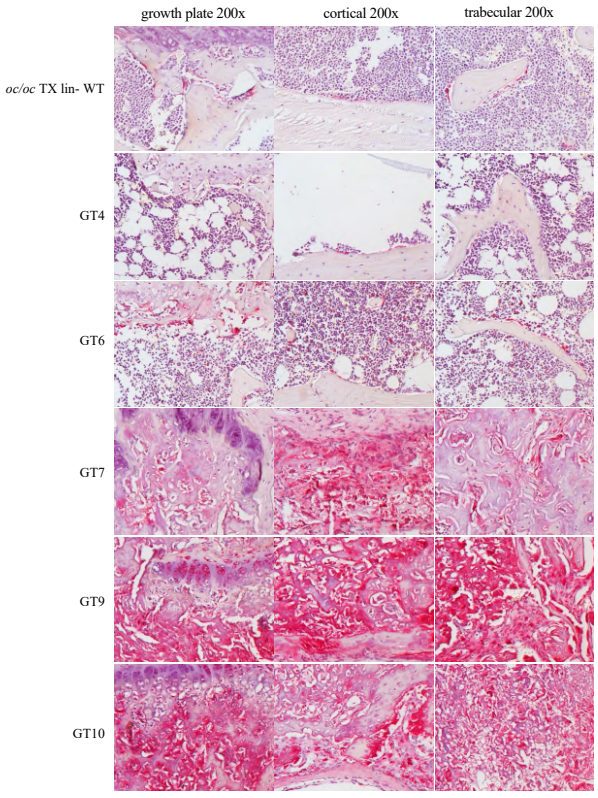


**Figure 16. Femora histology.** Images show TRAP staining of femora sections of GT mice (n=5) and *oc/oc* mice transplanted with WT Lin-

cells. Images have been obtained from adult mice (8-20 weeks of age). Images were acquired with a 200X magnification of the growth plate (left), in the cortical (middle) and in the trabecular (right) area of the bone.

Bone mineralization and architecture of the femora were also evaluated by microcomputed tomography (µCT) (Figure 17). Femora of GT4 and GT6 mice showed bone architecture and cortical thickness comparable to the WT control and to *oc/oc* mice transplanted with WT Lin-, suggesting a full reconstitution of the bone phenotype, coherently with histological results. As opposite, GT7, GT8, GT9 and GT10, despite the significant improvement of the lifespan, display a predominant cortical portion of the bone, typical sign of osteopetrosis (Figure 17). Of note, the femur of *oc/oc* UT control mouse was too small for µCT analysis, since only 2-3 weeks old mice could be analysed.

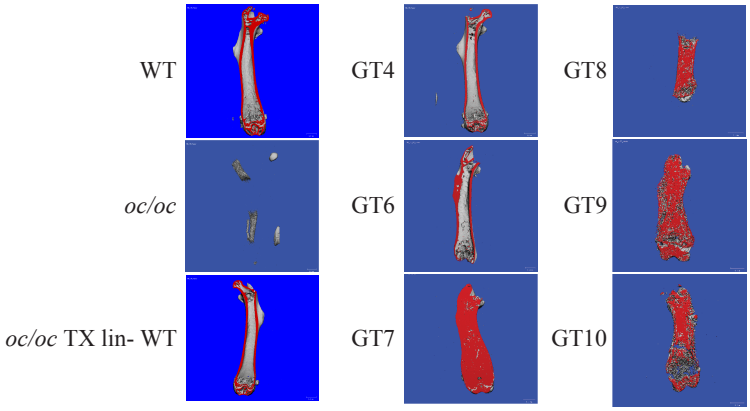


**Figure 17. Cortical and trabecular bone analysis in the femur using micro-computed tomography (µCT).** Representative images showing µCT scanning of the femur of adult GT mice compared to *oc/oc* mice

transplanted with WT Lin- cells and WT littermates. The cortical area of the bone is highlighted in red. Image of *oc/oc* have been obtained from a 2-3 weeks days old mouse, but the dimension is inadequate for µCT.

µCT analysis of the skull confirmed the eruption of the incisors in GT mice (except for GT7), which are typically absent in osteopetrotic *oc/oc* mice. We observed that the small size of the skull of GT8, GT9, GT10 and GT11 mice precludes the adequate scanning by µCT, resulting in the poor quality of the images (Figure 18).

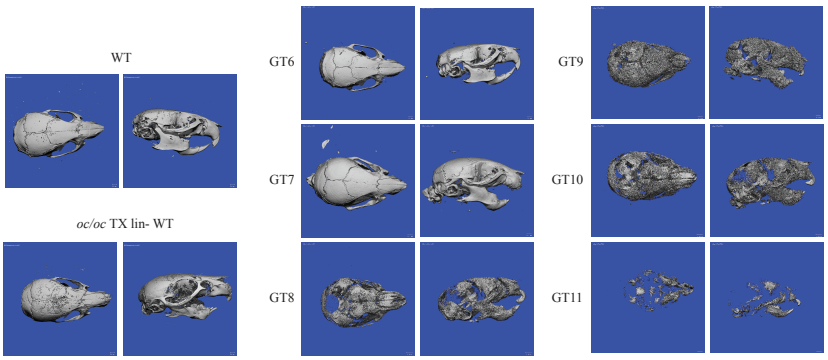


**Figure 18. micro-computed tomography (µCT) of the skull.** Representative images of the skull of adult GT mice compared to *oc/oc* mice transplanted with WT Lin- cells and WT littermates.

### *GT rescued the ratio of white and red pulp of the spleen of oc/oc mice*

*oc/oc* mice are characterized by increased extramedullary hematopoiesis, resulting in disbalanced white/red pulp ratio in the spleen. The majority of analysed GT mice displayed a normal distribution of white and red pulp in the spleen, comparable to

those observed in *oc/oc* transplanted with WT Lin- and WT controls (Figure 19). This result suggests that compensatory extramedullary hematopoiesis is limited, as a result of increased hematopoiesis in the BM.

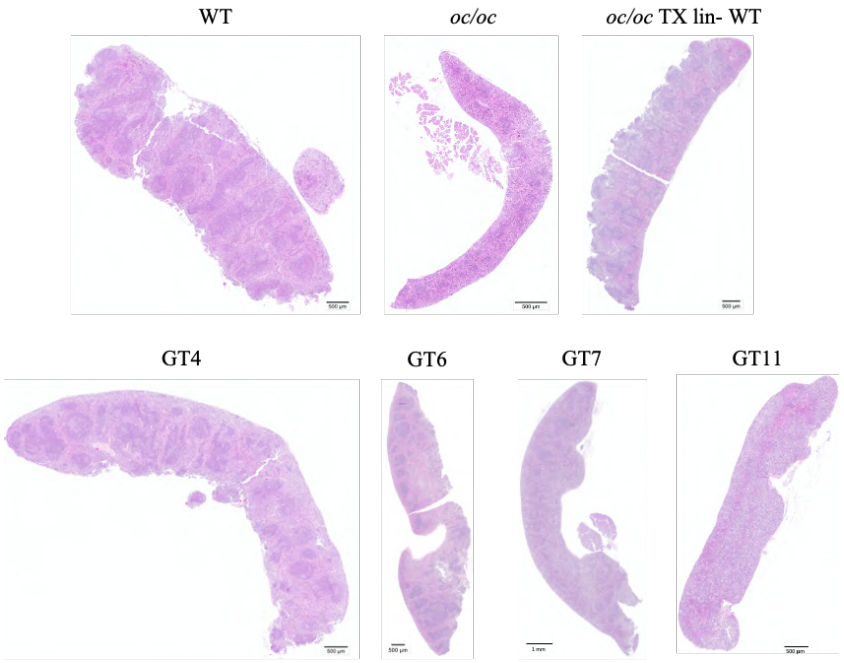


**Figure 19. Spleen histology.** Images show haematoxylin and eosin (H&E) staining of spleen sections of GT mice (n=4), WT mice, *oc/oc* mice transplanted with WT Lin- cells and *oc/oc* UT mice. Spleen samples of *oc/oc* transplanted with WT Lin- cells, GT mice and WT controls have been obtained from adult mice (8-20 weeks of age), while samples of *oc/oc* UT from 2-3 weeks old mice.

### *Feasibility of HSC mobilization in oc/oc mouse model*

HSC mobilization is an unexplored solution to overcome the impossibility of BM harvest in osteopetrosis, due to the characteristic fibrosis of the BM niche of ARO patients resulting

in increased frequency of circulating HSC in the PB. *oc/oc* mouse, which closely resembles the human disease, gave us the chance to investigate the effect of AMD3100 (Plerixafor)-based HSC mobilization on a pathological BM niche. In particular, we adapted a protocol reported in literature for adult mice [26] to *oc/oc* and WT pups at 3 and 7 days of life, to mimic the hypothetic therapeutic conditions of ARO patients. We injected subcutaneously 5 mg/kg of Plerixafor in *oc/oc* and WT pups and sacrificed them one hour after the injection, when the maximum rate of mobilization occurs. We collected whole blood samples and white blood cell count (WBC) was analysed by haemocytometer. We observed higher WBC count after Plerixafor injection in both *oc/oc* and WT mice at 7 days of life (Figure 20a). Higher number of circulating HSC was observed, as shown by colony forming unit assay in methylcellulose. The number of colonies was higher in blood samples of *oc/oc* and WT mice treated with Plerixafor at 7 days of life, compared to untreated controls (Figure 20b). Since mobilization induces HSPC egress from the hematopoietic niches, we performed methylcellulose culture of BM cells and splenocytes. Colony count tends to decrease in BM cells and splenocytes samples of both *oc/oc* and WT treated with plerixafor at 7 days of life, compared to untreated groups (Figure 20c). Since these data have been obtained on a limited number of mice, these experiments are still ongoing, and we plan to add 3 days old untreated *oc/oc* mice to these analysis as control group to evaluate the effect of plerixafor on 3 days old *oc/oc* pups. Thus, we can speculate that Plerixafor-based HSC mobilization induces the egress of HSC

from their hematopoietic niche and the increase of WBC counts in *oc/oc* pups at 7 of life, suggesting that this procedure is feasible also in the context of pathological BM fibrosis.

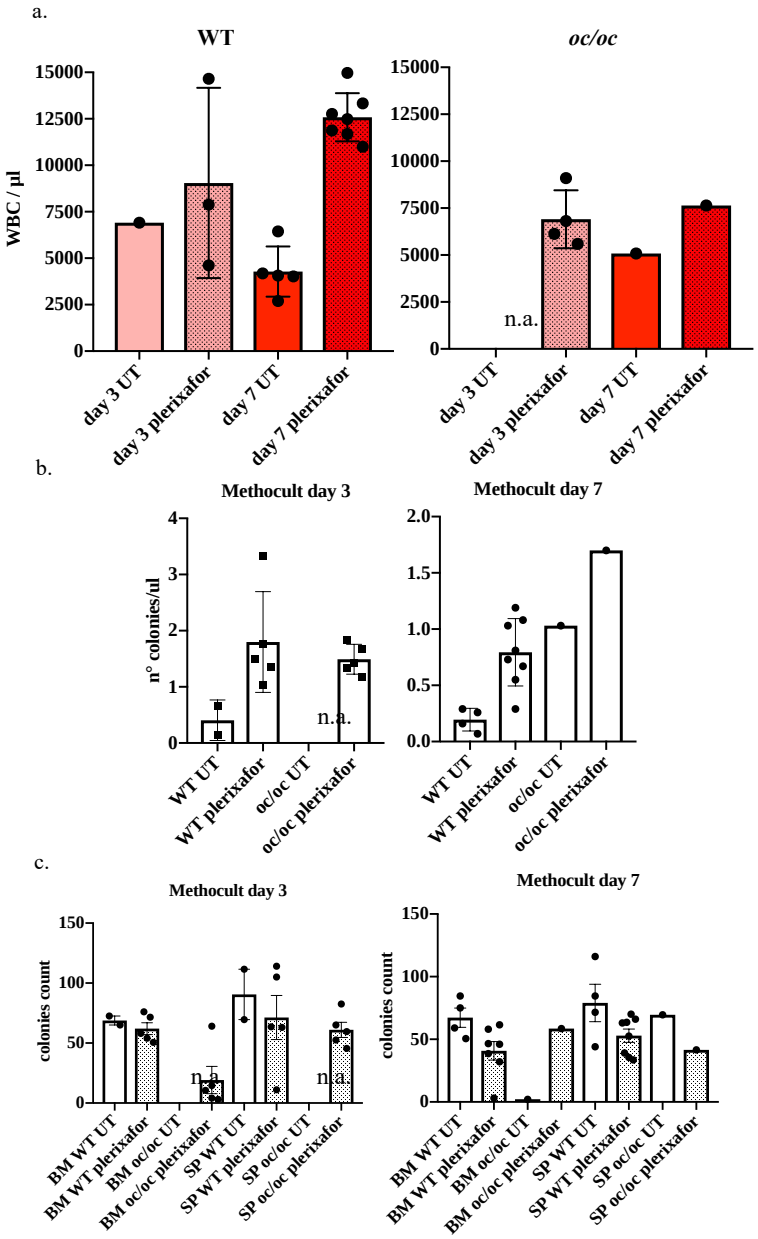

**Figure 20. Feasibility of Plerixafor-based HSC mobilization** (a) White blood cell (WBC) count/µl of WT (left) and *oc/oc* (right) pups untreated (UT) or subcutaneously injected with a dose of 5 mg/kg of Plerixafor (AMD3100) at 3 and 7 days of life (WT UT day3, n=1; WT plerixafor day3, n=3; WT UT day7, n=5; WT plerixafor day7, n=7; *oc/oc* UT day3, n=not available; *oc/oc* plerixafor day3, n=4; *oc/oc* UT day7, n=1; *oc/oc* plerixafor day7, n=1). Each dot represents a single mouse. (b) Graphs show counts of hematopoietic progenitor colonies obtained in methylcellulose cultures for each µl of whole blood. (c) Graphs show absolute counts of hematopoietic progenitor colonies obtained in methylcellulose cultures of the BM and spleen of *oc/oc* and WT pups untreated (UT) or treated with plerixafor at 3 and 7 days of life. Data show mean ± SEM.

## Methods

### *Mice*

Animal experimental procedures were approved by the Institutional Animal Care and Use Committee of San Raffaele Hospital and Italian Ministry of Health. C57Bl/6 wild-type (WT) mice were obtained from Charles River Laboratories (Calco, Italy). The knock-out *oc/oc* mouse (JAX strain no. 000230) colony was maintained on site in heterozygosis [4].

### *Mouse genotyping*

Mice were genotyped by PCR using DNA extracted from a tail biopsy. The PCR conditions for the *Tcirg1* mutation were: 95 °C for 5 min, then 40 cycles, 95 °C for 30 s, 60 °C for 30 s and 72 °C for 30 sec, then 72 °C for 5 min, with *oc/oc* forward primer 5′-GGCCTGGCTCTTCTGAAGCC-3′, *oc/oc* reverse primer 5′-CCGCTGCACTTCTTCCCGCA-3′, WT forward primer 5'-TCATGGGCTCTATGTTCCGG-3' and WT reverse primer 5'-GAAGGCGCTCACGGATTCGT-3'. WT mice present a PCR product of 431 bp, while *oc/oc* mice display a 563 bp PCR product. Heterozygous mice have both products.

### *Lentiviral vector (LV) production*

PGK.TCIRG1 lentiviral vector was produced as previously described [27], substituting the IDUA transgene with the TCIRG1 cDNA sequence (GeneArt Gene Synthesis, Thermo Fisher Scientific). Briefly, VSV-pseudotyped third-generation LVs were

produced by cotransfection of the transfer, packaging (pMD2.Lg/p.RRE and pRSV.Rev) and envelope constructs (pMD2.G) into 293T cells by a Ca3PO4 transfection. Supernatants were collected, passed through a 0.22μm filter, and purified by ultracentrifugation. Vector particles were measured by HIV-1 gag p24 antigen immunocapture (NEN Life Science Products, USA). Vector titer (transducing units/ml) was estimated by digital droplet PCR (ddPCR) on 293T cells, previously infected with different dilutions of concentrated vector supernatant.

***Lin- isolation and transduction***

10-12 days old donor WT and *oc/oc* mice were euthanized by decapitation and spleen was collected. Single cell suspension was obtained by smashing on 40μm mesh to collect splenocytes for Lineage-negative (Lin–) separation. Moreover, on embryonic day 14.5, pregnant mice were euthanized. Fetal livers (FLs) were dissected out of embryos and smashed to obtain a single-cell suspension. Individual FLs were genotyped by PCR of a small biopsy. Lin- cells were enriched from total splenocytes or FL cells with the Lineage Cell Depletion Kit and MS or LS columns (Miltenyi Biotec, Bergisch Gladbach, Germany), according to the manufacturer's instructions. *oc/oc* Lin– cells were transduced overnight with LVs at a multiplicity of infection (MOI) of 10 (vector titer 0.50–1.9 × $10^9$ transducing units per mL) in StemSpan SFEM medium (STEMCELL Technologies, Vancouver, British Columbia, Canada), 1% penicillin/streptomycin, 1% glutamine (Gibco, Carlsbad, Calif), and the following cytokines (PeproTech,

Rocky Hills, NJ): recombinant murine thromobopoietin (rmTPO), 20 ng/mL; recombinant murine stem cell factor (rmSCF), 50 ng/mL; recombinant human Fms-related tyrosine kinase 3 ligand (rhFLT3L), 10 ng/mL; recombinant human interleukin 3 (rmIL-3), 10 ng/mL; and recombinant human interleukin 6 (rhIL-6), 20 ng/ml. *oc/oc* transduced Lin- and WT Lin- were frozen alive in fetal bovine serum (FBS) (Euroclone, Milan, Italy) with 10% dimethyl sulfoxide (DMSO) and stored at -80°C.

***oc/oc mice transplantation***

Recipient 1-2 day-old *oc/oc* mice were conditioned by sublethal total-body irradiation (300 rad) at least 2 hours before transplantation. Then, they were injected intra-hepatically with freshly thawed 0.66-1.4 × $10^6$ Lin– cells (*oc/oc* Lin- transduced with LV PGK.TCIRG1 or WT Lin-). Gentamicin sulphate (Italfarmaco, Milan, Italy) was administered in drinking water (8 mg/mL) for the first 2 weeks after transplantation to prevent infections. 18-20 days after transplant mice were weaned and fed with high calories diet gel food (Clear$H_2O$) due to the absence of teeth. Mice were checked for health status and weight 3 times a week until the sacrifice, performed 4 months after GT or earlier in case of prolonged weight loss, by $CO_2$ asphyxiation. Splenocytes, BM cells, bones, blood and thymus were collected for analysis.

***Osteoclasts differentiation***

OCs were generated from splenic or fetal liver Lin- cells *in vitro*, differentiating them toward myeloid lineage in StemSpan SFEM

medium (STEMCELL Technologies, Vancouver, British Columbia, Canada), 2% FBS (Euroclone, Milan, Italy), 1% penicillin/streptomycin, 1% glutamine (Gibco, Carlsbad, Calif), and the following cytokines (PeproTech, Rocky Hills, NJ): rmTPO, 20 ng/mL; rmSCF, 50 ng/mL; rhFLT3L, 10 ng/mL; rmIL-3, 10 ng/mL; and rhIL-6, 20 ng/mL for at least 10 days, splitting cells every 3 days. OC precursors from differentiated Lin-, BM and splenic cells were seeded on plastic tissue-culture treated 96-well plates or dentine slices at a density of $5 \times 10^5$ in 200µl of alpha-Minimum Essential Medium (aMEM) containing 10% FBS, 1% penicillin, 1% streptomycin and the following cytokines: recombinant murine macrophage colony-stimulating factor (rmM-CSF), 25 ng/ml; recombinant human transforming growth factor-beta (rhTGFβ), 5 ng/ml; dexamethasone 1 mM (Sigma); recombinant murine receptor activator of nuclear factor kappa-B ligand (rmsRankL), 100 ng/ml. Half of the medium was chanced twice a week for at least 7 days for OCs seeded on plastic 96-well plates and for 21 days for OCs seeded on dentine slices. Cells were incubated at 37°C and 5% $CO_2$.

***Osteoclast activity***

Osteoclasts cultured on plastic were stained using the Tartrate Resistant Acid Phosphatase (TRAP) Kit (Sigma-Aldrich), following the manufacturer's instruction. To evaluate OCs resorptive function, OCs were differentiated on dentin discs (Immunodiagnostic Systems, Ltd., Scottsdale, AZ). After 3 weeks, dentin discs were rinsed with water, scraped to remove attached

cells, stained with 1% toluidine blue solution for 3 minutes, and then washed with water to visualize resorption pits. TRAP and toluidine blue images were acquired on a Zeiss AxioImager microscope.

### *CFU evaluation by methylcellulose culture*

Hematopoietic progenitor cultures were performed plating 375000 splenocytes or 187000 BM cells in 2.5ml MethoCult GF M3434 methylcellulose-based medium (STEMCELL Technologies) and cultured for 12 days. MethoCult assay were also performed on Lin- cells, plating 2500 transduced and untransduced Lin- in 2.5ml MethoCult GF M3434 methylcellulose-based medium cultured for 12 days incubated at 37°C and 5% $CO_2$. For plerixafor-based HSC mobilization experiments we performed Methocult assay on whole blood, normalizing the number of colonies on the volume of blood drawn.

### *PTH ELISA assay*

Serum samples were collected from mice and stored at -20 °C. Sera were thawed and maintained on ice until the use and were diluted 1:5. Mouse PTH 1-84 ELISA Kit (Quidel Corporation, USA) was used to evaluate PTH concentration in the serum samples, following the manufacturer's instruction.

### *Histopathology*

Mice were sacrificed by $CO_2$ asphyxiation; spleen tissue were harvested, and half of the spleen was fixed in formalin fro 24 hours,

washed and maintained in ethanol 70% at 4°C. Then samples were embedded in paraffin for Haematoxylin and Eosin (H&E) staining. Selected bones were fixed in 4% paraformaldehyde (PFA) and decalcified in 14% ethylenediaminetetraacetic acid (EDTA), pH 7.4 with Acetic Acid, then dehydrated and embedded in paraffin for Haematoxylin and Eosin (H&E) staining and TRAP staining (Sigma-Aldrich, Saint Louis, MO).

### *Micro-computed tomography (μCT)*

Selected bones were fixed in 4% formalin for 24 hours at 4°C. Then formalin was replaced with 70% EtOH for 24 hours and finally with 80% EtOH. For μCT analysis, the femur and skull of each mouse were placed into a radiotranslucent sample holder. To prevent desiccation, the holder was filled with PBS (Life technologies, Carlsbad, CA, USA). μCT scanning and analysis was performed as previously described [28] using a μCT 40 desktop cone-beam μCT (Scanco Medical AG, Bruüttisellen, Switzerland).

### *Vector copy number*

Genomic DNA was extracted with QIAamp DNA Blood mini kit (QIAGEN), according to manufacturer's instructions. Vector copy number/genome (VCN) was calculated on transduced cells and transduced hematopoietic progenitors as previously described [29] using murine RPP30 housekeeping gene.

### *Plerixafor-based HSC mobilization*

*oc/oc* and WT mice at 3 or 7 days of life were injected subcutaneously with one dose of 5 mg/kg of AMD3100 (Plerixafor) as already described [26]. A cohort of *oc/oc* and WT mice remains untreated as control group. One hour after the injection, mice were sacrificed and the blood drawn was mixed with 50 ul anticoagulant citrate phosphate dextrose solution. We collected whole blood, BM and spleen tissue for Methocult assay. White blood cells count was determined with Procyte DX Analyser (Idexxbioanalytics).

## Discussion

ARO is a rare genetic disease and HSCT is the only cure available up to date. However, the clinical need for innovative therapies is urgent, since ARO patients experience high transplant related mortality and HLA-matched donor are available to a minority of patients [2, 9]. We and other groups previously demonstrated that the LV based GT represent an effective and feasible approach to restore bone resorptive function of ARO patient-derived OCs *in vitro* [22, 30]. The murine model of ARO, the *oc/oc* mouse, offers the unique opportunity to test the GT efficacy *in vivo*. The *oc/oc* mouse presents early onset of the symptoms with a rapid degeneration, similar to disease progression in patients. However, its severe phenotype poses challenges to the technical feasibility of the GT approach. In the past, Richter's group demonstrated the efficacy of LV EFS.TCIRG1 on *oc/oc* neonates, showing that 9 out of 12 GT mice survived long-term with improved bone phenotype [24].

In the present work, we elaborated a proof of concept study that demonstrates the efficacy of our PGK.TCIRG1 LV to cure *TCIRG1*-dependent ARO in the *oc/oc* mouse model.

We first demonstrated that *oc/oc*-derived OCs obtained from *oc/oc* transduced Lin- cells were able to resorb the bone *in vitro*, comparably to OCs obtained from WT Lin-. Then we applied the GT strategy to rescue the osteopetrotic phenotype of *oc/oc* mice *in vivo*, presenting a very severe osteopetrotic phenotype already in the first 3-4 days of life (Figure 9).

To correct the phenotype as early as possible, we transplanted transduced *oc/oc* Lin- cells into irradiated *oc/oc* neonates of 1-2 days old. At the beginning of this study, we used splenic Lin- cells as source to treat 3 GT mice. One of them (GT4) showed the complete rescue of bone phenotype with absence of circling behaviour and eruption of the incisors, consistent with the high VCN in the analysed organs. However, splenic Lin- cells, independently on the LV transduction, showed high level of mortality after isolation, significantly limiting our experimental purposes. For this reason, we were forced to use Lin- cells isolated from *oc/oc* fetal liver as cell source for the GT in the subsequent experiments [25]. The use of fetal liver also allowed us to collect a high number of Lin- cells, increasing the possibility to exploit a higher number of *oc/oc* donors as fetuses, if compared to *oc/oc* neonates that presents a high rate of perinatal death. We transplanted a total number of 14 *oc/oc* mice with *oc/oc* Lin- cells transduced with LV PGK.TCIRG1 and 15 *oc/oc* mice with WT Lin- cells as control group. Ten out of fourteen GT mice survived longer then 3 weeks, and 6 of them reached the age of 4 months which was set as the final end point of the experiment. Moreover, most long-term surviving GT mice showed absence of circling behaviour and eruption of the incisors. However, GT mice remain smaller in size compared to WT littermates, despite their growth improvement. This could result from the presence of osteopetrotic features already at birth, despite phenotype is still not visible. Adult GT mice were sacrificed 4 months after the treatment and BM, spleen, thymus and blood were analysed. Surprisingly, the number

of HSC colonies in BM of GT mice was comparable to control groups, suggesting that BM of *oc/oc* mice had been repopulated with HSC after GT. However, we still observed signs of compensatory extramedullary hematopoiesis due to reduced BM space and HSC niches, since we did not obtain full correction of osteopetrosis. This result was further confirmed by the partial and variable normalization of spleen architecture in GT mice. *Ex vivo* bone resorption capacity showed variable results in GT mice. We hypothesized that VCN could reflect the differences obtained in the mice. However, most of them had the very low VCN observed in BM and spleen at the sacrifice. On the other hand, GT mice had long-term survival, that could be accountable to the presence of transduced cells. Since we observed loss of weight during last follow up, we speculate that a loss of engraftment is occurring overtime, likely due to the limited number of transduced Lin- able to engraft the pathological bone niche. However, we cannot exclude that additional factors could play a role in the outcome of the proposed strategy, such as the pre-existent inflammation and damage of bone marrow niche which strongly limit the therapeutic approach to ARO patients.

Variable results, not always correlating with survival and clinical status, were also observed in PTH level in the serum. Indeed, calcium homeostasis is dramatically impaired in *oc/oc* mice, closely resembling the hypocalcaemia and hyperparathyroidism of ARO patients [6, 31]. Moreover, bone architecture studies by histology or μCT confirmed the poor correction of bone phenotype in most GT mice.

The explanation for these conflicting data, in which the significant improvement in survival does not coincide with an adequate level of gene transfer expressed in terms of VCN, could reside in the fact that a low expression of *TCIRG1* is sufficient to guarantee the improvement of the osteopetrotic phenotype, as demonstrated by the studies of Flores et al., in which only 3-5% of engraftment in PB, after WT cells transplantation led to the rescue of the disease [32].

The cell source and the number of LV-corrected autologous HSC, transplantable in *oc/oc* mice, are one of the major issues faced during the application of the GT protocol. These problems are also encountered in the therapy of osteopetrotic patients. Drug-based HSC mobilization, used to harvest HSC before transplantation as autologous back up, is still an unexplored solution for ARO patients. We hypothesized that HSC mobilization could increase the number of HSC obtained from ARO patient, in spite of the pathological BM niche. To this end, we applied AMD3100 (Plerixafor)-based HSC mobilization protocol to *oc/oc* mice, at 3 and 7 days of life, when phenotype is not visible but bone already presents overt signs of osteopetrosis, in order to mimic patient health status. We observed an increase in WBC counts and in HSC colonies, suggesting that mobilization is feasible from the limited and pathological BM niche. However, these preliminary results still need to be confirmed and corroborated by deep analysis of hematopoietic niches after mobilization.

In conclusion, the application of drug-based mobilization of ARO patients could have the great potential to decrease the amount of

blood to harvest as autologous back up before transplantation and could facilitate the development of autologous HSC-based gene therapy (GT) strategy to cure osteopetrosis. Moreover, GT results obtained in the *oc/oc* model, showed the efficacy of LV PGK.TCIRG1-mediated gene transfer in ameliorating lifespan and bone defects of osteopetrotic mice, despite the severity of *oc/oc* phenotype, which significantly limits the manipulation of this model.

## Supplementary

| mouse ID | source of transplanted lin- | number of transplanted cells | VCN in vitro of transplanted lin- | age at sacrifice (weeks) | VCN in the organs | | | VCN of methocult pool | |
|---|---|---|---|---|---|---|---|---|---|
| | | | | | spleen | bone marrow | thymus | spleen | bone marrow |
| GT1 | spleen | 0,715x106 | 31,4 | 3 | n.a. | n.a. | n.a. | n.a. | n.a. |
| GT4 | spleen | $1x10^6$ | 31,4 | 17 | 4,11 | 4,69 | 5,00 | 12,00 | 6,21 |
| GT6 | fetal liver | 2,1x106 | 15,6 | 20 | 0,00 | 0,01 | 0,00 | 0,50 | 0,01 |
| GT7 | fetal liver | 0,76x106 | n.a. | 17 | 0,01 | 0,01 | n.a. | n.a. | n.a. |
| GT8 | fetal liver | 0,66x106 | n.a. | 8 | 0,00 | 0,00 | 0,01 | 0,00 | n.a. |
| GT9 | fetal liver | 1,2x106 | n.a. | 14 | 0,00 | 0,01 | 0,04 | 0,00 | n.a. |
| GT10 | fetal liver | 1,2x106 | n.a. | 14 | 0,01 | 0,00 | 0,02 | 0,03 | n.a. |
| GT11 | fetal liver | 1,4x106 | n.a. | 3 | n.a. | n.a. | n.a. | n.a. | n.a. |
| GT12 | fetal liver | 1,3x106 | 1,71 | 16 | 0,01 | 0,07 | 0,01 | 0,00 | 0,00 |
| GT13 | fetal liver | $0,86x10^6$ | n.a. | 4 | n.a. | n.a. | n.a. | n.a. | n.a. |
| GT14 | fetal liver | $0,86x10^6$ | n.a. | 4 | n.a. | n.a. | n.a. | n.a. | n.a. |
| GT16 | fetal liver | $1,2x10^6$ | n.a. | 3 | n.a. | n.a. | n.a. | n.a. | n.a. |
| GT17 | fetal liver | $1,2x10^6$ | n.a. | 3 | n.a. | n.a. | n.a. | n.a. | n.a. |
| GT18 | spleen | $0,79x10^6$ | n.a. | 4 | 0,96 | n.a. | n.a. | n.a. | n.a. |

**Supplementary Table 1.** Data from individual GT mice transplanted with LV PGK.TCIRG1 transduced *oc/oc* Lin-. VCN, vector copy number; lin-, lineage negative cells; n.a. not available.

## References


1. Teti, A. and S.L. Teitelbaum, *Congenital disorders of bone and blood.* Bone, 2019. **119**: p. 71-81.
2. Sobacchi, C., et al., *Osteopetrosis: genetics, treatment and new insights into osteoclast function.* Nat Rev Endocrinol, 2013. **9**(9): p. 522-36.
3. Frattini, A., et al., *Defects in TCIRG1 subunit of the vacuolar proton pump are responsible for a subset of human autosomal recessive osteopetrosis.* Nat Genet, 2000. **25**(3): p. 343-6.
4. Scimeca, J.C., et al., *The gene encoding the mouse homologue of the human osteoclast-specific 116-kDa V-ATPase subunit bears a deletion in osteosclerotic (oc/oc) mutants.* Bone : official journal of the international and mineral society, 2000. **26**(3): p. 207-213.
5. Marks, S.C., M.F. Seifert, and P.W. Lane, *Osteosclerosis, a recessive skeletal mutation on chromosome 19 in the mouse.* J Hered, 1985. **76**(3): p. 171-6.
6. Schinke, T., et al., *Impaired gastric acidification negatively affects calcium homeostasis and bone mass.* Nat Med, 2009. **15**(6): p. 674-81.
7. Natsheh, J., et al., *Improved Outcomes of Hematopoietic Stem Cell Transplantation in Patients With Infantile Malignant Osteopetrosis Using Fludarabine-Based Conditioning.* Pediatr Blood Cancer, 2016. **63**(3): p. 535-40.
8. Stepensky, P., et al., *Stem cell transplantation for osteopetrosis in patients beyond the age of 5 years.* Blood Adv, 2019. **3**(6): p. 862-868.
9. Schulz, A.S., et al., *Osteopetrosis. Consensus guidelines for diagnosis, therapy and follow-up*. 2015, ESID and the EBMT WP Inborn Errors.
10. Steward, C.G., et al., *High peripheral blood progenitor cell counts enable autologous backup before stem cell transplantation for malignant infantile osteopetrosis.* Biol Blood Marrow Transplant, 2005. **11**(2): p. 115-21.
11. De Clercq, E., *The bicyclam AMD3100 story.* Nat Rev Drug Discov, 2003. **2**(7): p. 581-7.

12. Hatse, S., et al., *Chemokine receptor inhibition by AMD3100 is strictly confined to CXCR4.* FEBS Lett, 2002. **527**(1-3): p. 255-62.
13. Seifert, M.F. and S.C. Marks, Jr., *Congenitally osteosclerotic (oc/oc) mice are resistant to cure by transplantation of bone marrow or spleen cells from normal littermates.* Tissue Cell, 1987. **19**(1): p. 29-37.
14. Johansson, M., et al., *Neonatal hematopoietic stem cell transplantation cures oc/oc mice from osteopetrosis.* Exp Hematol, 2006. **34**(2): p. 242-9.
15. Johansson, M.K., et al., *Hematopoietic stem cell-targeted neonatal gene therapy reverses lethally progressive osteopetrosis in oc/oc mice.* Blood, 2007. **109**(12): p. 5178-85.
16. Naldini, L., *Genetic engineering of hematopoiesis: current stage of clinical translation and future perspectives.* EMBO Molecular Medicine, 2019. **11**(3): p. e9958.
17. Naldini, L., *Gene therapy returns to centre stage.* Nature, 2015. **526**(7573): p. 351-60.
18. Aiuti, A., et al., *Lentiviral hematopoietic stem cell gene therapy in patients with Wiskott-Aldrich syndrome.* Science, 2013. **341**(6148): p. 1233151.
19. Cavazzana-Calvo, M., et al., *Transfusion independence and HMGA2 activation after gene therapy of human β-thalassaemia.* Nature, 2010. **467**(7313): p. 318-322.
20. Cartier, N., et al., *Hematopoietic stem cell gene therapy with a lentiviral vector in X-linked adrenoleukodystrophy.* Science, 2009. **326**(5954): p. 818-23.
21. Biffi, A., et al., *Lentiviral hematopoietic stem cell gene therapy benefits metachromatic leukodystrophy.* Science, 2013. **341**(6148): p. 1233158.
22. Capo, V., et al., *Expanded circulating hematopoietic stem/progenitor cells as novel cell source for the treatment of TCIRG1 osteopetrosis.* Haematologica, 2020.
23. Moscatelli, I., et al., *Targeting NSG Mice Engrafting Cells with a Clinically Applicable Lentiviral Vector Corrects Osteoclasts in Infantile Malignant Osteopetrosis.* Hum Gene Ther, 2018. **29**(8): p. 938-949.
24. Löfvall, H., et al., *Hematopoietic Stem Cell-Targeted Neonatal Gene Therapy with a Clinically Applicable Lentiviral Vector Corrects Osteopetrosis in.* Hum Gene Ther, 2019. **30**(11): p. 1395-1404.

25. Papathanasiou, P., et al., *Evaluation of the long-term reconstituting subset of hematopoietic stem cells with CD150.* Stem cells (Dayton, Ohio), 2009. **27**(10): p. 2498-2508.
26. Broxmeyer, H.E., et al., *Rapid mobilization of murine and human hematopoietic stem and progenitor cells with AMD3100, a CXCR4 antagonist.* J Exp Med, 2005. **201**(8): p. 1307-18.
27. Visigalli, I., et al., *Preclinical Testing of the Safety and Tolerability of Lentiviral Vector-Mediated Above-Normal Alpha-L-Iduronidase Expression in Murine and Human Hematopoietic Cells Using Toxicology and Biodistribution Good Laboratory Practice Studies.* Hum Gene Ther, 2016. **27**(10): p. 813-829.
28. Yorgan, T.A., et al., *The Anti-Osteoanabolic Function of Sclerostin Is Blunted in Mice Carrying a High Bone Mass Mutation of Lrp5.* Journal of Bone and Mineral Research, 2015. **30**(7): p. 1175-1183.
29. Scala, S., et al., *Dynamics of genetically engineered hematopoietic stem and progenitor cells after autologous transplantation in humans.* Nature Medicine, 2018. **24**(11): p. 1683-1690.
30. Moscatelli, I., et al., *Lentiviral gene transfer of TCIRG1 into peripheral blood CD34(+) cells restores osteoclast function in infantile malignant osteopetrosis.* Bone, 2013. **57**(1): p. 1-9.
31. Wu, C.C., et al., *Diagnosis and Management of Osteopetrosis: Consensus Guidelines From the Osteopetrosis Working Group.* J Clin Endocrinol Metab, 2017. **102**(9): p. 3111-3123.
32. Flores, C., et al., *Nonablative neonatal bone marrow transplantation rapidly reverses severe murine osteopetrosis despite low-level engraftment and lack of selective expansion of the osteoclastic lineage.* J Bone Miner Res, 2010. **25**(9): p. 2069-77.

## Chapter 3

# Expanded circulating hematopoietic stem/progenitor cells as novel cell source for the treatment of TCIRG1 osteopetrosis

Valentina Capo[1], Sara Penna[1,2], Ivan Merelli[3], Matteo Barcella[1], Serena Scala[1], Luca Basso-Ricci[1], Elena Draghici[1], Eleonora Palagano[4,5], Erika Zonari[1], Giacomo Desantis[1], Paolo Uva[6], Roberto Cusano[6], Lucia Sergi Sergi[1], Laura Crisafulli[4,5], Despina Moshous[7,8], Polina Stepensky[9], Katarzyna Drabko[10], Zühre Kaya[11], Ekrem Unal[12,13], Alper Gezdirici[14], Giuseppe Menna[15], Marta Serafini[2], Alessandro Aiuti[1], Silvia Laura Locatelli[16], Carmelo Carlo-Stella[16,17], Ansgar S. Schulz[18], Francesca Ficara[4,5], Cristina Sobacchi[4,5], Bernhard Gentner[1] and Anna Villa[1,4]

[1]San Raffaele Telethon Institute for Gene Therapy (SR-Tiget), IRCCS San Raffaele Scientific Institute, Milan (Italy);[2]DIMET, University of Milano-Bicocca, Monza (Italy); [3]Institute for Biomedical Technologies, National Research Council, Segrate (Italy); [4]CNR-IRGB, Milan Unit, Milan (Italy); [5]Humanitas Clinical and Research Center - IRCCS, Rozzano (Italy); [6]CRS4, Science and Technology Park Polaris, Pula (Italy); [7]Unité d'Immunologie, Hématologie et Rhumatologie Pédiatriques (UIHR), Assistance Publique-Hôpitaux de Paris, Hôpital Necker-Enfants Malades, Paris (France); [8]INSERM UMR1163, Institut Imagine, Université Paris Descartes-Sorbonne Paris Cité, Paris (France); [9]Department of Bone Marrow Transplantation and

Cancer Immunotherapy, Hadassah University Hospital, Jerusalem (Israel); [10]Medical University of Lublin, Lublin (Poland); [11]Department of Pediatric Hematology, Gazi University, School of Medicine, Ankara (Turkey); [12]Erciyes University, Pediatric Hematology Oncology, Kayseri (Turkey); [13]Molecular Biology and Genetic Department, Gevher Nesibe Genom and Stem Cell Institution, Genome and Stem Cell Center (GENKOK), Erciyes University, Kayseri (Turkey); [14]Department of Medical Genetics, Istanbul Health Science University, Kanuni Sultan Suleyman Training and Research Hospital, Istanbul (Turkey); [15]Hemato-Oncology Unit, Department of Oncology, Pausilipon Hospital, Naples (Italy); [16]Department of Oncology and Hematology, Humanitas Cancer Center, Humanitas Clinical and Research Center, Rozzano (Italy); [17]Department of Biomedical Sciences, Humanitas University, Rozzano (Italy) 18Department of Pediatrics and Adolescent Medicine, University Medical Center, Ulm (Germany)

This article was published on *Haematologica* in 2020 January 16.
DOI: 10.3324/haematol.2019.238261

**Abstract**

Allogeneic hematopoietic stem cell transplantation is the treatment of choice for autosomal recessive osteopetrosis caused by defects in the *TCIRG1* gene. Despite recent progress in conditioning, a relevant number of patients are not eligible for allogeneic stem cell transplantation because of the severity of the disease and significant transplant-related morbidity. We exploited peripheral $CD34^+$ cells, known to circulate at high frequency in the peripheral blood of TCIRG1-deficient patients, as a novel cell source for autologous transplantation of gene corrected cells. Detailed phenotypical analysis showed that circulating CD34+ cells have a cellular composition that resembles bone marrow, supporting their use in gene therapy protocols. Transcriptomic profile revealed enrichment in genes expressed by hematopoietic stem and progenitor cells (HSPCs). To overcome the limit of bone marrow harvest/ HSPC mobilization and serial blood drawings in TCIRG1 patients, we applied UM171-based *ex-vivo* expansion of HSPCs coupled with lentiviral gene transfer. Circulating $CD34^+$ cells from TCIRG1-defective patients were transduced with a clinically-optimized lentiviral vector (LV) expressing *TCIRG1* under the control of phosphoglycerate promoter and expanded *ex vivo*. Expanded cells maintained long-term engraftment capacity and multi-lineage repopulating potential when transplanted *in vivo* both in primary and secondary NSG recipients. Moreover, when $CD34^+$ cells were differentiated *in vitro*, genetically corrected osteoclasts resorbed the bone efficiently. Overall, we provide evidence that expansion of circulating HSPCs coupled to gene therapy can

overcome the limit of stem cell harvest in osteopetrotic patients, thus opening the way to future gene-based treatment of skeletal diseases caused by bone marrow fibrosis.

## Introduction

Autosomal recessive osteopetrosis (ARO) is a rare and heterogeneous genetic disease, caused by defects in the differentiation or resorption activity of osteoclasts. Patients present with dense and brittle bones, severe anemia, hepatosplenomegaly, macrocephaly, progressive deafness and blindness due to pressure on nerves, and limited bone marrow (BM) cavities [1,2]. The incidence of the disease is 1 in 250000 live births, with higher rates in specific geographic areas where consanguineous marriages are frequent [3]. More than 50% of the cases are due to defects in the *TCIRG1* gene, encoding for the a3 subunit of ATPase H+ transporting V0 complex, necessary for the acidification of organelles and resorption lacuna [4].

The disease is usually lethal in the first decade of life, with poor quality of life. To date, the only curative treatment is hematopoietic stem cell transplantation (HSCT) from an allogeneic donor, which has to be performed as early as possible, before compression of nerves and irreversible neurological damages have occurred [5,6]. Children with osteopetrosis suffer from high rates of graft failure and transplant-related mortality, mostly due to severe graft-versus-host disease, liver toxicity (veno-occlusive disease), infections or lung toxicity (idiopathic pneumonia syndrome and acute respiratory distress syndrome) [7,8]. In particular, transplants from HLA-matched related or unrelated donors have an 80-88% five-year disease-free survival, whereas the success rate is lower for haploidentical transplants (66%) [2]. Recently, improvements in

the outcome and overall survival has been observed in patients treated with fludarabine-based conditioning regimens and T cell depleted haploidentical donors [9,10]. However, HLA-compatible donors are readily available only to a minority of patients. Umbilical cord blood transplantation (UCBT) has also been used as an alternative source, but overall survival rate at 6 years was 43%, so it is no longer recommended [11].

To overcome donor-related issues, gene therapy has been proposed as an alternative strategy. In the past, a retroviral vector, in which the TCIRG1 gene was driven by the strong viral SFFV (spleen focus-forming virus) promoter, has been tested in *oc/oc* mice, the murine model of TCIRG1-deficient osteopetrosis [12], showing that *ex vivo* gene therapy for ARO is effective. More recently, TCIRG1-expressing lentiviral vectors, driven by different promoters, were designed and tested in ARO CD34+ cells *in vitro* and in the *oc/oc* mouse model [13–15]. Since BM harvest cannot be performed in these patients due to severe bone marrow fibrosis and susceptibility to bone fractures, peripheral blood (PB) $CD34^+$ cells represent a potential source of autologous HSPCs. The majority of ARO patients have high frequencies of circulating $CD34^+$ cells, because of the limited BM cavities and the reduction of hematopoietic stem cell (HSC) niches [16,17]. Of note, previous studies showed that peripheral blood of osteopetrotic patients is highly enriched in cells with myeloid and erythroid clonogenic potential [16,18]. However, a detailed characterization of ARO PB $CD34^+$ cell stemness markers is still lacking, a prerequisite before considering their clinical use.

Finally, despite the high frequency of PB $CD34^+$ cells, the amount of collectable HSPC for *ex vivo* manipulation is constrained by the severity of the disease, the young age of the patients and low amount of blood that can be drawn. Data reported in literature indicates the feasibility of exchange transfusion in osteopetrotic patients for back-up purpose [16]. Since gene therapy protocols usually require higher amounts of $CD34^+$ cell/kg, we might speculate that an adequate number of autologous $CD34^+$ cells can be obtained through the collection of both spontaneously circulating and mobilized HSPC. We hypothesized that an efficient expansion of short-term progenitors and HSCs may facilitate reaching adequate cell dose, allowing timely hematopoietic recovery and durable engraftment by genetically-engineered cells, respectively. To this end, we tested an HSPC expansion protocol previously used for cord blood (CB), BM or mobilized PB $CD34^+$ cells from healthy donors [19,20]. We exploited the pyrimidoindole derivative UM171 to expand ARO-derived PB $CD34^+$ cells with repopulating potential, after transduction with a clinically optimized *TCIRG1*-expressing lentiviral vector driven by the phosphoglycerate kinase (*PGK1*) promoter. We demonstrated that transduced and expanded cells generated functional bone-resorbing osteoclasts *in vitro*. Our deep phenotypic characterization unveiled that ARO-derived spontaneously mobilized $CD34^+$ cells contained *bona fide* primitive HSCs and that the stem cell output and BM homing capacity were maintained in NSG mice after the expansion protocol. Overall, we have established a novel protocol that will allow performing

transplantation of gene-corrected and expanded PB $CD34^+$ cells in human disorders characterized by bone marrow fibrosis.

## Methods

### *Patients and healthy donors.*

Peripheral blood of ARO patients and healthy donors was obtained according to the Declaration of Helsinki with the approval of the local Medical Ethical Committees. A description of patients is reported in Table 1. ARO17 and ARO18 patients were previously described (patients 13 and 19 respectively) [21]. Details on healthy donors are reported in Online Supplementary Methods.

| Patient | Sample type | Age | TCIRG1 mutation | % CD34+ in WB | CD34+/uL | blood volume (ml) | isolated CD34+ |
|---|---|---|---|---|---|---|---|
| ARO2 | peripheral blood | 5.5 months | c.713+1G>A, r.spl; c.1555-2A>C, r.spl | 4.97 | 1831 | 2.0 | 3,53E+05 |
| ARO6 | frozen PBMC | 11 months | c.1674-1G>A, r.spl; c.1674-1G>A, r.spl | 0.94 | na | na | 2,20E+04 |
| ARO7 | peripheral blood | 8 months | c.2321C>G, p.(Pro774Arg); c.2321C>G, p.(Pro774Arg) | 1.59 | 282 | 3.2 | 2,70E+05 |
| ARO9 | frozen PBMC | 12 months | c.1874-1G>A, r.spl; c.1874-1G>A, r.spl | 4.26 | na | na | 5,00E+05 |
| ARO12 | frozen PBMC | 2 months | c.2233+1G>A, r.spl; c.2233+1G>A, r.spl | 7.52 | na | na | 1,30E+05 |
| ARO13 | peripheral blood | 5 months | c.2233+1G>A, r.spl; c.2233+1G>A, r.spl | 5.90 | 539 | 6.7 | 1,90E+05 |
| ARO16 | frozen PBMC | 10 months | c.2233+1G>A, r.spl; c.2233+1G>A, r.spl | 1.93 | na | na | 2,00E+05 |
| ARO17 | frozen PBMC | 7 months | c.1875C>A, p.(Tyr625X); c.1875C>A, p.(Tyr625X) | 1.61 | na | na | 1,60E+05 |
| ARO18 | frozen PBMC | 7 months | c.1226G>A, p.(Gly410Arg); c.2374G>C, p.(Gly792Arg) | 8.91 | na | na | 1,16E+06 |
| ARO19 | peripheral blood | 12 months | r.223_224inst; r.223_224inst | 2.90 | 1466 | 6.0 | 1,89E+06 |
| | peripheral blood | 13 months | | | | 8.8 | 1,08E+06 |
| ARO20 | peripheral blood | 7 months | c.2005C>T; p.(Arg669X); r.694_695insa | 0.10 | 25 | 7.0 | 4,10E+05 |
| ARO21 | peripheral blood | 2.5 months | c.1682delinsTT, p.(Gly561Valfs); c.2383_2384del, p.(Ala796Leufs) | 14.45 | 19 | 4 | 8,00E+05 |
| ARO25 | frozen PBMC | 3.5 months | g.8280_9560del; g.8280_9560del | 6.70 | na | na | 1,02E+05 |
| | peripheral blood | 5.5 months | | | 1353 | 16.5 | 1,11E+06 |
| ARO26 | peripheral blood | 8 months | c.2218_2219del, (p.Leu740Glufs); c.2218_2219del, (p.Leu740Glufs) | 4.07 | 899 | 5.6 | WBD only |
| ARO27 | peripheral blood | 8 months | c.1230del; c.1230del | 5.20 | 770 | 5.6 | WBD only |
| ARO28 | peripheral blood | 6 months | c.1213G>A, p.(Gly405Arg); c.1674-1G>A, r.spl | 3.23 | 341 | 2.7 | WBD only |
| ARO29 | peripheral blood | 6.5 months | c.1674-1G>A, r.spl; c.1674-1G>A, r.spl | 2.40 | 458 | 3.0 | WBD only |

PBMC, peripheral blood mononuclear cells; WB, whole blood; WBD, whole blood dissection analysis
Accession number of the TCIRG1variant1 cDNA: NM_006019; the numbering used starts with nucleotide +1 for the A of the ATG-translation initiation codon
Sequence variant nomenclature conforms to the HGVS recommendations for the description of sequence variants – 2016 update, Den Dunnen et al, Hum Mutat 37:564-569, 2016.

**Table 1.** ARO patients

***CD34$^+$ isolation and culture.***

Lymphoprep (STEMCELL Technologies) density gradient was used to isolate PBMCs. CD34$^+$ cells were isolated from PBMCs using human CD34 MicroBead Kit and autoMACS Pro Separator (Miltenyi Biotec), according to the manufacturer's instruction. CD34$^+$ were prestimulated for 24 hours and transduced with 1-hit of LV at MOI 100 overnight, as previously described [22,23]. Hematopoietic progenitor cultures were performed plating 2500 cells in 2.5ml MethoCult H4434 Classic methylcellulose-based medium (STEMCELL Technologies) and cultured for 12 days.

After transduction, cells were expanded using UM171 compound until day 7, as previously described [19]. A fraction of expanded cells was differentiated *in vitro* towards the myeloid lineage for 1 week and then into osteoclasts for 2 or 3 weeks on plastic wells or bone slices (Immunodiagnostic Systems), as previously described [14].

***Mice.***

Animal experimental procedures were approved by Institutional Animal Care and Use Committee of San Raffaele Hospital and Italian Ministry of Health. NOD *scid* gamma common chain (NSG) mice, obtained from Charles River Laboratories, were irradiated at 180 RAD and transplanted after 2 hours, as detailed in Online Supplementary Table S1.

***RNAseq.***

Total RNA of $CD34^+$ cells was extracted using ReliaPrep RNA Cell Miniprep System (Promega), according to manufacturer's instructions. Libraries generation and data analysis were performed as detailed in Online Supplementary Methods.

***Osteoclast activity.***

Osteoclasts cultured on plastic were stained using the Tartrate Resistant Acid Phosphatase (TRAP) Kit (Sigma-Aldrich), following the manufacturer's instruction. Osteoclasts differentiated on bone slices were stained using alendronate conjugated to Alexa Fluor 488 [24], TRITC-conjugated phalloidin (Sigma-Aldrich) and TO-PRO-3 (Thermo Fisher Scientific). To evaluate bone resorption, the same bone slices were used for toluidine blue staining as previously described [25]. TRAP and toluidine blue images were acquired on a Zeiss AxioImager M2m microscope, while immunofluorescence staining images were acquired on a Leica TCS SP5 Laser Scanning Confocal microscope.

Quantification of CTX-I was performed on culture supernatants using CrossLaps for Culture (CTX-I) ELISA (Immunodiagnostic Systems), according to the manufacturer's instruction.

***Statistics.***

Results are shown as mean ± standard error (SD) or standard error of the mean (SEM). Statistical significance was determined by non-parametric Mann Whitney test, Kruskal-Wallis test, one-way ANOVA, two-way ANOVA, Dunn's post-test, Bonferroni post-

test or Spearman correlation, as detailed in figure legends. * indicates $p<0.05$, ** $p<0.01$, *** $p<0.001$, **** $p<0.0001$.

Additional methods are presented in the Supplementary Methods.

## Results

### *High number of circulating stem/progenitor cells in TCIRG1-defective autosomal recessive patients*

Human HSPCs are known to circulate at low frequencies in steady-state peripheral blood of healthy adult donors (0.11% ± 0.01) [26]. Interestingly, patients affected by *TCIRG1*-defective ARO show high $CD34^+$ cell counts in the peripheral blood [16], due to the reduced bone marrow cavities. To confirm this finding in our cohort of patients, we analyzed the frequencies of circulating $CD34^+$ cells in 17 *TCIRG1*-mutated patients. The vast majority had elevated $CD34^+$ frequencies, with age-dependent differences (Figure 21A). In particular, ARO patients younger than 6 months of age had a mean percentage of 4.57% ± 2.3, while children of 7-12 months showed 2.38% ± 1.7 CD34+ cells.

We further characterized the composition of ARO PB $CD34^+$ cells by deep multi-parametric phenotyping, since $CD34^+$ cells are composed by subpopulations with distinct differentiation and survival capability. Blood samples from 5 ARO patients (age range 5.5-8 months, mean 6.8 months) were analyzed using whole blood dissection (WBD) technology, a novel flow cytometry protocol, which allows to evaluate and quantify all major hematopoietic lineages including 10 distinct HSPC subpopulations circulating in the periphery [27]. As reference, we also analyzed peripheral blood samples from 4 age-matched pediatric healthy donors (age range 4-7 months, mean 5.3 months) and bone marrow samples of 7

pediatric healthy donors (age range 3-17 years, mean 10.5 years) (Figure 21B). The hematopoietic composition of PB from *TCIRG1*-deficient patients was more similar to pediatric BM than to PB from age-matched healthy children, as evidenced by the presence of classical BM-restricted progenitors such as erythroblasts, myeloblasts and B cell progenitors (Online Supplementary Figure S1). Quantitative analysis of the absolute number/µl of various HSPC subpopulations further confirmed similarities with BM. Importantly, we found that ARO patients display a content of primitive phenotypic HSC ($CD90^+$ $CD45RA^-$) comparable to BM of pediatric HD (Figure 21C). Additionally, ARO patients showed increased number of primitive multipotent progenitors (MPP) and multi-lymphoid progenitors (MLP) with respect to BM of healthy children and, most importantly, to the PB of healthy age-matched controls (Figure 21D-E).

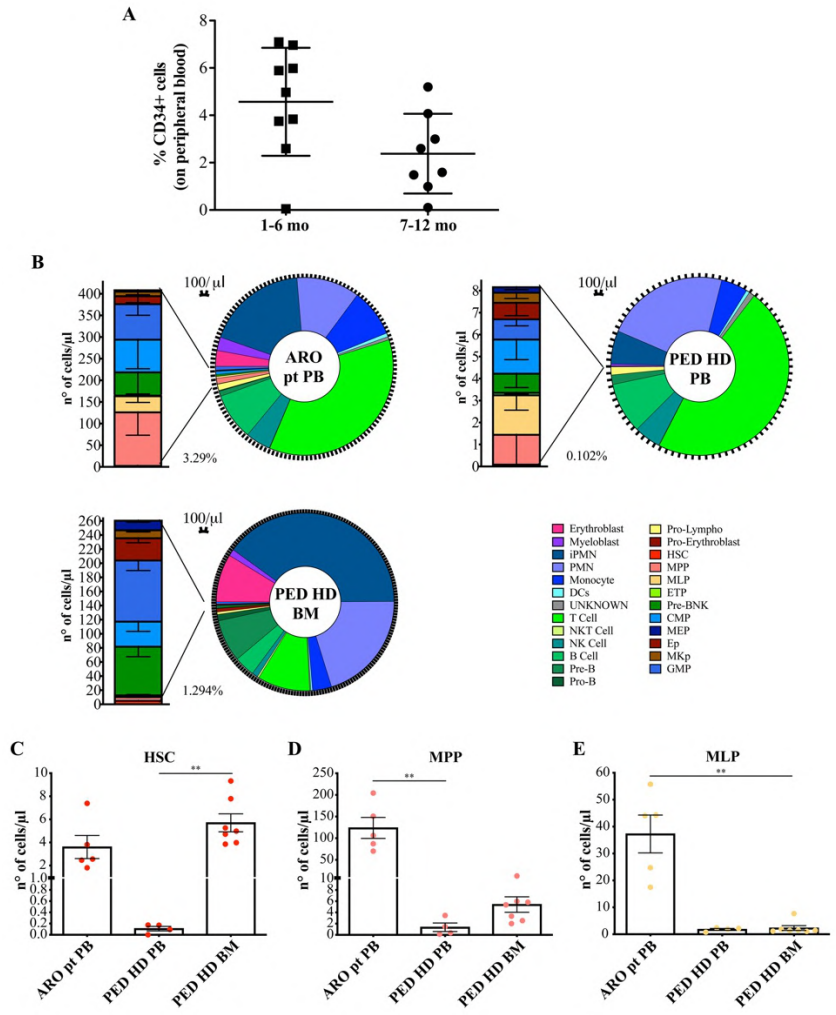


**Figure 21. Circulating CD34$^+$ cells.** (A) The graph shows the percentage of CD34$^+$ in the peripheral blood of ARO patients, divided in the indicated age groups. (B) Pie charts show distribution of 25 subsets within the CD45$^+$ gate in ARO patient peripheral blood (n=5), healthy donor peripheral blood (n=4) and bone marrow (n=7). Black outer ticks indicate 100 cells/µl. Percentages indicate the frequency of HSPC population (CD34$^+$ LIN$^-$) on total CD45$^+$ cells. The stacked bar graphs indicate the absolute cell count/µl of the HSPC compartment, composed

of 10 primitive subsets. CMP, common myeloid progenitors; DC, dendritic cells; Ep, erythroid progenitors; ETP, early T progenitors; GMP, granulocyte-monocyte progenitors; HSC, hematopoietic stem cells; iPMN, immature polymorphonucleated cells; MEP, megakaryo-erythroid progenitors; MKp, megakaryocyte progenitors; MLP, multi-lymphoid progenitors; MPP, multipotent progenitors; NKT, natural killer-T cells; NK, natural killer cells; PMN, mature polymorphonucleated cells. (C,D,E) Graphs show cell count/µl of HSC (C), MPP (D) and MLP (E) in ARO patient peripheral blood, healthy donor peripheral blood and bone marrow. Data show mean ± SD (panels A and B) or mean ± SEM (panels C, D and E). Statistical significance was determined by non-parametric Mann Whitney test (panel A) or Kruskal-Wallis test with Dunn's multiple comparison post-test (panels C, D and E).

Next, we performed whole trascriptome profiling through RNA sequencing (RNA-seq) to determine the transcriptional signature of ARO $CD34^+$ cells, in comparison to $CD34^+$ cells circulating in CB and mobilized peripheral blood (mPB) healthy donor cells, the two main sources for HSCT. Explorative data analysis performed by principal component analysis (PCA) revealed three clusters (ARO, CB and mPB) corresponding to the cell source (Figure 22A). ARO samples are closer to CB cell cluster rather than to mPB. Using unsupervised hierarchical clustering on differentially expressed genes (DEGs), ARO patients clustered together when compared to both CB and mPB (Figure 22B and Online Supplementary Figure S2), confirming the unique nature of the osteopetrotic circulating $CD34^+$ cells.

To study the HSPC composition at the RNA level, we used different gene lists reported in literature [28-36]. Gene set enrichment analysis (GSEA) revealed that ARO CD34+ cells were enriched for committed progenitors (MLP, CLP and GMP) in comparison to mPB, similarly to CB. No definitive conclusions could be drawn on the most primitive HSC population, since heterogeneous results were obtained depending on the gene set used (Figure 22C).

Overall, these analyses confirmed that $CD34^+$ cells are present at high numbers in the peripheral blood of *TCIRG1*-defective patients and that these cells are enriched for primitive subsets both phenotypically and transcriptionally, providing the first indication that unmobilized PB could be a suitable stem cell source for gene therapy.

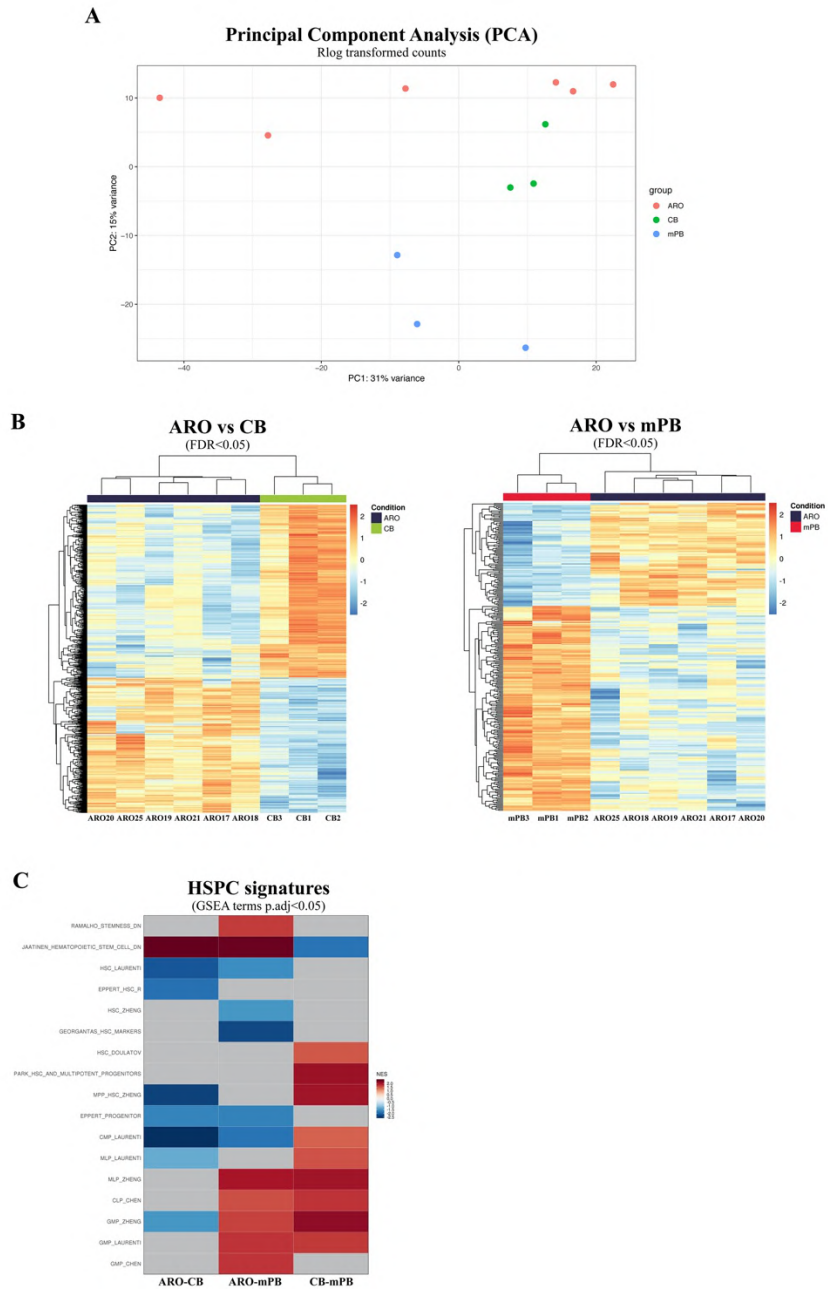


**Figure 22. RNA sequencing.** (A) Principal component analysis of ARO, CB and mPB samples. (B) Heatmaps show unsupervised hierarchical clustering on differentially expressed genes (DEGs) of ARO patients

versus CB (left) or mPB (right). (C) Heatmap shows normalized enrichment score (NES) from gene set enrichment analysis (GSEA) in the indicated categories.

***Transduction and expansion of TCIRG1-defective CD34+ cells***

We designed a gene therapy approach based on the transduction with *TCIRG1*-expressing LVs coupled with a HSPC expansion protocol, to overcome the limitation imposed by the restricted amount of *TCIRG1*-defective $CD34^+$ cells. In order to reduce the total culture period, we adapted the gene-correction protocol currently in use for gene therapy clinical trials [22,23], using only 1 hit of LV transduction.

We designed two different LVs expressing *TCIRG1* cDNA under the control of the phosphoglycerate kinase (*PGK1*) promoter (Figure 23A). The first vector (PGK.TCIRG1) was designed as a clinically-applicable vector, using the same backbone currently used in clinical trials. The second LV (PGK.TCIRG1/dNGFR) has a bidirectional design containing a marker gene, allowing easy detection/selection of transduced cells for research purposes [37].

Circulating $CD34^+$ cells, isolated from 2-16.5 ml of peripheral blood from 12 *TCIRG1*-mutated ARO patients (Table 1), were pre-stimulated with cytokines and then transduced either with PGK.TCIRG1 or PGK.TCIRG1/dNGFR (Figure 23B). Similar frequencies of BFU-E (burst-forming unit of erythroid cells) and CFU-GM (colony-forming unit of granulocyte/macrophage) colonies in transduced and non-transduced cells (Figure 23C) demonstrated that transduction did not impact on the clonogenic potential of HSPCs.

To compensate for HSPC shortage and the difficulties in collecting them from the PB of very young patients, we exploited a recently described *ex vivo* expansion protocol based on UM171 small molecule [19,20,38]. After transduction, cells were expanded for 5 additional days in the presence of early-acting cytokines and the pyrimidoindole derivative UM171, reaching a total culture time of 7 days (Figure 23B), as practiced in the UM171-based cord blood expansion trials [39].

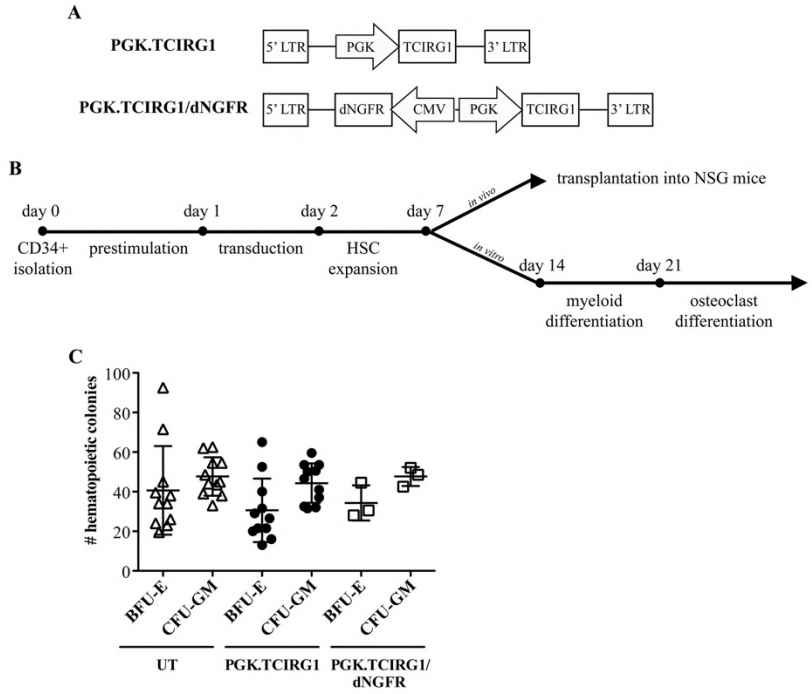


**Figure 23. Transduction and expansion.** (A) Schematic representation of the 2 vector constructs driving *TCIRG1* expression: the PGK.TCIRG1 vector and PGK.TCIRG1/dNGFR bidirectional vector. LTR, long terminal repeat; PGK, phosphoglycerate kinase promoter; TCIRG1, T

cell immune regulator 1; dNGFR, deleted nerve growth factor receptor; CMV, cytomegalovirus promoter. (B) Time-line of transduction, expansion and in vivo and in vitro studies. (C) Absolute counts of hematopoietic progenitor colonies obtained in MethoCult cultures. BFU-E, burst-forming unit of erythroid cells; CFU-GM, colony-forming unit of granulocyte/macrophage. Data show mean ± SD.

In line with published data [38], UM171 exposure induced the expansion of the total $CD34^+$ cells. We observed a 10.4 mean fold expansion, with differences probably due to patient-to-patient variability, regardless of UM171 dose (Figure 24A). Cells exposed to the TCIRG1-expressing LVs showed a similar fold expansion as compared to their untransduced counterparts, confirming that UM171 expansion protocol can also be used in the setting of gene therapy [19]. Importantly, the HSC-containing $CD34^+$ $CD90^+$ $EPCR^+$ (endothelial protein C receptor) cell subpopulation expanded both in terms of absolute counts (Figure 24B) and relative frequency within the $CD34^+$ population (Figure 24C and Online Supplementary Figure S3A-B). The triple positive $CD34^+$ $CD90^+$ $EPCR^+$ population was present at comparable frequency in both transduced and untransduced cells (Online Supplementary Figure S3C).

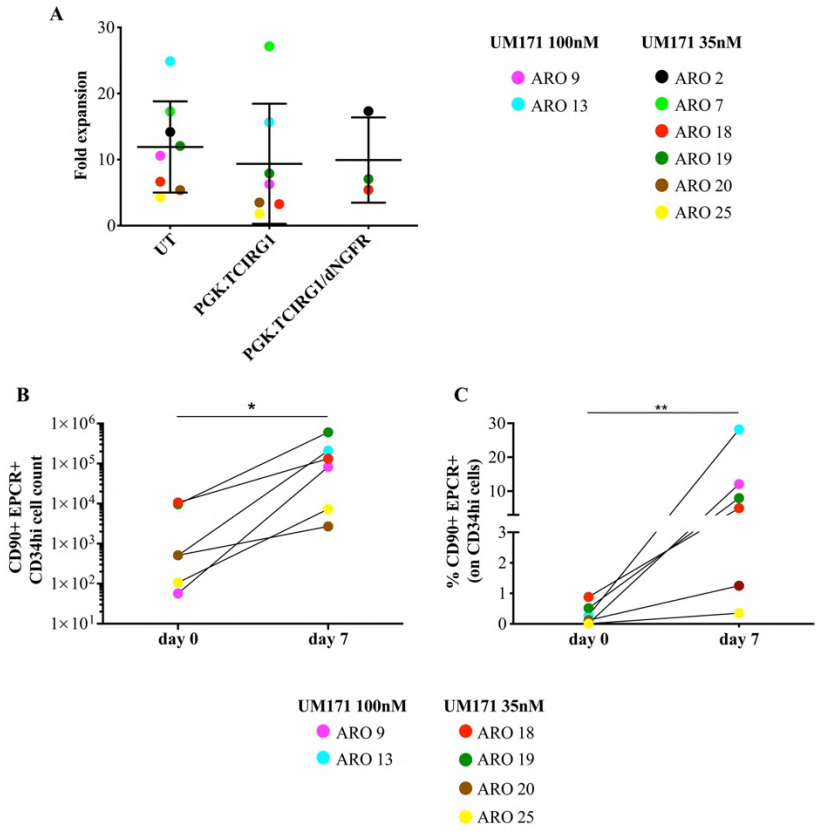


**Figure 24. HSPC expansion.** (A) Fold expansion, calculated as a ratio between total CD34$^+$ cells at the start of the culture and at the end of expansion phase in untransduced (UT) or transduced (PGK.TCIRG1 and PGK.TCIRG1/dNGFR) patient cells. (B) Absolute counts of the CD34high CD90$^+$ EPCR$^+$ population, which is enriched for the long-term HSC, at day 0 (freshly isolated CD34$^+$ cells) and day 7 (end of expansion phase). Each color represents a different untransduced patient, cultured with 35 or 100 nM UM171, as indicated in figure. (C) Frequency of the CD90$^+$ EPCR$^+$ population on the CD34high cells at day 0 and at day 7. As in panel A, each color represents a different untransduced patient, cultured with 35 or 100 nM UM171, as indicated in figure. Statistical significance was determined by non-parametric one-way ANOVA with

Dunns post-test (panel A) or non-parametric Mann Whitney test (panels B and C). * $p<0.05$, ** $p<0.01$. Data show mean ± SD.

### *In vitro correction of osteoclast defect*

Transduced and expanded $CD34^+$ cells were differentiated *in vitro* into myeloid progenitors and then into osteoclasts, in order to assess the correction of osteoclast resorptive function.

As expected, osteoclasts derived from *TCIRG1*-mutated patients were able to normally fuse and differentiate into mature, multinucleated, tartrate-resistant acid phosphatase (TRAP)-positive osteoclasts, although not functional (Online Supplementary Figure S4). We verified that osteoclasts from ARO patients did not express TCIRG1 protein. Transduction with the LV PGK.TCIRG1 restored the expression of the TCIRG1 protein, as assessed by Western Blot (Online Supplementary Figure S5).

To assess the functionality of gene-corrected cells, we cultured osteoclasts derived from untransduced and transduced patient cells on bone slices and analyzed the bone resorption by immunofluorescence and confocal microscopy after 2-3 weeks. The assembled nuclei (stained with TO-PRO-3) and the presence of actin rings (stained with phalloidin) confirmed osteoclast differentiation on the bone slices (Figure 25A). Untransduced patient cells were not able to resorb bone slices, as shown by the absence of alendronate-positive resorption pits. Conversely, gene-corrected patient-derived $CD34^+$ were able to form fully functional osteoclasts, even at low vector copy number/genome (VCN). These findings were confirmed by toluidine blue staining, that was

performed on bone slices after cell removal. Resorption pits were visible only on bone discs in the presence of patient corrected cells (Figure 25B). To quantify the resorption levels, we measured the C-terminal telopeptide fragment of type I collagen (CTX-I), a degradation marker of collagen released during bone and cartilage resorption. We quantified the CTX-I concentration in the culture supernatant at day 0 (start of the culture), at day 8 (intermediate time point), and at day 21 (end of the culture) by ELISA. Transduced patient cells resorbed bone slices at levels comparable to healthy donor cells at both days 8 and 21. Conversely, untransduced patient cells were not able to resorb bone (Figure 25C). The CTX-I levels did not show a statistically significant correlation with the VCN, probably due to the variability of the osteoclast differentiation assay (Online Supplementary Figure S6). However, high levels of resorption were found also in cells with low VCN, supporting the hypothesis that osteoclasts may be functional even in case of a minor fraction of corrected nuclei.

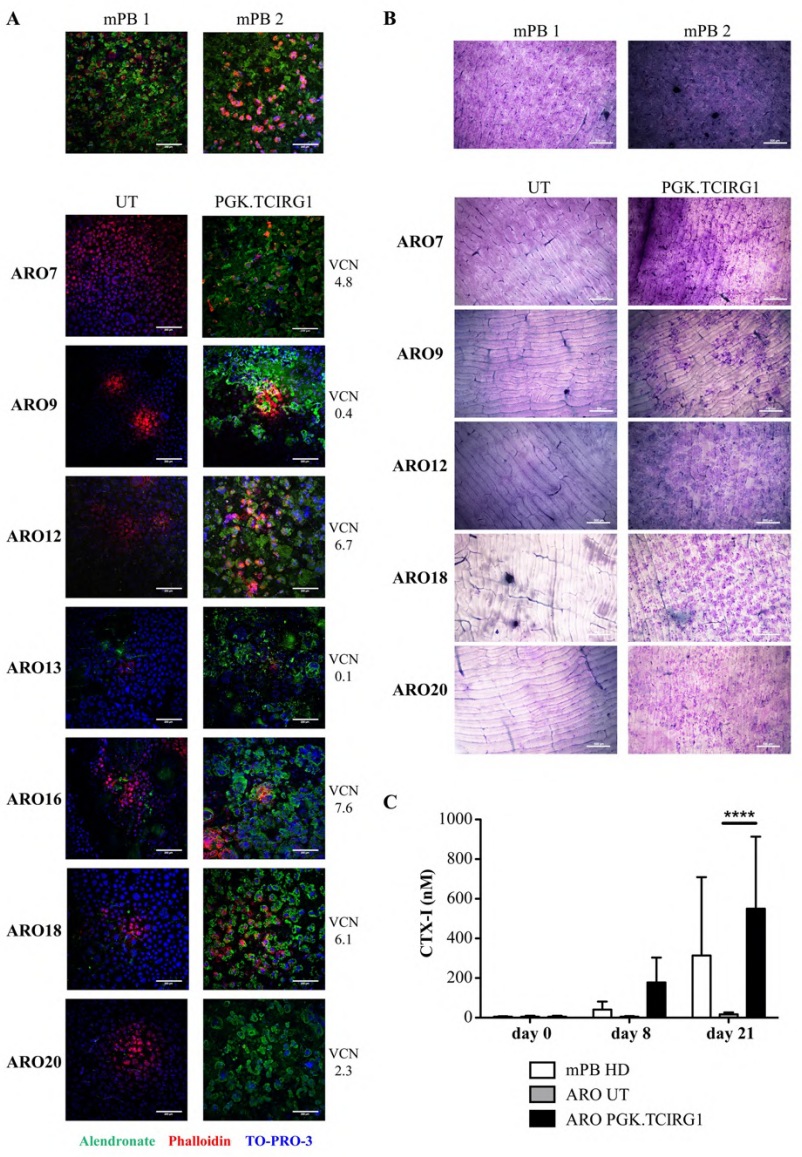


**Figure 25. Osteoclast bone resorption.** (A) Immunofluorescence staining of osteoclasts differentiated from $CD34^+$ cells and cultured on bone slices. Images show the merge result of alendronate-AF-488 (resorption pits in green), phalloidin-TRITC (actin rings in red) and TO-PRO-3 (nuclei in blue). The upper part shows representative images of osteoclasts obtained from mobilized peripheral blood $CD34^+$ cells from

2 healthy donors (mPB), while the panels below show representative images of untransduced (UT) or transduced (PGK.TCIRG1) osteoclasts from 7 ARO patients. Vector copy numbers (VCN) of the transduced cells are indicated for each patient. Images were acquired with Leica TCS SP5 laser scanning confocal, equipped with HC PL FLUOTAR 10X (NA 0.3) dry and Leica Application Suite Advanced Fluorescence (LASAF) software. (B) Toluidine blue staining of bone slices that were previously cultured with osteoclasts from healthy donor peripheral blood mobilized $CD34^+$ cells (mPB) and ARO patient untransduced (UT) or transduced (PGK.TCIRG1) cells. Vector copy numbers (VCN) of the transduced cells are shown for each patient. Images were acquired with Nikon ECLIPSE E600 microscope equipped with Nikon DS-Ri2 camera, using Plan Fluor 4x/0.13 objective and NIS-Elements F 4.30.01 software. (C) C-terminal telopeptide fragment of type I collagen (CTX-I) quantification in the osteoclast culture supernatant at day 0, day 8 and day 21. Healthy donor peripheral blood mobilized $CD34^+$ cells (mPB HD) in white, ARO patient untransduced (ARO UT) cells in grey and ARO patient transduced (ARO PGK.TCIRG1) in black. Statistical significance was determined by two-way ANOVA with Bonferroni post-test (panel C). **** $p<0.0001$. All data show mean ± SD.

### *In vivo repopulating capacity of expanded $CD34^+$ cells*

To evaluate the capability of gene-corrected ARO-$CD34^+$ cells to engraft and to fully differentiate in all hematopoietic lineages, we transplanted a median of $0.75x10^6$ expanded $CD34^+$ cells (range $0.5\text{-}1x10^6$ cells) in NSG mice, which corresponded to 0.11-0.47 day0 equivalents per mouse (Online Supplementary Table S1 and Figure 23B). Mice were bled at 6 and 10 weeks, and euthanized at

13 weeks to study human cell engraftment. We observed the presence of stable human hematopoietic ($CD45^+$) multilineage cell engraftment in peripheral blood, starting from 6 weeks after transplant (Figure 26A). The engraftment showed donor-dependent variability, not correlating with the transplanted day0 equivalents, the transduction status of the cells, or the UM171 dosage.

At 13 weeks post-transplant, we sacrificed the mice and analyzed the hematopoietic organs. In accordance to the results obtained in the peripheral blood, we observed similar level of human $CD45^+$ cell engraftment in the spleen and in the BM. In the thymus, nearly 100% of the cells were of human origin as expected (Figure 26B). The majority of human cells were B cells ($CD19^+$), as a consequence of the human cell differentiation bias in NSG mice. Nonetheless, we could observe the presence of myeloid (CD13+) and T ($CD3^+$) cells in the hematopoietic organs and also of CD34+ HSPCs in the BM (Figure 26C). Importantly, transduced cells were retrieved in the analyzed tissues, in line with the VCN of the *in vitro* cultures (Figure 26D), indicating long-term engraftment ability by TCIRG1-expressing HSPCs.

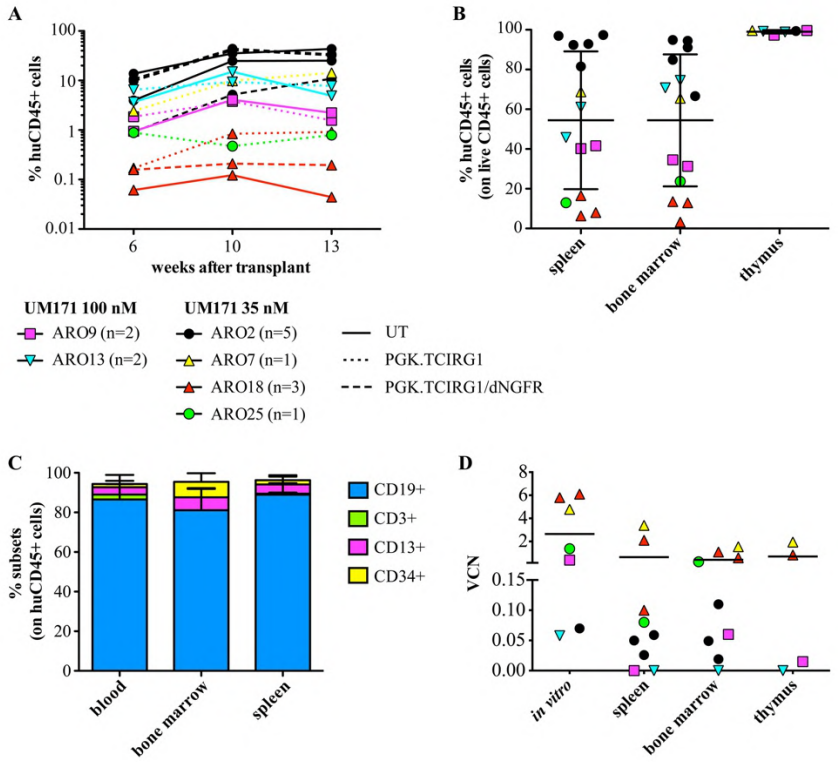


**Figure 26. Transplants in primary NSG recipients.** (A) Percentage of human hematopoietic (huCD45+) cells in the peripheral blood of primary NSG recipients overtime. Each colour represents a different patient, as indicated in figure. UM171 dosage used for $CD34^+$ cell expansion is also indicated. Continuous line indicates untransduced (UT) cells, dotted line indicates cells transduced with PGK.TCIRG1 vector and dashed line indicates cells transduced with PGK.TCIRG1/dNGFR vector. (B) Percentage of human hematopoietic ($huCD45^+$) cells on total $CD45^+$ cells in spleen, bone marrow and thymus at sacrifice. (C) Percentage of $CD19^+$ (B lymphocytes, in blue), $CD3^+$ (T lymphocytes, in green), $CD13^+$ (myeloid cells, in pink) and $CD34^+$ (hematopoietic stem and progenitor cells, in yellow) subsets on the total human $CD45^+$ cells. (D) Vector copy number (VCN) of in vitro transplanted cells and in tissues (spleen, bone

marrow and thymus). Data show mean (panel A) or mean ± SD (panels B and C).

After sacrifice of NSG mice, human $CD34^+$ cells were re-isolated from the BM and transplanted in secondary NSG recipients. We isolated 0.7-1x$10^6$ $CD34^+$ cells from each mouse and transplanted them into a different recipient. We observed low but stable human engraftment overtime in secondary recipients up to 13 weeks after transplantation, indicating that our transduction and expansion strategy allowed the maintenance of long-term HSCs (Figure 27A). Similarly, to the results obtained in primary recipients, variable $CD45^+$ frequencies were observed in the spleen and in the BM, whereas the thymus showed nearly 100% of human $CD45^+$ cells (Figure 27B). In the secondary grafts, multi-lineage cell repopulation was observed, with the expected prevalence of $CD19^+$ cells (B lymphocytes) and the presence of $CD34^+$ cells in the BM (Figure 27C). Vector copy number in the hematopoietic organs was consistent with the transduction levels of the primary recipients (Figure 27D), indicating the long-term maintenance of gene-corrected primitive HSPCs.

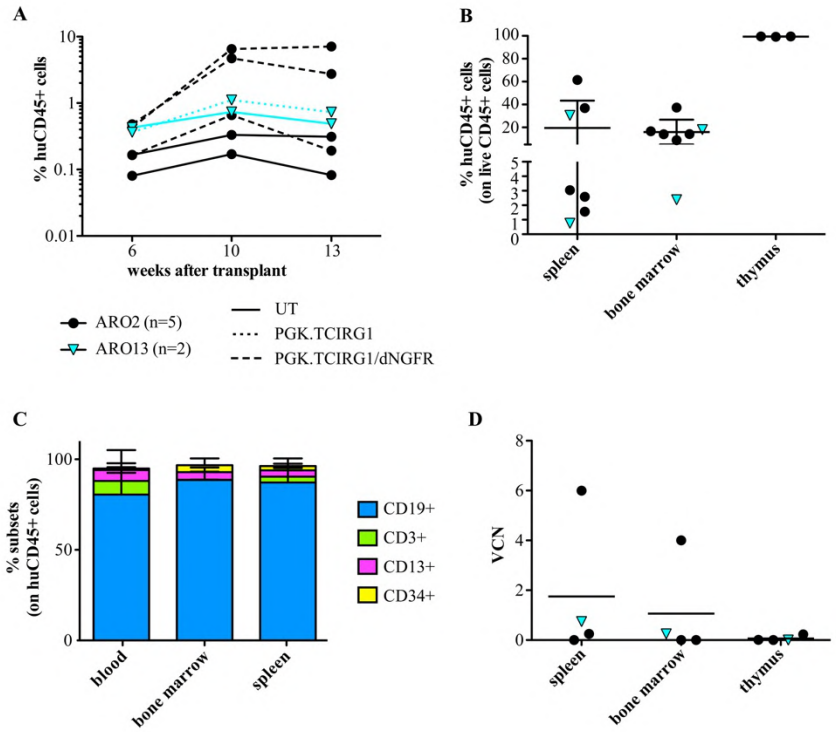


**Figure 27. Transplants in secondary NSG recipients**. (A) Percentage of human hematopoietic (huCD45$^+$) cells in the peripheral blood of secondary NSG recipients overtime. Each color represents a different patient, as indicated in figure. Continuous line indicates untransduced (UT) cells, dotted line indicates cells transduced with PGK.TCIRG1 vector and dashed line indicates cells transduced with PGK.TCIRG1/dNGFR vector. (B) Percentage of human hematopoietic (huCD45$^+$) cells on total CD45$^+$ cells in spleen, bone marrow and thymus at sacrifice. (C) Percentage of CD19$^+$ (B lymphocytes, in blue), CD3$^+$ (T lymphocytes, in green), CD13$^+$ (myeloid cells, in pink) and CD34$^+$ (hematopoietic stem and progenitor cells, in yellow) subsets on the total human CD45$^+$ cells. (D) Vector copy number (VCN) of in vitro transplanted cells and in tissues (spleen, bone marrow and thymus). Data show mean (panel D) or mean ± SD (panel B and C).

## Discussion

To date, hematopoietic stem cell transplantation is the treatment of choice in patients with severe forms of autosomal recessive osteopetrosis, a rare genetic disease characterized by defective osteoclast function and bone marrow fibrosis. Infusion of autologous gene corrected HSPCs may represent an attractive therapy to avoid the risk of severe graft-versus-host-disease reactions and limit complications caused by intensive myeloablative conditioning. Gene therapy would also allow treatment of patients without compatible donors or whose severe clinical conditions and/or age preclude conventional therapy [7,40]. In addition, mild forms of *TCIRG1* osteopetrosis have been recently identified in adult patients rising concerns about the risk of life-threating complications during conventional therapy [41]. However, contrary to other inherited diseases treated with gene therapy [42], the development of novel strategies is required in osteopetrosis to overcome clinical limitations that may hamper gene therapy applicability [43]. For this reason, we developed a tailored approach for the treatment of *TCIRG1*-mutated osteopetrosis exploiting autologous HSPC gene correction and expansion.

Although previous studies have demonstrated the feasibility of gene therapy [12-15], its clinical applicability remains constrained by the scarcity of a bone marrow niche and the limited amount of blood that can be drawn in these patients to collect circulating hematopoietic precursors. Remarkably, $CD34^+$ cells isolated from

peripheral blood of ARO patients have been reinfused successfully in two transplanted osteopetrotic patients with no engraftment and other complications, providing clinical evidence that circulating $CD34^+$ cells can engraft and speed count recovery [16]. In spite of these observations, studies on the phenotypic composition and transcriptome of these spontaneously mobilized HSPCs were lacking in literature. To assess relative frequencies and absolute counts/µl of blood cellular components, we took advantage of a multiparametric flow-cytometry analysis that allows the dissection of 23 different blood cell types, including HSPCs, myeloid and lymphoid progenitors [27]. Notably, HSC counts/µl were comparable to those observed in the bone marrow of healthy children, supporting the feasibility of exploiting non-mobilized peripheral blood as an easily accessible source for hematopoietic stem cells in these patients.

These results were corroborated by the transcriptomic profile of circulating $CD34^+$ cells from ARO patients, showing a positive enrichment for committed progenitors signatures, in particular for granulocyte-monocyte progenitor (GMP) cells. As recently described [44], osteoclast defects can be rescued by monocytic cells transfusion in osteopetrotic mice. The simultaneous presence of HSCs and myeloid lineage cells makes the circulating $CD34^+$ cells a favorable cell source for gene therapy. The heterogeneity of the population, containing both committed and primitive progenitors, would allow for an initial reconstitution after transplant sustained by differentiated progenitors, followed by a later output of transduced cells from long-term engrafting cells

[45]. The long-term survival capability of PB ARO-CD34$^+$ cells is supported by our *in vivo* transplantation analyses, indicating that expanded gene-modified PB HSPCs from ARO patients are able to maintain long-term multi-lineage engineered hematopoiesis both in primary and in secondary transplanted mice.

To further enhance the number of HSPC that can be collected by exchange transfusion, here we proposed an innovative strategy coupling transduction protocol with efficient *ex vivo* expansion of genetically modified HSCs. We exploited the small molecule pyrimidoindole derivate UM171, that has been demonstrated to stimulate the *in vitro* expansion of human HSC and to enhance lentiviral transduction efficiency of CB derived CD34$^+$ cells, maintaining their short and long-term repopulating potential [19,20,38,46].

The availability of UM171-expanded gene corrected CD34$^+$ cells may allow the cryopreservation of corrected HSPC backup available for potential repeated administration. We can speculate that patients with low chimerism may benefit from repeated infusions in the absence of conditioning, as modelled in osteopetrotic mice [44,47]. Remarkably, we demonstrated multi-lineage engraftment of PB CD34$^+$ cells in immunodeficient mice upon *ex vivo* manipulation, including transduction and/or expansion. Of note, for the first time, we assessed the maintenance of long-term repopulating capacity in NSG secondary recipients of UM171-expanded CD34$^+$ cells, indicating the presence of *bona fide* LT-HSC in the expanded and corrected cell population.

In order to pursue the clinical applicability of our approach, we designed a *TCIRG1*-expressing LV based on the vector approved and currently in use in the clinical trial for mucopolysaccharidosis type I (clinical trial TigetT10_MPSIH, NCT03488394) [48,49]. In our *in vitro* studies *TCIRG1*-corrected CD34+ with low VCN are able to resorb bone substrate, indicating that a limited number of corrected nuclei could provide for adequate protein levels in the mature multinucleated osteoclast. These results are in line with previous studies showing *in vivo* bone resorption in *oc/oc* mice with 1-3% of BM engraftment, likely due to the fusion of corrected hematopoietic progenitors to uncorrected cells [14,47,50].

Importantly, the unregulated expression of TCIRG1 protein driven by the cellular ubiquitous *PGK* promoter does not impact on the clonogenic potential of HSPCs, as shown by methylcellulose cultures.

In conclusion, here we provide a clinically applicable multi-step approach for autosomal recessive osteopetrosis based on the use of an optimized vector, an accessible HSPC source and reliable HSC expansion culture conditions. Our strategy may overcome all the major limitations related to the low number of $CD34^+$ cells retrievable from ARO patients. Namely, peripheral blood $CD34^+$ cells with primitive phenotype were easily collected and transduced with the corrective PGK.TCIRG1 vector. Then, the UM171-based HSC expansion culture overcame the limited access to high blood volumes in severely affected children. These major improvements would allow the implementation of a clinical trial for autosomal recessive osteopetrosis in the next future and the

exploitation of circulating $CD34^+$ cells in other clinical conditions characterized by bone marrow fibrosis.

## References


1. Teti A, Teitelbaum SL. Congenital disorders of bone and blood. Bone 2019;11971–81.
2. Sobacchi C, Schulz A, Coxon FP, Villa A, Helfrich MH. Osteopetrosis: Genetics, treatment and new insights into osteoclast function. Nat Rev Endocrinol 2013;9(9):522–536.
3. Palagano E, Menale C, Sobacchi C, Villa A. Genetics of Osteopetrosis. Curr Osteoporos Rep 2018;16(1):13–25.
4. Frattini A, Orchard PJ, Sobacchi C, et al. Defects in TCIRG1 subunit of the vacuolar proton pump are responsible for a subset of human autosomal recessive osteopetrosis. Nat Genet 2000;25(3):343–346.
5. Wu CC, Econs MJ, DiMeglio LA, et al. Diagnosis and management of osteopetrosis: Consensus guidelines from the osteopetrosis working group. J Clin Endocrinol Metab 2017;102(9):3111–3123.
6. Stepensky P, Grisariu S, Avni B, et al. Stem cell transplantation for osteopetrosis in patients beyond the age of 5 years. Blood Adv 2019;3(6):862–868.
7. Teti A, Econs MJ. Osteopetroses, emphasizing potential approaches to treatment. Bone 2017;10250–59.
8. Steward CG. Hematopoietic Stem Cell Transplantation for Osteopetrosis. Pediatr Clin NA 2010;57(1):171–180.
9. Orchard PJ, Fasth AL, Le Rademacher JL, et al. Hematopoietic stem cell transplantation for infantile osteopetrosis. Blood 2015;126(2):270–276.
10. Schulz AS, Moshous D, Steward CG, Villa A, Sobacchi C. Osteopetrosis Consensus guidelines for diagnosis, therapy and follow-up. ESID EBMT 2015;1–35.
11. Chiesa R, Ruggeri A, Paviglianiti A, et al. Outcomes after Unrelated Umbilical Cord Blood Transplantation for Children with Osteopetrosis. Biol Blood Marrow Transplant 2016;22(11):1997–2002.
12. Johansson MK, De Vries TJ, Schoenmaker T, et al. Hematopoietic stem cell-targeted neonatal gene therapy reverses lethally progressive osteopetrosis in oc/oc mice. Blood 2007;109(12):5178–5185.
13. Moscatelli I, Löfvall H, Schneider Thudium C, et al. Targeting NSG Mice Engrafting Cells with a Clinically Applicable

Lentiviral Vector Corrects Osteoclasts in Infantile Malignant Osteopetrosis. Hum Gene Ther 2018;29(8):938–949.
14. Moscatelli I, Thudium CS, Flores C, et al. Lentiviral gene transfer of TCIRG1 into peripheral blood CD34+ cells restores osteoclast function in infantile malignant osteopetrosis. Bone 2013;57(1):1–9.
15. Löfvall H, Rothe M, Schambach A, Henriksen K, Richter J, Moscatelli I. Hematopoietic Stem Cell-Targeted Neonatal Gene Therapy with a Clinically Applicable Lentiviral Vector Corrects Osteopetrosis in oc/oc Mice. Hum Gene Ther 2019;Jul 3. [Epub ahead of print].
16. Steward CG, Blair A, Moppett J, et al. High peripheral blood progenitor cell counts enable autologous backup before stem cell transplantation for malignant infantile osteopetrosis. Biol Blood Marrow Transplant 2005;11(2):115–121.
17. Blin-Wakkach C, Rouleau M, Wakkach A. Roles of osteoclasts in the control of medullary hematopoietic niches. Arch Biochem Biophys 2014;56129–37.
18. Marcus JR, Fibach E, Aker M. Circulating myeloid and erythroid progenitor cells in malignant osteopetrosis. Acta Haematol 1982;67(3):185–189.
19. Zonari E, Desantis G, Petrillo C, et al. Efficient *Ex Vivo* Engineering and Expansion of Highly Purified Human Hematopoietic Stem and Progenitor Cell Populations for Gene Therapy. Stem Cell Reports 2017;8(4):977–990.
20. Fares I, Chagraoui J, Gareau Y, et al. Pyrimidoindole derivatives are agonists of human hematopoietic stem cell self-renewal. Science (80- ) 2014;345(6203):1509–1512.
21. Mazzolari E, Forino C, Razza A, Porta F, Villa A, Notarangelo LD. A single-center experience in 20 patients with infantile malignant osteopetrosis. Am J Hematol 2009;84(8):473–479.
22. Aiuti A, Biasco L, Scaramuzza S, et al. Lentiviral hematopoietic stem cell gene therapy in patients with wiskott-aldrich syndrome. Science (80- ) 2013;341(6148):1233151–1233151.
23. Biffi A, Montini E, Lorioli L, et al. Lentiviral hematopoietic stem cell gene therapy benefits metachromatic leukodystrophy. Science (80- ) 2013;341(6148):1233158–1233158.
24. Coxon FP. Fluorescence imaging of osteoclasts using confocal microscopy. In: Methods in Molecular Biology. 2012. p401–

424.
25. Menale C, Campodoni E, Palagano E, et al. Mesenchymal Stromal Cell-Seeded Biomimetic Scaffolds as a Factory of Soluble RANKL in Rankl-Deficient Osteopetrosis. Stem Cells Transl Med 2019;8(1):22–34.
26. Cimato TR, Furlage RL, Conway A, Wallace PK. Simultaneous measurement of human hematopoietic stem and progenitor cells in blood using multicolor flow cytometry. Cytometry B Clin Cytom 2016;90(5):415–423.
27. Basso-Ricci L, Scala S, Milani R, et al. Multiparametric Whole Blood Dissection: A one-shot comprehensive picture of the human hematopoietic system. Cytom Part A 2017;91(10):952–965.
28. Ramalho-Santos M, Yoon S, Matsuzaki Y, Mulligan RC, Melton DA. "Stemness": Transcriptional profiling of embryonic and adult stem cells. Science (80- ) 2002;298(5593):597–600.
29. Jaatinen T, Hemmoranta H, Hautaniemi S, et al. Global Gene Expression Profile of Human Cord Blood-Derived CD133 + Cells . Stem Cells 2005;24(3):631–641.
30. Eppert K, Takenaka K, Lechman ER, et al. Stem cell gene expression programs influence clinical outcome in human leukemia. Nat Med 2011;17(9):1086–1094.
31. Georgantas RW, Tanadve V, Malehorn M, et al. Microarray and serial analysis of gene expression analyses identify known and novel transcripts overexpressed in hematopoietic stem cells. Cancer Res 2004;64(13):4434–4441.
32. Doulatov S, Vo LT, Chou SS, et al. Induction of multipotential hematopoietic progenitors from human pluripotent stem cells via respecification of lineage-restricted precursors. Cell Stem Cell 2013;13(4):459–470.
33. Laurenti E, Doulatov S, Zandi S, et al. The transcriptional architecture of early human hematopoiesis identifies multilevel control of lymphoid commitment. Nat Immunol 2013;14(7):756–763.
34. Park IK, He Y, Lin F, et al. Differential gene expression profiling of adult murine hematopoietic stem cells. Blood 2002;99(2):488–498.
35. Zheng S, Papalexi E, Butler A, Stephenson W, Satija R. Molecular transitions in early progenitors during human cord blood hematopoiesis. Mol Syst Biol 2018;14(3):e8041.

36. Clien L, Kostadraia M, Martens JHA, et al. Transcriptional diversity during lineage commitment of human blood progenitors. Science (80- ) 2014;345(6204):1251033.
37. Amendola M, Venneri MA, Biffi A, Vigna E, Naldini L. Coordinate dual-gene transgenesis by lentiviral vectors carrying synthetic bidirectional promoters. Nat Biotechnol 2005;23(1):108–116.
38. Fares I, Chagraoui J, Lehnertz B, et al. EPCR expression marks UM171-expanded CD34+ cord blood stem cells. Blood 2017;129(25):3344–3351.
39. Cohen S, Roy J, Lachance S, et al. Single UM171 Expanded Cord Blood Permits Transplantation of Better HLA Matched Cords with Excellent Gvhd Relapse Free Survival. Blood 2018;132(Suppl 1):4658–4658.
40. Askmyr M, Flores C, Fasth A, Richter J. Prospects for Gene Therapy of Osteopetrosis. Curr Gene Ther 2009;9(3):150–159.
41. Palagano E, Blair HC, Pangrazio A, et al. Buried in the middle but guilty: Intronic mutations in the TCIRG1 gene cause human autosomal recessive osteopetrosis. J Bone Miner Res 2015;30(10):1814–1821.
42. Gawthorpe P. Gene Therapy Gene Therapy. Nurs Stand 2003;17(33):29–29.
43. Penna S, Capo V, Palagano E, Sobacchi C, Villa A. One disease, many genes: Implications for the treatment of osteopetroses. Front Endocrinol (Lausanne) 2019;10(Feb):85.
44. Jacome-Galarza CE, Percin GI, Muller JT, et al. Developmental origin, functional maintenance and genetic rescue of osteoclasts. *Nature* 2019;568(7753):541–545.
45. Scala S, Basso-Ricci L, Dionisio F, et al. Dynamics of genetically engineered hematopoietic stem and progenitor cells after autologous transplantation in humans. Nat Med 2018;24(11):1683–1690.
46. Ngom M, Imren S, Maetzig T, et al. UM171 Enhances Lentiviral Gene Transfer and Recovery of Primitive Human Hematopoietic Cells. Mol Ther - Methods Clin Dev 2018;10156–164.
47. Flores C, De Vries TJ, Moscatelli I, et al. Nonablative neonatal bone marrow transplantation rapidly reverses severe murine osteopetrosis despite low-level engraftment and lack of selective expansion of the osteoclastic lineage. J Bone Miner

Res 2010;25(9):2069–2077.
48. Gentner B, Bernardo ME, Zonari E, et al. Ex-Vivo Gene Therapy for Hurler Disease: Initial Results from a Phase I/II Clinical Study. Mol Ther 2019;27(4S1):abstr. 2.
49. Squeri G, Passerini L, Ferro F, et al. Targeting a Pre-existing Anti-transgene T Cell Response for Effective Gene Therapy of MPS-I in the Mouse Model of the Disease. Mol Ther 2019;27(7):1215–1227.
50. Thudium CS, Moscatelli I, Löfvall H, et al. Regulation and Function of Lentiviral Vector-Mediated TCIRG1 Expression in Osteoclasts from Patients with Infantile Malignant Osteopetrosis: Implications for Gene Therapy. Calcif Tissue Int 2016;99(6):638–648.

**Supplementary Methods**

***Patients and healthy donors.*** We collected samples of bone marrow (BM) and peripheral blood (PB) from healthy donors for which exceeding materials were available. BM samples from pediatric HD were previously described [1].
Cord blood (CB) cells were purchased from Lonza. Mobilized PB $CD34^+$ cells were positively selected using the RoboSep device (Stemcell Technologies) from peripheral blood of consenting donors of allogeneic stem cells undergoing blood stem cell mobilization.

***Vector production.*** PGK.TCIRG1 lentiviral vector was produced as previously described [2,3], substituting the IDUA transgene with the TCIRG1 cDNA sequence (GeneArt Gene Synthesis, Thermo Fisher Scientific). In the PGK.TCIRG1/dNGFR, we added the dNGFR marker gene, driven by the CMV promoter.

***Vector copy number.*** Genomic DNA was extracted with QIAamp DNA Blood mini kit (QIAGEN), according to manufacturer's instructions. Vector copy number/genome (VCN) was calculated on transduced cells and transduced hematopoietic progenitors as previously described [4].

***Expansion.*** Transplanted day0 equivalents are calculated as ratio between total cells at the end of the expansion and the number of transplanted cells in each NSG mice.

***Flow cytometry analysis.*** Cells were stained with the following anti-human antibodies (BD Pharmingen, Miltenyi Biotec, Biolegend or eBioscience): CD3 clone BW264/56, CD4 clone VIT4, CD8 clone BW135/80, CD13 clone WM15, CD19 clone SJ25C1, CD34 clones AC136 and 581, CD38 clone HIT2, CD45 clones 5B1 and 2D1, CD45RA clone HI100, CD90 clone 5E10, dNGFR clone ME20.4-1.H4. Viability was determined with live/dead fixable dead cell stain kit (ThermoFisher Scientific). Samples were acquired on FACS Canto II or LSRFortessa (BD) and analyzed with FlowJo software.
The multiparametric whole blood dissection was performed as previously described [1].

***RNAseq.*** Total RNA was used to generate mRNA-Seq libraries using the SMART- Seq v4 Ultra low-input RNA kit for sequencing according to the manufacturer's instructions (Takara Bio). The quality of PCR library products was evaluated with the Bioanalyzer (Agilent). Pooled libraries were sequenced in one lane of a single-end flow-cell on an Illumina HiSeq 3000. On average, 25 million of 50bp single-end reads were generated for each sample.
RNA-seq data were aligned to the human reference genome (GRCh38/hg38) using STAR (v2.7.0d) with standard input parameters. Gene counts were produced with featureCounts

(Subread v1.6.3) using GENCODE v29 as reference gene annotation. Read counts were processed using edgeR (v3.20.9), using the standard protocol as reported in the respective manual. Differentially expressed genes were determined considering FDR corrected p-values (FDR <0.05). Gene Set Enrichment Analysis (GSEA) were computed using clusterProfiler (v 3.8.1, http://bioconductor.org/packages/release/bioc/html/clusterProfiler.html) on gene lists ranked by logFC considering different datasets (Gene Ontology, KEGG Pathway Database, Reactome Pathway Database, Disease Ontology, Molecular Signatures Database). Heatmaps were produced using pheatmap (v1.0.12) R package.

***Data Sharing Statement.*** Microarray data are available at GEO under accession number GSE132889.

***Western Blot.*** Osteoclasts were lysed with RIPA buffer (ThermoFisher Scientific) and proteins were quantified using Bio-Rad protein assay kit II (Bio-Rad). Proteins were denatured in Laemmli loading buffer and a total of 10-15 μg of proteins were separated by gel electrophoresis in a precast gel SDS-PAGE 7.5% (Mini- PROTEAN® TGXTM Gels, Bio-Rad) followed by blotting onto nitrocellulose membrane. After blocking in 5% skim milk in Tris-buffered saline (TBS) with 0.05% Tween 20 (TBST), the membrane was incubated overnight with mouse monoclonal anti-TCIRG1 (Abnova) or rabbit polyclonal anti-p38 MAPK (Cell Signalling Technology) and appropriate secondary antibody: anti-mouse IgG-HRP or anti-rabbit IgG-HRP (Cell Signalling

Technology). Blots were developed using Western Lightning Plus-ECL (Perkin Elmer) and images were acquired using ChemiDoc Imaging System (Bio-Rad).

**References (Supplementary materials)**


1. Basso-Ricci L, Scala S, Milani R, et al. Multiparametric Whole Blood Dissection: A one-shot comprehensive picture of the human hematopoietic system. Cytom Part A 2017;91(10):952–965.
2. Visigalli I, Delai S, Ferro F, et al. Preclinical Testing of the Safety and Tolerability of Lentiviral Vector-Mediated Above-Normal Alpha-L- Iduronidase Expression in Murine and Human Hematopoietic Cells Using Toxicology and Biodistribution Good Laboratory Practice Studies. Hum Gene Ther 2016;27(10):813–829.
3. Visigalli I, Delai S, Politi LS, et al. Gene therapy augments the efficacy of hematopoietic cell transplantation and fully corrects mucopolysaccharidosis type I phenotype in the mouse model. Blood 2010;116(24):5130–5139.
4. Scala S, Basso-Ricci L, Dionisio F, et al. Dynamics of genetically engineered hematopoietic stem and progenitor cells after autologous transplantation in humans. Nat Med 2018;24(11):1683–1690.

## Supplementary figures

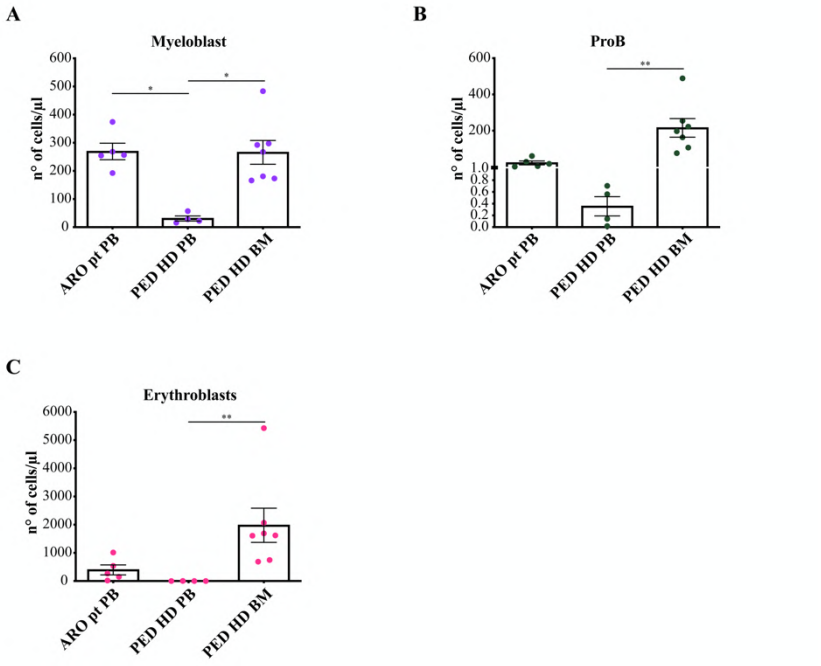


**Supplementary figure S1.** Immature subsets. Cell count/µl of myeloblasts (a), proB (b) and erythroblasts (c) in ARO patient peripheral blood (n=5), healthy donor peripheral blood (n=4) and bone marrow (n=7). Data show mean ± SEM. Statistical significance was determined by Kruskal-Wallis test with Dunn's multiple comparison post-test.

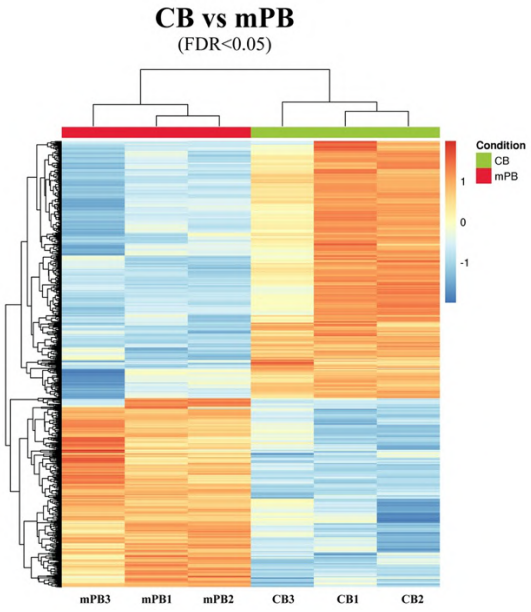


**Supplementary figure S2. RNA sequencing.** Heatmap shows unsupervised hierarchical clustering on differentially expressed genes (DEGs) of CB versus mPB.

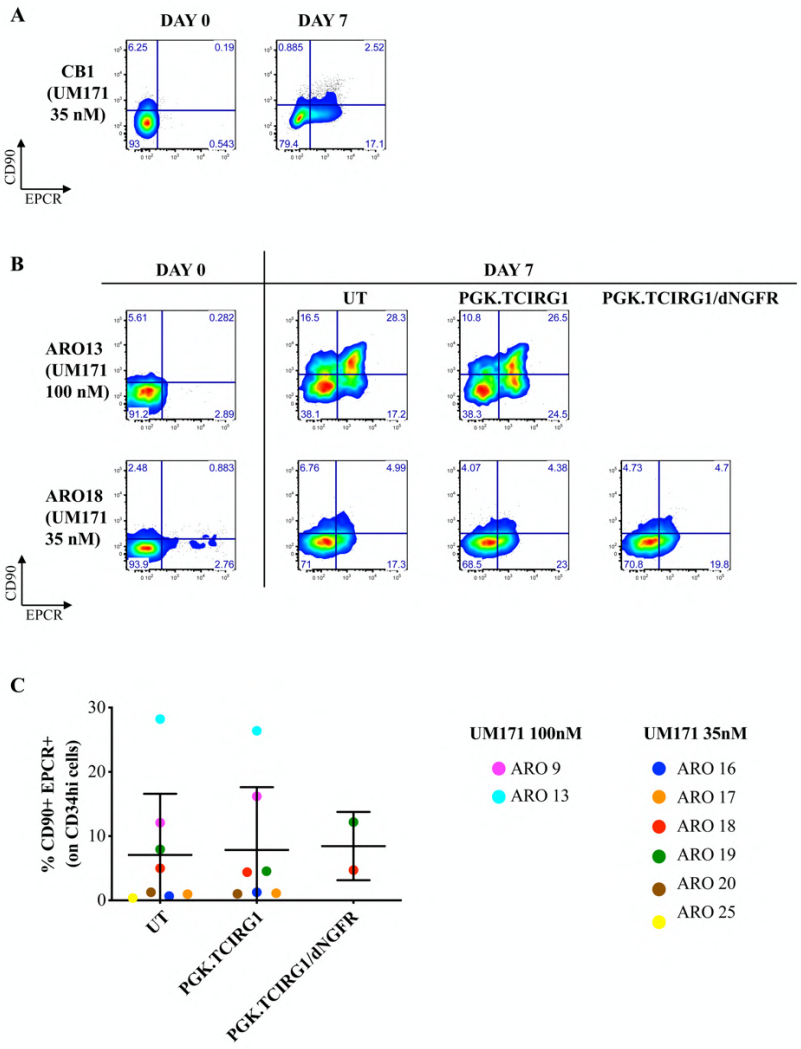


**Supplementary figure S3. HSPC expansion protocol.** (a) Representative FACS plot of $CD34^+$ cells from a healthy donor cord blood (CB) at day 0 and at day 7. (b) Representative FACS plot of $CD34^+$ cells from 2 ARO patients at day 0 and at day 7, cultured with UM171 at a concentration of 35 (ARO18) or 100 nM (ARO13). Plots in panels a and b show CD90 and EPCR marker expression on the $CD34^+$

population. (c) Percentage of the $CD90^+$ $EPCR^+$ population on the CD34high cells at day 7 in untransduced (UT) or transduced (PGK.TCIRG1 and PGK.TCIRG1/dNGFR) patient cells, cultured with 35 or 100 nM UM171, as indicated in figure.

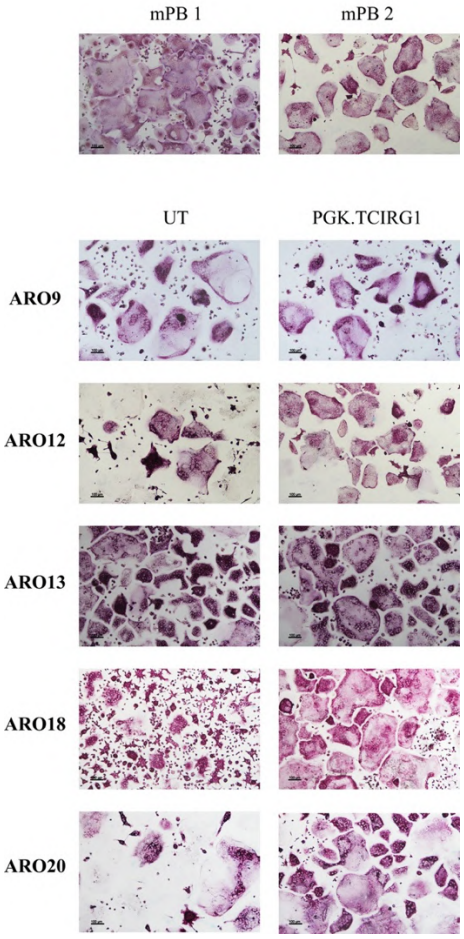


**Supplementary figure S4. TRAP staining.** Osteoclasts differentiated on plastic well plates and stained for tartrate-resistant acid phosphatase (TRAP) activity. Images were acquired with Nikon ECLIPSE E600 microscope equipped with Nikon DS-Ri2 camera, using Plan Fluor 4x/0.13 objective and NIS-Elements F 4.30.01 software.

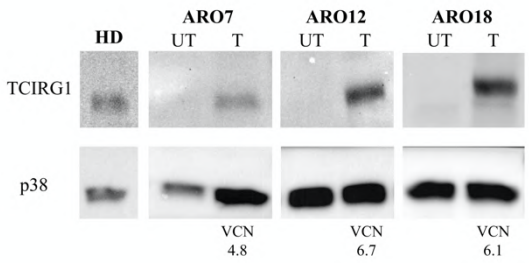


**Supplementary figure S5. Western Blot.** Western Blot analysis on total cell lysate of osteoclasts of a healthy donor (HD) and 3 different ARO patients. UT = untransduced, T = transduced with LV.PGK.TCIRG1

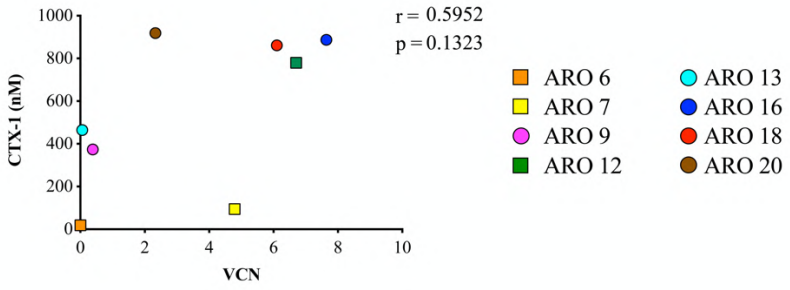


**Supplementary figure S6. Correlation VCN/resorption.** Correlation between vector copy number/genome (VCN) of $CD34^+$ cells and C-terminal telopeptide fragment of type I collagen (CTX-I) release in supernatant of $CD34^+$ derived osteoclast cultures. Statistical significance was determined by Spearman correlation and r value is indicated in figure.

**Supplementary Table S1.** Primary NSG transplants

| Patient | Mouse # | Transplanted with | | Transplanted d0 equivalents | % engraftment at 13w | | | *In vitro* VCN |
|---|---|---|---|---|---|---|---|---|
| | | Sample | Cell number | | Blood | Spleen | Bone marrow | |
| ARO2 | 1 | ARO2 PGK.TCIRG1/dNGFR | 7,00E+05 | 0.15 | 34.7 | 92.9 | 91.1 | 0.1 |
| | 2 | | 7,00E+05 | 0.15 | 33.3 | 97.0 | 94.4 | |
| | 3 | | 5,00E+05 | 0.11 | 11.1 | 81.5 | 66.6 | |
| | 4 | ARO2 UT | 5,00E+05 | 0.11 | 25.9 | 92.4 | 84.8 | 0.0 |
| | 5 | | 7,00E+05 | 0.15 | 49.8 | 97.3 | 94.9 | 0.0 |
| ARO7 | 6 | ARO7 PGK.TCIRG1 | 9,40E+05 | 0.31 | 14.7 | 68.8 | 65.5 | 4.8 |
| ARO9 | 7 | ARO9 PGK.TCIRG1 | 8,00E+05 | 0.41 | 1.6 | 41.6 | 34.6 | 0.4 |
| | 8 | ARO9 UT | 5,00E+05 | 0.26 | 2.3 | 40.2 | 31.3 | 0.0 |
| ARO13 | 9 | ARO13 UT | 6,50E+05 | 0.39 | 5.0 | 45.8 | 70.8 | 0.0 |
| | 10 | ARO13 PGK.TCIRG1 | 8,00E+05 | 0.47 | 7.9 | 61.0 | 74.5 | 0.1 |
| ARO18 | 11 | ARO18 UT | 1,00E+06 | 0.16 | 0.1 | 8.0 | 3.2 | 0.0 |
| | 12 | ARO18 PGK.TCIRG1 | 8,00E+05 | 0.13 | 0.9 | 16.6 | 13.6 | 6.1 |
| | 13 | ARO18 PGK.TCIRG1/dNGFR | 1,00E+06 | 0.16 | 0.2 | 6.4 | 13.0 | 5.8 |
| ARO25 | 14 | ARO25 PGK.TCIRG1 | 8,74E+05 | 0.30 | 0.8 | 13.0 | 23.7 | 1.4 |

**Acknowledgments**

The authors would like to thank Miep Helfrich for helping with immunofluorescence and for valuable discussion. We would also like to thank ALEMBIC, an advanced microscopy laboratory established by IRCCS Ospedale San Raffaele and Università Vita-Salute San Raffaele. This research was supported by a grant from the Telethon Foundation (TGT16C05) to A.V. and partially by a fellowship from the European Calcified Tissue Society (ECTS) to V.C..

**Contributions**

V.C., S.P., S.S, L.B.R., E.D., L.S.S and L.C. performed experiments and analyzed the data. E.P., E.Z., G.D. and M.S. provided intellectual input, reagents, and protocols. I.M., M.B., P.U. and R.C. performed and analyzed RNAseq experiments. D.M., P.S., K.D., Z.K., E.U., A.G., G.M., A.A., S.L.L., C.C.S. and A.S. provided patient samples and data. V.C., S.P, F.F. and C.S. contributed to write the manuscript. B.G. and A.V. designed and coordinated the research. All authors critically revised the manuscript.

**Conflict of interest and disclosure**

All authors declare no conflict of interest.

**Chapter 4**

# Investigation of the bone damage in Mucopolysaccharidosis type I Hurler Syndrome: pathophysiological mechanisms and impact of *ex-vivo* gene therapy

Sara Penna[1,2#], Stefania Crippa[1#], Valentina Capo[1,3#], Ludovica Santi[1#], Roberto Bosotti[1], Marta Serafini[2], Bernhard Gentner[1], Alessandro Aiuti[1], Anna Villa[1,3], Maria Ester Bernardo[1]

[1]San Raffaele-Telethon Institute for Gene Therapy (SR-Tiget); San Raffaele Scientific Institute, Milan, Italy.
[2]DIMET, University of Milano-Bicocca, School of Medicine and Surgery, Monza, Italy.
[3]Milan Unit, Istituto di Ricerca Genetica e Biomedica, Consiglio Nazionale delle Ricerche, Milan, Italy.
#contributed equally to this work

**Preface**

A phase I/II clinical trial of gene therapy to treat Mucopolysaccharidosis type I, Hurler variant (MPSIH) is currently ongoing in our Institute (NCT03488394). In the last year of my PhD program, I contributed to study the effect of *ex-vivo* gene therapy on defective mechanisms of bone homeostasis in Hurler syndrome, in close collaboration with the group directed by Prof. Bernardo. To this end, we have developed an *in vitro* cellular platform to study the crosstalk between the main bone cells, mesenchymal stem cells-derived osteocytes and osteoclasts before and after the treatment. In this collaborative framework, my activity has been focused on the characterization of MPSIH patient derived-osteoclasts in terms of osteoclastogenesis, function and IDUA production. In particular, this analysis has been performed on osteoclasts derived from monocytes obtained from the peripheral blood and from the drug product (MPSIH $CD34^+$ cells transduced with the clinical vector LV.PGK.IDUA). Here I describe preliminary results of this *in vitro* study and show clinical achievement provided by Prof. Bernardo to corroborate *in vitro* data.

**Abstract**

Hurler syndrome is a severe form of mucopolysaccharidosis type 1 (MPSIH), one of the most frequent autosomal recessive lysosomal storage diseases. MPSIH is caused by mutations in IDUA gene, encoding for IDUA enzyme, which is involved in the catabolism of glycosaminoglycans. MPSIH patients experience severe symptoms such as dysostosis multiplex, cognitive impairment, heart disease, respiratory problems, hepatosplenomegaly and reduced life expectancy. Despite several therapeutic interventions have been developed, including enzyme replacement therapy (ERT) and allogeneic hematopoietic stem cell transplantation (HSCT), the delivery of sufficient enzyme to the bones and, consequently, the correction of bone defects remains an unmet clinical need. A phase I/II clinical trial based on *ex-vivo* hematopoietic stem cell (HSC) gene therapy (GT) in MPSIH patients is ongoing at our institute SR-Tiget. Preliminary results showed sustained engraftment of gene-corrected cells accompanied by supraphysiologic IDUA levels in peripheral blood and from a clinical standpoint, improved motor function and joint mobility. However, the pathogenesis of bone defects in MPSIH is still debated. For this reason, we decide to characterize the different bone components of MPSIH patients and healthy donor controls. Osteoclast (OC) differentiation and bone resorption activity *in vitro* were not affected by IDUA absence in MPSIH OCs pre-GT. However, we observed the presence of abnormal electron dense lysosome-like organelles that confirms the pathological GAGs

engulfment of MPSIH OCs *in vitro* by transmission electron microscopy (TEM). Similarly, we observed pathological GAG engulfment signs in MPSIH bone biopsies by TEM. At different time points after GT, we detected supraphysiologic IDUA levels in MPSIH-derived OCs and in their culture media, suggesting that OCs are gene corrected, produce and release IDUA enzyme in the bone microenvironment, cross-correcting osteoblast precursors and their progeny. In conclusion, these results contribute to clarify the role of OC in the delivery IDUA enzyme to other bone cells and suggest the potential clinical efficacy of GT in ameliorating bone defects of MPSIH patients.

## Introduction

Mucopolysaccharidosis type I (MPSI) is an autosomal recessive disease caused by the defect of the lysosomal enzyme α-L-iduronidase (IDUA) with the consequent intracellular accumulation of glycosaminoglycans (GAG), dermatan- and heparan-sulphate [1], and progressive onset of clinical manifestations [2]. The most severe form of the disease is the Hurler Syndrome (MPSIH), characterized by typical facies with a gargoyle appearance, hepatosplenomegaly, heart disease, respiratory infections, corneal opacity, reduced hearing acuity and mental retardation. Multiple dysostosis is the main osteoarticular manifestation caused by impaired bone remodelling, ectopic endochondral and intramembranous ossification and GAG infiltration into ligaments, joint capsules and other soft tissue [3-5]. Skeletal manifestations become clinically evident at 6 months of age and progress until 2-3 years of age, when patients start to present with growth retardation and joint contractures with stiffness [6].

In MPSIH patients allogeneic hematopoietic stem cell transplantation (HSCT) is the standard treatment, often preceded by a phase of enzyme replacement therapy (ERT) administration that alleviates non-neurological symptoms [7]. ERT and HSCT have been effective in treating major manifestations of MPSI [3, 8, 9], but HSCT needs to performed within 18-24 months of life to obtain beneficial effects [10, 11]. Importantly, ERT and HSCT are

not effective on mental retardation and neurological symptoms [12].

The effect of HSCT on skeletal manifestations remains controversial, since the IDUA enzyme levels do not adequately penetrate the bone tissue and support skeletal development. Altered endochondral and membranous ossification still exist after HSCT despite the improvement in joint mobility [4]. Moreover, clinicians report the worsening of other important symptoms such as odontoid dysplasia and facial deformities, joint pain and stiffness, genu valgum, carpal tunnel syndrome and vertebral changes, resulting in spinal cord compression that significantly impair patients quality life [13]. Despite amelioration of ERT and HSCT procedure, the delivery of sufficient enzyme to the bones and, consequently, the correction of bone defects remains an unmet clinical need.

Serafini's group reported that early intervention can improve the skeletal outcome, and that HSCT performed in the neonatal period prevents the progression of bone damaging in the animal model of the disease [14, 15]. However, early intervention with HSCT is not possible for patients lacking compatible HLA donors. For this reason, gene therapy (GT) has been proposed as an alternative therapy, being potentially available to all patients.

*Ex vivo* GT based on lentiviral vector correction of the genetic defect in autologous hematopoietic stem cell (HSC) has recently been developed for the treatment of rare genetic diseases, including some lysosomal disorder [16-19]. In particular, in the animal model of MPSI, it has been demonstrated that *ex vivo* HSC GT approach

is more effective than HSCT in terms of GAG clearance and enzymatic levels recovery, since it confers supraphysiological levels of enzyme instead of physiological. Moreover, Visigalli et al. demostrated that *ex vivo* HSC GT allows the correction of the skeletal phenotype and the amelioration of neurological symptoms [18].

Based on these important preclinical studies, a phase I/II clinical trial has been initiated at SR-Tiget for the treatment of MPSIH patients (NCT03488394). This procedure is based on *ex vivo* transduction of autologous HSCs with a lentiviral vector carrying the cDNA of the *IDUA* gene. Transduced HSCs are re-infused to the patient after myeloablative chemotherapy. Patients are monitored before and after HSC GT at a multidisciplinary level, including evaluation of the skeletal system with accurate clinical, instrumental and biological examinations.

However, little is known about the mechanisms responsible for multiple dysostosis and about the crosstalk between the cell types involved in the pathogenesis of bone defects in MPSIH [20]. To better elucidate these phenomena, in this project we investigated the mechanisms underlying bone damage in MPSIH and its correction. For this purpose, we generated mesenchymal stromal cells (MSCs), osteoblasts (OBs) and osteoclasts (OCs) from bone marrow and peripheral blood samples of MPSIH patients and healthy subjects as controls. We dissected OC functionality, testing MPSIH derived OCs capacity to differentiate and to resorbe the bone. We also evaluated the level of lysosomal engulfment in MPSIH-derived OCs and their IDUA production after GT.

Conditioned-medium cultures were set up to evaluate the capacity of MPSIH MSCs to uptake the IDUA enzyme, released from OCs post-GT. We also had the chance to collect a bone biopsy from a MPSIH patient to observe the level of GAGs lysosomal engulftment pre- and post-GT *in vivo*.

In conclusion, we provided new insights on the pathogenetic aspects of bone damage underlying MPSIH, and the effect of GT on the dysregulation of bone remodeling.

## Results

### *Ex vivo HSC GT restores IDUA activity and ameliorates muscle-skeletal manifestations of MPSIH patients: preliminary clinical data of MPSIH SR-Tiget GT trial*

*Ex-vivo* HSC GT clinical trial ongoing at SR-Tiget (NCT03488394) enrolled 8 patients from May 2018 (MPSIH001-MPSIH008) with preserved neurocognitive function (DQ/IQ>70) that had no access to a suitable allogeneic donor (Table 2). The median age of treatment was 24 months (range: 14-34) with a median follow up of 12 months (range: 6-24). A high number of autologous $CD34^+$ cells were collected from the leukapheresis following mobilization with Lenograstim and Plerixafor, resulting in drug products with a median of 21 million $CD34^+$ cells/kg (range: 13-29). Drug products were obtained applying a shortened 36-hours transduction protocol that included prostaglandin E2, reaching a median VCN of 1.7 (range: 1.0-5.2).

| Patient ID | Sex | IDUA protein variants | DQ/IQ (Bayley scale) | Age at GT | CD34+ cells/kg infused | LV vector copies per genome (drug product) | Latest Follow up |
|---|---|---|---|---|---|---|---|
| MPSIH001 | M | p.Y201*/p.Y201* | 75 | 24 months | $24 \times 10^6$ | 2.1 | +24 months |
| MPSIH002 | M | p.Y64*/Y64* | 100 | 14 months | $15 \times 10^6$ | 5.2 | +12 months |
| MPSIH003 | M | p.W402*/p.V470Afs*55 | 76 | 35 months | $13 \times 10^6$ | 1.3 | +12 months |
| MPSIH004 | F | p.Q70*/p.Q70* | 75 | 23 months | $18 \times 10^6$ | 2.3 | +12 months |
| MPSIH005 | M | p.Q70*/p.Q70* | 95 | 14 months | $29 \times 10^6$ | 1.0 | +12 months |
| MPSIH006 | M | p.W402*/p.A327P | 85 | 25 months | $28 \times 10^6$ | 1.1 | +12 months |
| MPSIH007 | M | p.L308Hfs*8/p.L308Hfs*8 | 80 | 20 months | $22 \times 10^6$ | 3.4 | +9 months |
| MPSIH008 | F | p.G219E/p.F369Pfs*29 | 90 | 24 months | $19 \times 10^6$ | 3.4 | +6 months |

**Table 2. Baseline patient characteristics.** The table summarizes patient characteristics, updated on July 2020. ERT was discontinued in all patients 3 weeks before GT. DQ/IQ is measured by Bayley Scale III (BDSI) pre-GT.

VCN of $CD15^+$ myeloid cells in the peripheral blood of MPSIH patients post-GT was evaluated overtime, as a surrogate marker of VCN in HSC (Figure 28a). Transduction levels were comparable to the correspondent drug product reinfused in the patients, containing MPSIH autologous $CD34^+$ transduced with the clinical lentiviral vector carrying *IDUA* gene, suggesting a stable gene correction of the myeloid lineage.

After GT, all patients showed stable supraphysiologic blood IDUA activity as measured by Tandem Mass Spectrometry on dried blood spot (DBS) assay. In particular, IDUA activity in GT treated patients was on average 3-fold above the upper normal limit (Figure 28b) and accompanied by Heparan- and Dermatan-sulphate depletion up to normalization in the urine after GT (Figure 38). Notably, MPSIH patients treated with allogeneic HSCT showed an IDUA activity ranging within the lowest quartile of normal, in spite of full donor chimerism, suggesting the important advantage of IDUA overexpression in *ex vivo* genetically modified autologous HSPC [21].

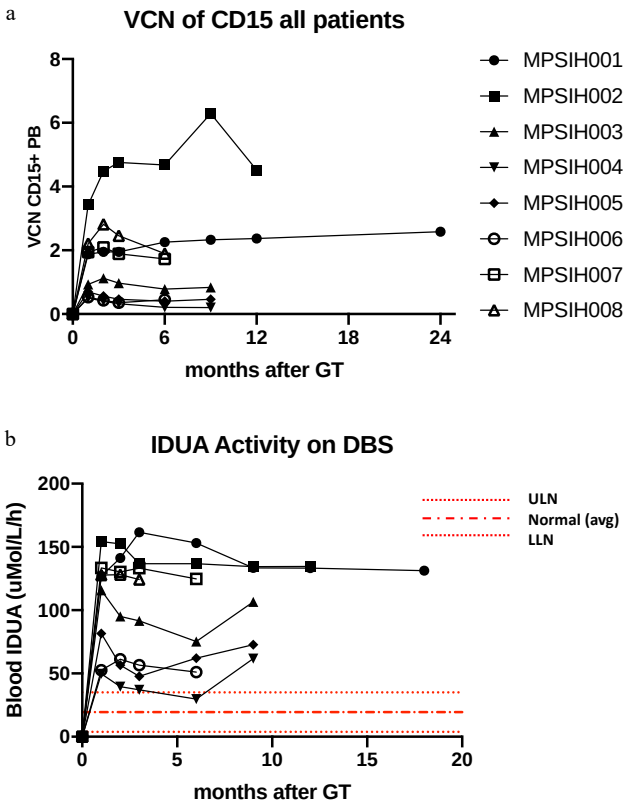


**Figure 28.VCN in myeloid lineage cells and IDUA activity on DBS.** (a) The graph represents the VCN of $CD15^{+}$ cells isolated from peripheral blood (PB) of MPSIH GT patient at different time points. Each symbol represents the VCN of different patient, as detailed in the figure legend. (b) The graph represents the quantification of IDUA enzyme activity (µMol/L/h) by tandem mass spectrometry in dried blood spots (DBS) overtime in the GT patients. Red dotted lines represent upper limit of normal (ULN) and lower limit of normal (LLN). The red dot dash line represents the average of normal value.

As readouts of the clinical efficacy of GT on MPSIH skeletal defects, magnetic resonance imaging (MRI) of the spine of MPSIH001 patient was performed pre- and post-GT together with

range of motion (ROM) and motor function evaluation (Figure 29). Cervical spinal stenosis was reduced, dorso-lumbar kyphosis angle and vertebral deformities improved in MPSIH001 patient at one year follow up (Figure 29). Moreover, motor functions and, in particular, joint mobility measured by ROM, improved in patient MPSIH001 1 year after treatment. These results revealed the potential of GT approach in correcting bone defects of MPSIH patients, emphasizing the importance of the study of bone cells crosstalk in maintaining the adequate bone remodelling process.

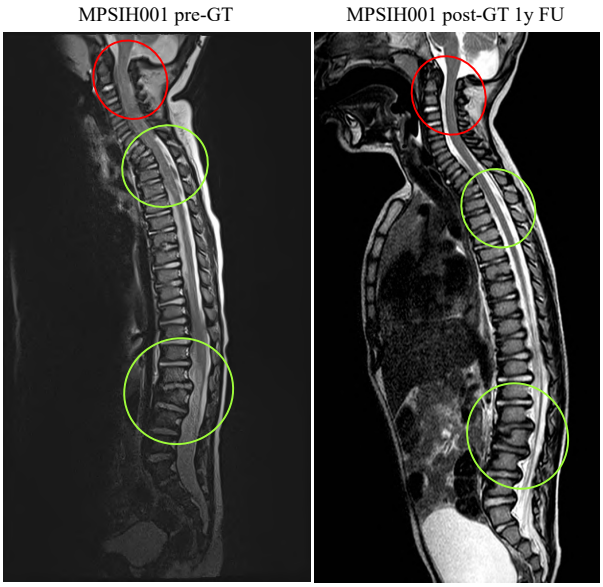


**Figure 29. Spine MRI of MPSIH001.** The pictures represent spine magnetic resonance imaging (MRI) of MPSIH001 patient pre- (left) and post-GT (right). Red circled highlight cervical spinal stenosis and odontoid process development. Green circles highlight kyphosis angles and vertebral shape.

### *Evaluation of differentiation and resorption activity of MPSIH patient-derived OCs*

Any detailed studies on the osteoclastogenesis process and OC function in MPSIH patients have been reported in the literature so far. To explore these aspects, we differentiated OCs from peripheral blood mononuclear cells (PBMCs) and from BM $CD34^+$ cells of MPSIH patients. We evaluated differentiation capacity of OC precursors on plastic tissue-culture treated 96-well plates, performing the tartrate-resistant acid phosphatase (TRAP) staining, after 7-10 days of cultures, as marker of OC differentiation. Both pre-GT PBMCs and transduced BM $CD34^+$ cells from MPSIH patients were able to differentiate into multinucleated TRAP positive OCs (Figure 30). To assess the functionality of MPSIH-derived OCs, we differentiated PBMCs and $CD34^+$ cells on bone slices and we analysed their bone resorption activity by immunofluorescence after 2-3 weeks of culture. The assembled nuclei and the presence of actin rings confirmed OC differentiation on the bone slices (Figure 30). MPSIH-OCs pre-GT are able to resorb the bone slice surface as well as OCs from healthy donor (HD) $CD34^+$ control (Figure 30), demonstrating that bone resorption capacity is not affected in MPSIH *in vitro*.

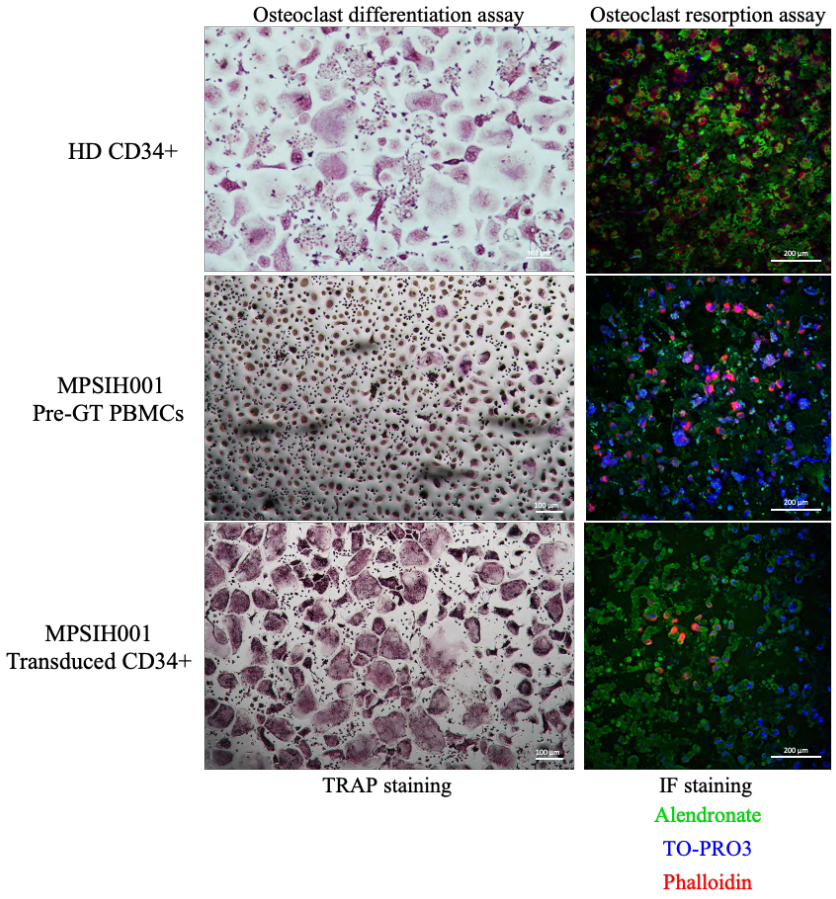


**Figure 30. Osteoclasts differentiation and bone resorption assay.** Representative pictures differentiation (on the left) and bone resorption assay (on the right) of osteoclasts derived from HD $CD34^{+}$ cells, MPSIH001 PBMCs pre-GT and MPSIH001 transduced CD34+ (drug product). On the left, OCs have been differentiated on plastic 96-well plates and stained for tartrate-resistant acid phosphatase (TRAP) activity. Images were acquired with Nikon ECLIPSE E600 microscope equipped with Nikon DS-Ri2 camera, using Plan Fluor 4x/0.13 objective and NIS-Elements F 4.30.01 software. On the right, immunofluorescence staining of OCs differentiated on bone slices shows the merge result of alendronate-AlexaFluor-488 (resorption pits in green), phalloidin-

TRITC (actin rings in red) and TO-PRO-3 (nuclei in blue). Images were acquired with Leica TCS SP5 laser scanning confocal, equipped with HC PL FLUOTAR 10X (NA 0.3) dry and Leica Application Suite Advanced Fluorescence (LASAF) software.

### *Analysis of the crosstalk between MSCs and OCs*

We collected MPSIH PBMCs pre- and post-GT at multiple follow ups of the clinical trial. To confirm gene marking in osteoclasts, we quantified the vector copy number/genome (VCN) in osteoclast precursors differentiated from the $CD34^+$ transduced with LV.PGK.IDUA (infused drug product, DP), which resulted in line with the DP VCN (Table 2) as expected. VCN was also measured overtime in the differentiated osteoclasts from PBMCs. Although we observed a general decrease in VCN between +30 days and +90 days after GT, we confirmed that *IDUA* gene is efficiently transferred to cells of the hematopoietic lineage and consequently to OCs after GT (Figure 31).

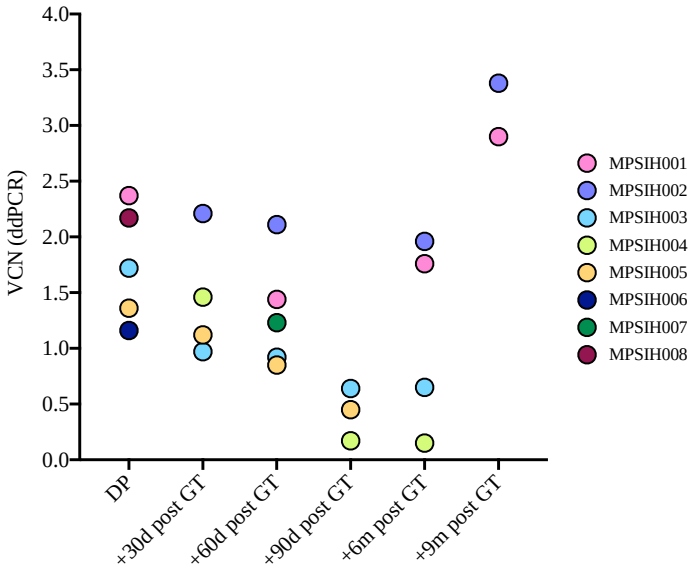


**Figure 31. VCN on MPSIH-derived OCs post-GT.** The graph represents the VCN of MPSIH OCs obtained from the infused drug product (DP, $CD34^+$ transduced with LV.PGK.IDUA) and PBMCs collected at different follow up. Each point represents a single patient, as detailed in figure legend.

In parallel, we quantified the IDUA activity in MPSIH PBMC-derived OCs pre- and post-GT and in paediatric HD. IDUA activity in OC pellets resulted undetectable in pre-GT. On the contrary, we observed supraphysiological level of IDUA activity in MPSIH-OCs post-GT, consistently with VCN results (Figure 32).

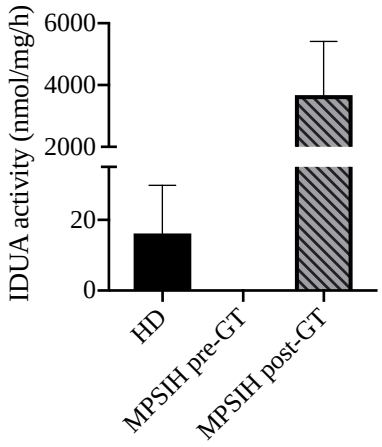


**Figure 32. IDUA activity in MPSIH-derived OCs pre- and post-GT.** The graph represents the mean IDUA activity (nmol/mg/h) of MPSIH OCs pre- and post-GT and HD OCs paediatric controls, measured in cell pellets using the fluorogenic substrate 4-methylumlliferyl-alpha-L-iduronide. The group of MPSIH OCs post-GT is the mean of a merge of multiple follow up of different patients.

Once demonstrated the presence of IDUA activity in post-GT MPSIH PBMCs-OCs pellets, we analysed the supernatant of their cultures to understand if OCs were able to release IDUA in bone environment and, potentially, to cross-correct the defective MSCs and their progeny, such as OBs, that are not directly corrected with GT. We measured IDUA activity in the supernatant of MPSIH-OCs pre- and at +60 days and at +90 days post-GT, by fluorometric assays. IDUA activity in the supernatant of MPSIH-OCs post-GT is higher than the level of IDUA activity detected in the supernatant of HD-OCs (Figure 33). These results suggest that transduced MPSIH-OCs are able to release high levels of IDUA enzyme to

MPSIH MSCs in the bone environment, being more effective than allogeneic HSCT in correcting the bone phenotype.

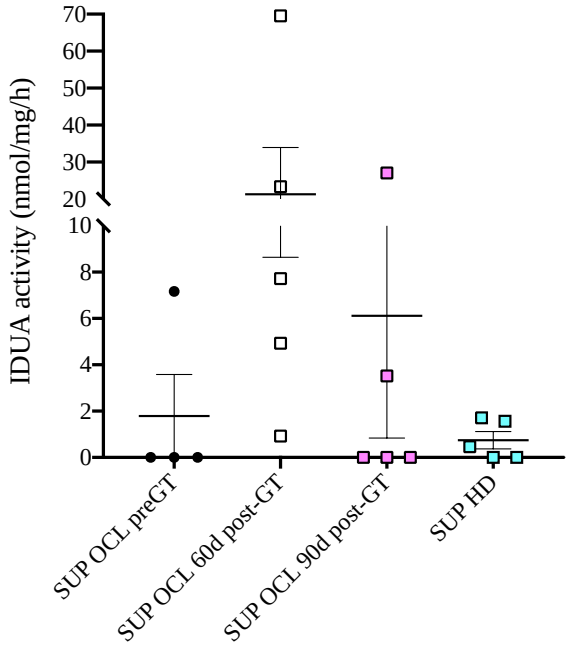


**Figure 33. IDUA activity in supernatants of MPSIH-derived osteoclasts pre- and post- GT.** The graph represents the mean IDUA activity (nmol/mg/h) in the supernatants of pre- and post-GT MPSIH OC cultures, measured using the fluorogenic substrate 4-methylumlliferyl-alpha-L-iduronide. Each point represents the level of IDUA activity in the supernatant of a single MPSIH OCs sample.

In order to investigate the kinetics of IDUA uptake by MPSIH MSCs and their progeny, we set up a conditioned culture experiment. Since patient samples are limited, we decided to use 293T cell line previously transduced with LV.PGK.IDUA as source of IDUA enzyme to define the culture conditions. MPSIH MSCs, isolated from the BM of MPSIH007 patient pre-GT, were

exposed to the supernatant of transduced 293T cells for different periods of time, in order to understand at which time point MSCs are able to efficiently uptake the IDUA enzyme from the culture medium. We observed IDUA activity in pre-GT MPSIH MSCs after the exposure to transduced 293T conditioned medium, especially after 6 and 24 hours of culture (Figure 34). Thus, we set the most efficient timing at 16 hours, being more favourable in term of experimental procedure.

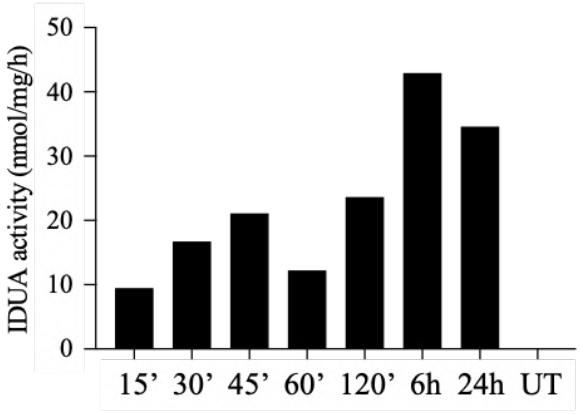


**Figure 34. IDUA activity of MPSIH MSCs at different timepoints, cultured with 293T medium.** The graph represents the IDUA activity (nmol/mg/h) in MPSIH007 MSCs pre-GT collected at different time points after the exposure to the medium of 293T cells transduced with LV.PGK.IDUA, compared with MPSIH MSCs cells exposed to the medium of untransduced 293T.

Once set the most favourable condition for MPSIH MSC exposure to the conditioned medium, we tested whether MPSIH MSCs were able to uptake IDUA enzyme from the supernatant of OC cultures. To this end, we exposed pre-GT MPSIH MSCs to the culture medium of post-GT MPSIH PBMC-OCs collected at different

follow up time points, compared to control groups (pediatric HD MSCs alone, pre-GT MPSIH MSCs alone, pre-GT MPSIH MSCs cultured with the supernatant of pre-GT MPSIH PBMCs-OCs, pre-GT MPSIH MSCs cultured with the supernatant of pediatric HD PBMCs-OCs and pre-GT MPSIH MSCs cultured with the supernatant of transduced 293T). Figure 35 shows the inability of pre-GT MPSIH MSCs to produce IDUA enzyme as compared to MSC derived from normal donors at baseline (without conditioned medium). Consistently, MPSIH MSCs exposed to MPSIH PBMC-OCs supernatant collected pre-GT, do not present IDUA activity. On the other hand, MPSIH MSCs cultured in the presence of the supernatant of MPSIH OCs generated from PBMC collected at +60 days and +90 days after GT showed IDUA activity, reaching supraphysiological level of the enzyme similarly to the level obtained from MSCs exposed to the medium of transduced 293T line. Remarkably, when MPSIH MSCs are cultured in the presence of the supernatant of HD OCs, they show very low or even absent IDUA activity, underlying the necessity for transgene overexpression. This result suggest that GT could be potentially more beneficial than allogeneic HSCT in the treatment of bone symptoms, allowing better enzyme distribution and cross-correction in the bone microenvironment.

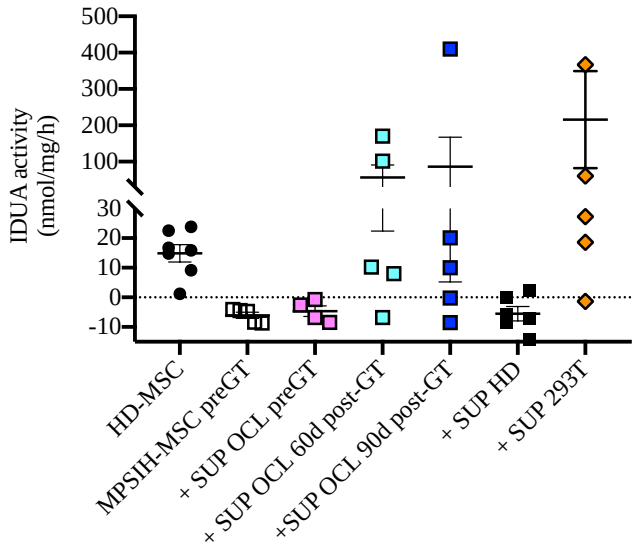


**Figure 35. IDUA uptake from MPSIH MSC exposed to OC supernatant**. IDUA activity was measured in pre-GT MPSIH MSCs using the fluorogenic substrate 4-methylumlliferyl-alpha-L-iduronide. The graph represents the IDUA activity in MPSIH MSCs pre-GT exposed to the medium of MPSIH OCs collected at +60 days and +90 days of follow up, compared to control groups (paediatric HD MSCs alone, MPSIH MSCs pre-GT cells, MPSIH MSCs cultured with the supernatant of MPSIH OCs pre-GT, OCs derived from paediatric HD and transduced 293T). Each dot represents the MSCs sample of a different patient. Data show mean ± SD.

### *Evaluation of lysosomal engulfment of MPSIH derived OCs by transmission electron microscopy (TEM)*

Skeletal manifestations in MPSIH patients are attributed to dysostosis multiplex caused by impaired bone remodelling. Lysosomal engulfment of bone cells due to GAG accumulation

could play a crucial role in the occurrence of these clinical manifestations. As reported in Kuehn et al., transmission electron microscopy (TEM) revealed that osteocytes from 24-week-old *Idua*-deficient mice display lysosomal accumulation of storage material, which was also found in OBs and in OCs. Additionally, authors observed that the ruffled border, a specialized membrane structure required for exocytosis and bone resorption, was less developed in *Idua*-deficient OCs [22]. These data revealed the important involvement of cells of bone compartment in the occurrence of skeletal manifestations in MPSIH disease. To better investigate the entity of bone damage due to GAG accumulation into lysosomes of MPSIH OCs, we differentiated MPSIH PBMCs, collected before GT, on bone slices and, once OCs were fully differentiated, we performed TEM. From the analysis of bone slice sections of MPSIH PBMCs-OCs in Figure 36, we observed the presence of abnormal lysosomes appearing as enlarged electron dense organelles, likely engulfed by the high concentration of GAGs. On the contrary, these engulfed structures were not visible in HD OC sections. We can speculate that reconstitution of physiological level of IDUA expression is sufficient to prevent the accumulation of electron dense material (likely GAGs) in lysosomes. However, these data need to be confirmed by the analysis of sections of OCs derived from PBMCs of post-GT MPSIH patients and HD controls, to exclude artefacts due to the long duration of the OC culture.

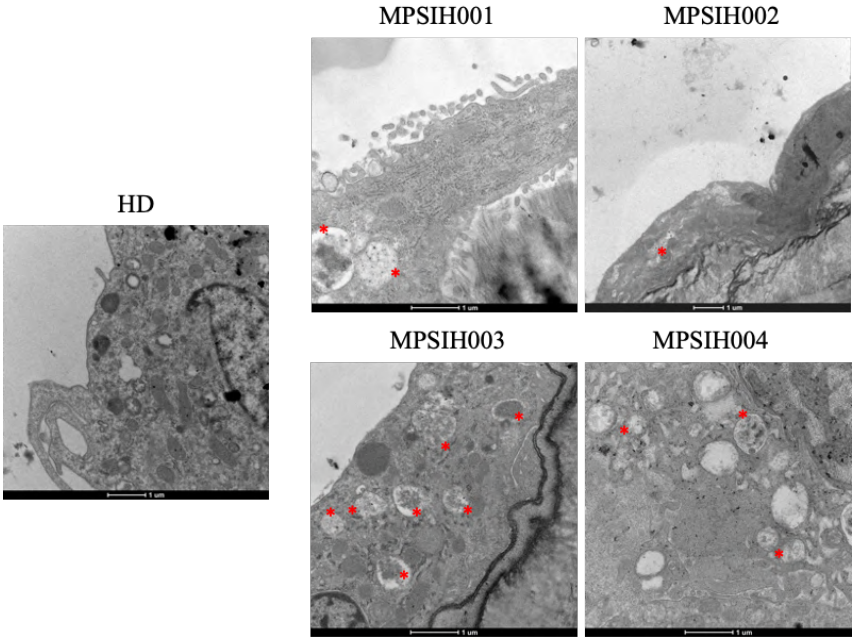


**Figure 36. TEM analysis of MPSIH OCs pre-GT.** Pictures represent TEM analysis of OCs differentiated on bone slices. On the left a representative picture of HD OCs, on the right representative pictures of OCs differentiated on bone slices from PBMCs of 4 different MPSIH patients pre-GT. Asterisks mark electron-dense organelles. Pictures have been acquired in Alembic facility (San Raffaele Hospital) using FEI Talos L120CG2 Transmission Electron Microscope.

To investigate the existence of an OC specific defect in MPSIH bone environment *in vivo*, we evaluated a bone biopsy (BOM) of MPSIH007 patient, performed before GT, by TEM. Importantly, as reported in Figure 37, we observed the presence of multinucleated OCs containing enlarged electron dense organelles, likely representing engulfed lysosomes (magnification highlighted in the red square). Up to now, we only had the possibility to analyse the BOM of MPSIH007 patient and these results need to be

compared to data obtained from TEM analysis of HD BOM. Moreover, we planned to analyse BOM sections of MPSIH patients at later time points of the follow up (one year after GT or later) to evaluate the level of clearance of GAGs in OC lysosomes *in vivo* in the physiological bone environment. These results will allow us to further dissect defects in osteoclast morphology and understand to which extent GT improves OC defects. Furthermore, the evaluation of cellular findings associated with clinical results will be instrumental to correlate changes of osteoblast-osteoclast crosstalk with improvements in skeletal features.

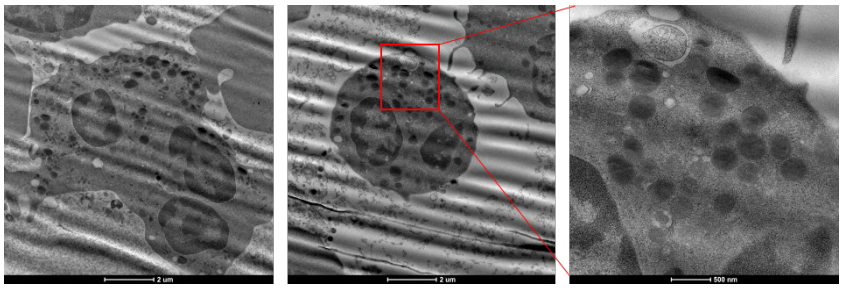

**Figure 37. TEM analysis of bone biopsy of MPSIH007 patient pre-GT**. The three pictures represent the TEM analysis of BOM of MPSIH007 patient pre-GT at different magnifications. The first picture on the left show a triple-nucleated OCs confirming the presence of these cells in the BOM section. The central picture represents a portion of an OC in the BOM; in the red square an electron dense organelle has been magnified (right picture). Pictures have been acquired in Alembic facility (San Raffaele Hospital) using FEI Talos L120CG2 Transmission Electron Microscope.

## Methods

### *MPSIH patients*

Clinical data of *ex-vivo* HSC GT trial of MPSIH patients have been collected from May 2018 to July 2020. Data have been provided by Maria Ester Bernardo and revised by Orchard Therapeutics (OTL).

### *Osteoclasts culture conditions*

PBMCs were seeded into 96-well plates on plastic or on bovine cortical bone slices (Immunodiagnostic System) at a density of $5\times10^5$/well and incubated at 37°C and 5% $CO_2$ in alpha minimum essential (αMEM) medium containing 10% heat-inactivated fetal bovine serum (FBS), 100X solution of penicillin/streptomycin, 2 mM L-Glutamine, 25 ng/ml human M-CSF, 30 ng/ml human sRANKL for 2 or 3 weeks. $CD34^+$ cells were expanded and differentiated toward myeloid lineage for 10 days by seeding them at a density of $5\times10^5$/ml and incubated at 37°C and 5% $CO_2$ in Iscove's Modified Dulbecco's Medium (IMDM) containing 10% heat-inactivated FBS, 100X solution of penicillin/streptomycin, 2 mM L-Glutamine, 300 ng/ml human SCF, 60 ng/ml human IL3 and 60 ng/ml human IL6. Myeloid precursors were seeded OCs into 96-well plates on plastic or on bovine cortical bone slices (ids) at a density of $2\times10^5$/well and incubated at 37°C and 5% $CO_2$ in (αMEM) containing 10% heat-inactivated FBS, 100X solution of penicillin/streptomycin, 2 mM L-Glutamine, 50 ng/ml human M-CSF, for 2 days. Then the medium was changed completely (90%)

and fresh medium containing 50 ng/ml human M-CSF and 50 ng/ml human sRANKL was added to the culture that was followed for 2 or 3 weeks. All the cytokines used for cell cultures have been taken from Peprotech.

***Osteoclast activity***

OCs cultured on plastic were stained using the Tartrate Resistant Acid Phosphatase (TRAP) Kit (Sigma-Aldrich), following the manufacturer's instruction. OCs differentiated on bone slices were stained using alendronate conjugated to Alexa Fluor 488 [23], TRITC-conjugated phalloidin (Sigma-Aldrich) and TO-PRO-3 (Thermo Fisher Scientific).

TRAP images were acquired on a Zeiss AxioImager M2m microscope, while immunofluorescence staining images were acquired on a Leica TCS SP5 Laser Scanning Confocal microscope.

***Vector copy number***

Genomic DNA was extracted from OCs pellets with QIAamp DNA Blood mini kit (QIAGEN), according to manufacturer’s instructions. Vector copy number/genome (VCN) was calculated on transduced cells and transduced hematopoietic progenitors by droplet digital (ddPCR) technique, detecting the DNA sequences on the common packaging signal region of LV (human immunodeficiency virus, HIV system) and using a DNA sequence specific to a region of the human Telomerase gene endogenous control, as previously described [24].

### *MSC culture conditions*

MPSIH patient BM aspirate was collected before HSC-GT or allogeneic HSCT, after obtaining patient or parental informed consent according to a protocol approved by the San Raffaele Ethical Committee. Control MSCs were obtained from BM cells of HDs who donated BM for transplantation at San Raffaele Scientific Institute. Mononuclear cells (MNCs) were isolated from BM by density gradient centrifugation; $CD34^+$ cells were purified from MNCs by immunomagnetic depletion with anti-CD34 microbeads (CD34 MicroBead Kit, Miltenyi Biotec) [25]. The remaining $CD34^-$ fraction was plated at a density of $2x10^5$/cm2 for MSC isolation by plastic adherence. MSCs were further expanded in DMEM+GlutaMAX (Thermo Fisher Scientific, catalog 10566-016) supplemented with 5% platelet lysate and 1% penicillin/streptomycin [20].

### *IDUA activity*

The activity of α-L-iduronidase (IDUA) was determined fluorometrically on OCs pellets and supernatant and on MSCs pellets as already described [26]. Cell suspension or supernatants (25 ul) were incubated for 1 hour at room temperature (22°C) with an equal volume of 50 uM 4-methylumbelliferyl-a-L-iduronide in 0.4 M Na formate buffer (pH 3.5, 0.1% $NaN_3$, 0.15M NaCl). Fluorescence of the 4-methylumbelliferone released was measured after addition of 200 ul of 0.5 M glycine–carbonate buffer (pH 10.3). Fluorescence was measured at 360 nm (excitation) and 465

nm (emission) on a HTS7000 plus BioAssay Reader (Perkinelmer) [27].

### *293T transduction*

293T cell line (provided by ATCC) have been transduced incubating cells with LV.PGK.IDUA at multiplicity of infection (MOI) of 50 in RPMI medium overnight. Cells were cultured and expanded for ten days and supernatant was collected and stored for conditioned culture experiments.

### *Transmission electron microscopy (TEM)*

After 3 weeks of culture, OCs on bovine cortical bone slices have been fixed in 2.5% glutaraldehyde, 0.1 M cacodylate buffer (pH 7.4) at overnight at 4°C and then samples have been decalcified in 2% glutaraldehyde, 0.15 M cacodylate buffer, 0.1 M EDTA (pH 7.4) at 4°C for at least 3 weeks.

MPSIH bone biopsies have been fixed in 2.5% glutaraldehyde, 0.1 M phosphate buffer (pH 7.4) at 4°C for 24 hours and then decalcified in a solution of 10% EDTA 0.1 M phosphate buffer (pH 7.4) at 4°C for at least 3 weeks.

Once the sample are decalcified, they were process for TEM by Alembic facility (San Raffaele Hospital) according to the following procedure: the samples were post fixed (1 hour) with 2% $OsO_4$ in 0.1 M cacodylate buffer (bone slices) or 0.1 M phosphate buffer (MPSIH bone biopsies), washed, dehydrated and embedded in Epon. Conventional thin sections were collected on uncoated

grids, stained with uranyl and lead citrate. Grids were examined at FEI Talos L120CG2 Transmission Electron Microscope at 120 kv.

## Discussion

Mucopolysaccharidosis type I, Hurler syndrome (MPSIH) is a lysosomal storage disease, which results in GAG accumulation in several tissues, including bones. Among other symptoms, MPSIH patients present with a severe bone disease, characterized by progressive skeletal dysplasia, abnormal joint mobility, and osteoarthritis, that requires multiple orthopedic procedures with poor quality of life [1]. ERT and HSCT have been historically exploited for the treatment of MPSIH patients; while ERT does not cross the blood-brain barrier, HSCT is only partially effective on the central nervous system and the bones, despite excellent survival curves. Therefore, the delivery of the IDUA enzyme to the bone still remains insufficient in most of the cases and hampers the resolution of the skeletal dysplasia [13]. Compared with HSCT, the use of genetically corrected HSPC presents important advantages in term of safety, limiting the risk of rejection and graft-versus-host disease and overcoming HLA-matched donor availability. In a proof-of-concept study in 2010, Visigalli et al. showed that MPSI lineage negative cells, transduced with LV.PGK.IDUA are capable of robust, effective delivery of the functional IDUA enzyme to damaged tissues, including the central nervous system in *Idua*$^{-/-}$ mice. Moreover, they observed amelioration of skeletal defects and the metabolic correction of the affected tissues through the clearance of GAGs within hematopoietic and nonhematopoietic cells [18]. Later on, they conducted preclinical biosafety studies obtaining robust evidence in support to safety and tolerability of

LV-mediated gene transfer and above-normal IDUA enzyme expression in both murine and human HSPCs and their in vivo progeny [19].

Based on these results, a hematopoietic stem cell–gene therapy (HSC-GT) phase I/II clinical trial for MPSIH has been started at SR-Tiget to test whether infusion of autologous $CD34^+$ HSPC transduced *ex vivo* with a LV coding for the IDUA gene is feasible, safe and efficient in restoring IDUA activity in MPSIH patients. The trial enrolled 8 patients with a median age of 22-23 months (range 14:35 months) (MPSIH001-MPSIH008), without neurocognitive dysfunction and no access to an HLA-compatible donor for HSCT. All treated patients showed a rapid hematopoietic recovery after myeloablative conditioning. The adverse events registered post-procedure were mild and compatible with the type of conditioning received. All evaluable GT patients showed sustained, supraphysiologic IDUA activity in the blood, reaching on average 3-fold above the upper limit of normal. Importantly, urinary GAG excretion fell to normal levels within 3-6 months after GT as shown in Figure 38.

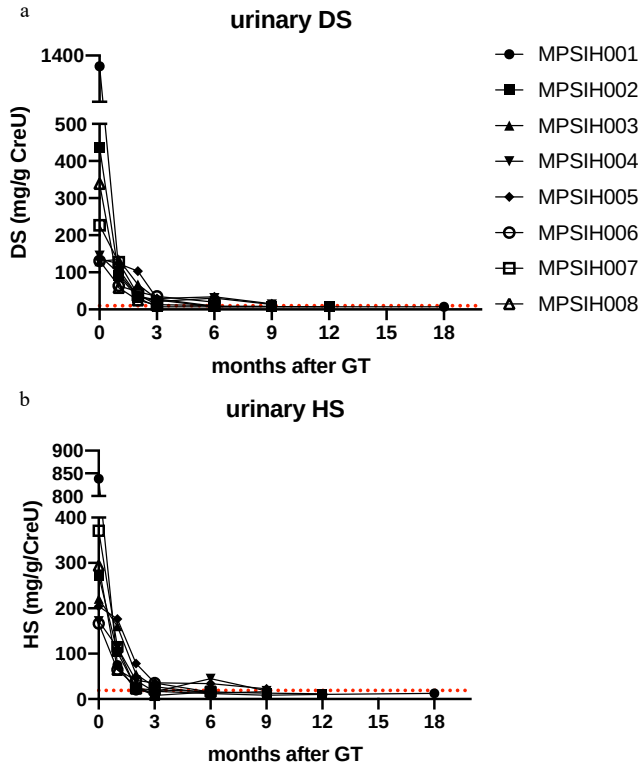


**Figure 38. GAGs detection in urines.** (a) The graph represents the concentration of urinary dermatan sulphate (DS) of MPSIH patients at subsequent follow up after GT. (b) The graph reports the concentration of urinary heparan sulphate (HS). The value of urinary GAGs is expressed as a ratio of DS or HS and creatinine (mg/g/CreU).

Clinical data on MPSIH001 and MPSIH002, the two patients with the longest follow-up after GT (24 months for MPSIH001 and 12 months for MPSIH002), showed stable cognitive performances and amelioration of skeletal features in terms of motor function and joint fitness, measuring the range of motion of the knees and shoulders. Moreover, they showed good growth curves after GT and a slow-down in the increase of head circumference. MRI

analysis of the spine of MPSIH001 at 1 year after GT revealed a reduced cervical spinal canal stenosis and odontoid process development and reduced kyphosis angle with improved vertebra deformity. Thus, improvement of the skeletal phenotype of MPSIH patients may reflect the beneficial effect of GT and highlights the relevance to investigate the pathophysiological mechanisms undergoing bone cell defects of this disease.

It has been reported that the *Idua*-deficient mouse presents a high bone mass phenotype due to impaired formation of osteoblasts and osteoclasts, and that this phenomenon is significantly influenced by HSCT. *Idua*-deficient mice transplanted with WT BM HSC showed an increased osteoclastogenesis [22]. Despite these studies in mouse models, the effects of lysosomal dysfunction in OCs derived from MPSI patients need to be fully clarified. To this end, we moved to the *in vitro* analysis of MPSIH OC differentiation and function. We collected MPSIH PBMCs samples at the baseline (pre-GT) and post-GT at different follow up time points and set up the culture conditions for the differentiation of PBMCs to OCs. In parallel, transduced BM $CD34^+$ cells, collected from the leftover of the infused product, were forced to differentiate into OCs. Comparing these different sources of OCs with HD OCs derived from $CD34^+$, we were able to confirm that MPSIH OCs can normally differentiate and do not present defects in bone resorption process.

To evaluate the level of transduction of MPSIH OCs post-GT, we quantified the VCN and we confirmed that *IDUA* gene is efficiently transferred to cells of the hematopoietic lineage, including OCs

after GT. Importantly, the efficient transduction of MPSIH OCs is coupled with IDUA enzyme production, as demonstrated by the quantification of IDUA activity on MPSIH OCs post-GT.

Once demonstrated that MPSIH OCs can produce functional IDUA enzyme after GT, we evaluated their ability to cross-correct MPSIH MSCs releasing IDUA in the medium. We observed supraphysiological IDUA activity in supernatant of MPSIH OCs at +30 and +90 days post-GT. This evidence allowed us to hypothesize that OCs could deliver IDUA in the bone environment restoring the deficit of MPSIH MSCs and reactivating GAG clearance.

To corroborate our hypothesis, we cultured MPSIH MSCs with the medium of MPSIH OCs post-GT and we observed that MSCs were able to uptake the enzyme after 16 hours of exposure to the conditioned medium and to reach supraphysiological level of functional IDUA.

These preliminary results suggest that MPSIH MSCs can be corrected by OCs, that after GT are efficient in providing IDUA enzyme to non-hematopoietic cell compartment. Moreover, MSCs are able to uptake the functional enzyme from the environment. However, important aspects of MSCs/OBs and OCs crosstalk still need to be elucidated. First, we would like to better investigate the molecular pathway of IDUA uptake, in particular, the expression of Mannose-6-Phosphate Receptor (M6PR), Lysosomal-associated membrane protein 1 (LAMP1) and Sortilin1, as receptors responsible for lysosomal protein uptake and the effect of GT on this mechanism. Moreover, to definitely prove that MSC defects

are reverted due to the *in vitro* cross-correction by OCs, we plan to assess the capacity of MSC, MSC-derived OB and chondroblasts to clear GAGs receiving functional IDUA enzyme from the culture medium. In particular, we will design *in vitro* conditions able to artificially engulf MSCs in culture, with the aim to observe their capacity to clear GAGs providing the functional IDUA enzyme through the use of MPSIH post-GT OCs supernatant.

Few studies reported in literature investigate the effects of lysosomal engulfment of bone cells due to GAGs accumulation in MPSIH. Kuehn et al. explored the consequences of accumulation of storage material in bone compartment of *Idua*$^{-/-}$ mouse model, observing among other defects, impaired ruffle border formation [22]. In our hands, OCs obtained from MPSIH PBMCs before GT, cultured on bone slices and analysed by TEM, showed abnormal highly concentrated electron dense organelles, resembling engulfed lysosomes. These in *vitro* results were confirmed by the TEM analysis of MPSIH007 bone biopsy collected before GT. However, although these results are encouraging, we planned to extend these analyses to other MPSIH patients before GT and at later follow ups (1-2 year post-GT) to confirm the existence of a lysosomal defect in MPSIH OCs *in vivo* and to confirm the rescue of this metabolic defect in bone cells after GT. Overall our data provide evidence that the supraphysiological production of IDUA enzyme by GT osteoclasts enables cross-correction in vitro of MPSIH MSCs. Osteoclasts VCN and IDUA production well correlate with improvement of the skeletal phenotype observed in MPSIH001. Long-term studies of bone defect in patients recruited

in the present project are needed to further confirm the efficacy of GT approach on bone remodelling.

## References


1. Neufeld, E. and J. Muenzer, *The Mucopolysaccharidoses.* 2005: *Online Metab. Mol. Bases Inherit. Dis.* p. 3421–52.
2. Clarke, L.A., *Mucopolysaccharidosis I*, in *Lysosomal Storage Disorders*, J.A. Barranger and M.A. Cabrera-Salazar, Editors. 2007, Springer US: Boston, MA. p. 389-405.
3. Field, R.E., et al., *Bone-marrow transplantation in Hurler's syndrome. Effect on skeletal development.* J Bone Joint Surg Br, 1994. **76**(6): p. 975-81.
4. Weisstein, J.S., et al., *Musculoskeletal manifestations of Hurler syndrome: long-term follow-up after bone marrow transplantation.* J Pediatr Orthop, 2004. **24**(1): p. 97-101.
5. Taylor, C., et al., *Mobility in Hurler syndrome.* J Pediatr Orthop, 2008. **28**(2): p. 163-8.
6. Aldenhoven, M., et al., *Musculoskeletal manifestations of lysosomal storage disorders.* Ann Rheum Dis, 2009. **68**(11): p. 1659-65.
7. Wynn, R.F., et al., *Use of enzyme replacement therapy (Laronidase) before hematopoietic stem cell transplantation for mucopolysaccharidosis I: experience in 18 patients.* J Pediatr, 2009. **154**(1): p. 135-9.
8. Peters, C., et al., *Hematopoietic cell transplantation for inherited metabolic diseases: an overview of outcomes and practice guidelines.* Bone Marrow Transplant, 2003. **31**(4): p. 229-39.
9. Aldenhoven, M., J.J. Boelens, and T.J. de Koning, *The clinical outcome of Hurler syndrome after stem cell transplantation.* Biol Blood Marrow Transplant, 2008. **14**(5): p. 485-98.
10. Aldenhoven, M., et al., *Hematopoietic cell transplantation for mucopolysaccharidosis patients is safe and effective: results after implementation of international guidelines.* Biol Blood Marrow Transplant, 2015. **21**(6): p. 1106-9.
11. Aldenhoven, M., et al., *Long-term outcome of Hurler syndrome patients after hematopoietic cell transplantation: an international multicenter study.* Blood, 2015. **125**(13): p. 2164-72.

12. Eisengart, J.B., et al., *Long-term outcomes of systemic therapies for Hurler syndrome: an international multicenter comparison.* Genetics in medicine : official journal of the American College of Medical Genetics, 2018. **20**(11): p. 1423-1429.
13. Parini, R., et al., *Open issues in Mucopolysaccharidosis type I-Hurler.* Orphanet J Rare Dis, 2017. **12**(1): p. 112.
14. Azario, I., et al., *Neonatal umbilical cord blood transplantation halts skeletal disease progression in the murine model of MPS-I.* Sci Rep, 2017. **7**(1): p. 9473.
15. Pievani, A., et al., *Neonatal bone marrow transplantation prevents bone pathology in a mouse model of mucopolysaccharidosis type I.* Blood, 2015. **125**(10): p. 1662-71.
16. Sessa, M., et al., *Lentiviral haemopoietic stem-cell gene therapy in early-onset metachromatic leukodystrophy: an ad-hoc analysis of a non-randomised, open-label, phase 1/2 trial.* The Lancet, 2016. **388**(10043): p. 476-487.
17. Fraldi, A., et al., *Gene therapy for mucopolysaccharidoses: in vivo and ex vivo approaches.* Ital J Pediatr, 2018. **44**(Suppl 2): p. 130.
18. Visigalli, I., et al., *Gene therapy augments the efficacy of hematopoietic cell transplantation and fully corrects mucopolysaccharidosis type I phenotype in the mouse model.* Blood, 2010. **116**(24): p. 5130-9.
19. Visigalli, I., et al., *Preclinical Testing of the Safety and Tolerability of Lentiviral Vector-Mediated Above-Normal Alpha-L-Iduronidase Expression in Murine and Human Hematopoietic Cells Using Toxicology and Biodistribution Good Laboratory Practice Studies.* Hum Gene Ther, 2016. **27**(10): p. 813-829.
20. Crippa, S., et al., *Bone Marrow-Derived Mesenchymal Stromal Cells: A Novel Target to Optimize Hematopoietic Stem Cell Transplantation Protocols in Hematological Malignancies and Rare Genetic Disorders.* Journal of clinical medicine, 2019. **9**(1): p. 2.
21. Gentner, B., et al., *Extensive Metabolic Correction of Hurler Disease By Hematopoietic Stem Cell-Based Gene Therapy: Preliminary Results from a Phase I/II Trial.* Blood, 2019. **134**(Supplement_1): p. 607-607.
22. Kuehn, S.C., et al., *Impaired bone remodeling and its correction by combination therapy in a mouse model of*

*mucopolysaccharidosis-I.* Hum Mol Genet, 2015. **24**(24): p. 7075-86.
23. Coxon, F.P. and A. Taylor, *Vesicular trafficking in osteoclasts.* Seminars in Cell & Developmental Biology, 2008. **19**(5): p. 424-433.
24. Scala, S., et al., *Dynamics of genetically engineered hematopoietic stem and progenitor cells after autologous transplantation in humans.* Nature Medicine, 2018. **24**(11): p. 1683-1690.
25. Ingo, D.M., et al., *Bone marrow-derived CD34(-) fraction: A rich source of mesenchymal stromal cells for clinical application*, in *Cytotherapy*. 2016: England. p. 1560-1563.
26. Kakkis, E.D., et al., *Overexpression of the human lysosomal enzyme alpha-L-iduronidase in Chinese hamster ovary cells*, in *Protein Expr Purif*. 1994: United States. p. 225-32.
27. Zheng, Y., et al., *Treatment of the mouse model of mucopolysaccharidosis I with retrovirally transduced bone marrow.* Mol Genet Metab, 2003. **79**(4): p. 233-44.

## Chapter 5

### Summary, Conclusions and Future Perspectives

Pediatric skeletal diseases severely affect the quality of life of young patients and in some forms the bone defect is so severe to lead to a reduced lifespan. Rare and severe monogenic disorders like Autosomal Recessive Osteopetrosis (ARO) and Mucopolysaccharidosis type 1 Hurler (MPSIH) are caused by primary and secondary bone defects, respectively. In particular, ARO patients suffer from high bone density and fragility, neurological defects and bone marrow fibrosis leading to extramedullary hematopoiesis and increased number of circulating $CD34^+$ cells [1]. The most frequent form of ARO is due to mutations in the *TCIRG1*, the gene encoding for the subunit a3 of the v0 complex of the V-ATPase proton pump necessary for bone resorptive activity of osteoclasts. MPSIH syndrome is one of the most frequent lysosomal storage disorders, caused by mutations of *IDUA* gene, that encodes for the alpha-L-iduronidase enzyme. Defective IDUA enzyme causes lysosomal engulfment due to impaired turnover of glycosaminoglycans (GAGs), leading to severe organ dysfunction and skeletal abnormalities. The pathogenesis of bone defects in MPSIH is still largely debated [2]. Allogeneic hematopoietic stem cells transplantation (HSCT) is the standard approach for ARO and MPSIH patients, but the high incidence of adverse outcomes and the low availability of

compatible donors, pave the way for the development of gene therapy (GT) strategies to cure these diseases.

In the first part of this PhD project, described in Chapter 2, we developed a novel GT strategy based on clinically-optimized lentiviral vectors, driving *TCIRG1* expression. We tested our GT protocol on the *oc/oc* mouse model, closely resembling the human ARO disease [3]. Firstly, once set up LV transduction of *oc/oc* $Lin^-$ cells and optimized *in vitro* OCs differentiation procedure, we demonstrated that OCs transduced with PGK.TCIRG1 LV are able to resorb bone substrate similarly to OCs obtained from WT $Lin^-$ cells. Next, we applied our GT protocol *in vivo* on newborn *oc/oc* mice, transplanting autologous transduced $Lin^-$ cells intra-hepatically after irradiation. Survival evaluation showed that while *oc/oc* mice die at 2-3 weeks if untreated, 10 out of 14 affected mice receiving GT survived longer then 3 weeks and 6 of them were sacrificed four months after the treatment to analyse bone and immune reconstitution. GT treated mice showed improvement of bone clinical signs corresponding to a dramatic amelioration of the bone phenotype. Despite the significative improvement in terms of survival and bone phenotype, the majority of the analysed mice showed very low VCN in BM, spleen and thymus likely reflecting progressive loss of engraftment of transduced fetal liver $Lin^-$ cells. Indeed, this hypothesis could be confirmed by the poor rescue of bone phenotype of *oc/oc* mice transplanted with fetal liver WT $Lin^-$ cells. This phenomenon has been exacerbated by the already compromised BM niche of *oc/oc* mice at the age of transplant (1-2

days). This evidence further highlights the importance of the timeliness of intervention in ARO [4]. However, in our hands 6 GT mice reached 4 moths of age and showed an improved lifespan and bone phenotype, despite the low VCN in the organs. Remarkably, our results are in line with data previously reported demonstrating that a low level of chimerism is sufficient to restore the bone phenotype of *oc/oc* mice and ameliorate their lifespan [5].

The severity of *oc/oc* mouse phenotype in terms of short lifespan and premature death due to cannibalism experienced in the colony, strongly limited our experimental plans, resulting in a small cohort of mice available for GT studies. To overcome the limited amount of $Lin^-$ cells that can be obtained from the *oc/oc* model and based on the promising results achieved in the human $CD34^+$ cell setting [6], we plan to set up a protocol to *in vitro* expand murine $Lin^-$ cells while maintaining stemness feature. To this end, we are currently performing preliminary experiments exploiting a protocol recently published, which allowed a 236- and 899-fold expansion of functional HSCs over 1 month of culture, starting from 50 primitive murine HSC [7].

In parallel, to enrich the number of autologous HSCP that can be retrieved, transduced and reinfused into the patients, we are evaluating the effects of mobilizing agents. To this end, we have exploited the *oc/oc* mouse model to assess the effect of Plerixafor-based HSC mobilization. To the best of my knowledge, no reports have been reported describing the effect of mobilization in ARO patients with the exception of two osteopetrotic patients, having a low count of circulating $CD34^+$ in the PB, in which mobilization

was cautiously exploited to store an autologous HSC back up before transplantation [8]. Preliminary data showed an increased white blood cells counts in mice treated with plerixafor in both WT and *oc/oc* mice and the analysis of methylcellulose colonies derived from the whole blood of treated mice showed higher number compared with the untreated groups. Therefore, these preliminary results suggest the feasibility of HSC mobilization even in the absence of a bone marrow niche and that HSCP harvested from peripheral blood after this procedure may represent a suitable cellular source for GT, since they maintained their stemness features. Moreover, the application of drug-based mobilization to ARO patients could have the great potential to increase the number of $CD34^+$ cells while limiting the amount of blood to be harvested as autologous back up before transplantation thus facilitating the development of autologous HSC-based GT strategy to cure osteopetrosis.

In the second part of this PhD project, described in Chapter 3, we performed *in vitro* studies to characterize circulating $CD34^+$ cells of ARO patients and in parallel, we developed a tailored approach for the treatment of *TCIRG1*-mutated osteopetrosis exploiting autologous HSPC gene correction and expansion.
Previous studies already demonstrated the feasibility of GT in the context of osteopetrosis [9-12], however, the pre-existent fibrotic condition of the bone marrow niche and the limited amount of blood that can be drawn to collect hematopoietic precursors in these patients limit the applicability of this approach at a clinical

level. Moreover, $CD34^+$ cells isolated from peripheral blood of ARO patients have been exploited as autologous back up before transplantation and reinfused successfully in two osteopetrotic patients with severe transplant complications, providing clinical evidence that circulating $CD34^+$ cells can engraft and speed count recovery [8].

Starting from these observations, we studied the phenotypic composition and transcriptome profile of these spontaneously mobilized HSPCs, that are not evaluated yet in literature.

We observed that HSCP counts/µl of blood were comparable to those observed in the BM of healthy children. Moreover, ARO patients display a content of primitive phenotypic HSCP comparable to BM of pediatric HD. Additionally, ARO patients showed increased number of primitive multipotent progenitors and multi-lymphoid progenitors compared to BM of healthy children and, most importantly, compared to the PB of healthy age-matched controls. These results were further corroborated by the transcriptomic analysis of ARO circulating $CD34^+$ cells, showing a positive enrichment for committed progenitors' signatures, in particular for granulocyte-monocyte progenitor cells. Overall, these data support the applicability of peripheral blood $CD34^+$ as an easily accessible source for HSC in ARO patients. Moreover, since this cell population contains both committed and primitive progenitors, it could favour an initial reconstitution after transplant sustained by differentiated progenitors, followed by the long term engraftment of transduced primitive cells [13]. We confirmed these hypotheses observing the long-term engraftment and multilineage

repopulating potential of these cells *in vivo* performing primary and secondary transplant of expanded and transduced ARO $CD34^+$ into NSG mice. Importantly, transduced and expanded ARO $CD34^+$ were differentiated into OCs that showed a complete rescue of bone resorptive function *in vitro* despite low VCN, confirming our *in vivo* results of GT experiments on *oc/oc* mice, and in line with data reported in literature [5, 11, 14].

In conclusion, we have provided a clinically applicable multi-step approach for ARO patient treatment, based on the use of a clinically-optimized lentiviral vector, an accessible source of long-term engrafting HSCP and reliable HSC expansion culture conditions able to overcome limitations related to the young age of patients and the pre-existence severity of their conditions.

In the third part of this PhD project, described in Chapter 4, we develop an *in vitro* technological platform to study the pathophysiological mechanisms of bone damage in Mucopolysaccharidosis type I, Hurler variant (MPSIH). The *ex vivo* HSC GT clinical trial ongoing at SR-Tiget is showing positive results in terms of rescue of supraphysiological level of the defective IDUA enzyme measured in the blood of the eight patients enrolled in the clinical trial. Additionally, urinary GAGs excretion fell to normal levels after GT. Importantly, the analysis of the MRI of the spine of MPSIH001 patient, the one reaching the longest follow up (24 months), revealed a significant reduction of cervical spinal canal stenosis and odontoid process development and reduced kyphosis angle with improved vertebra deformity. Based

on these promising clinical data on the muscle-skeletal system of MPSIH001 patients, we further investigated the pathophysiological mechanism undergoing bone cell defects of this disease. Idua deficiency in mice cause impaired osteoclastogenesis due to an unbalanced crosstalk between OCs and OBs resulting in severe bone defects. The lack of IDUA activity causes the accumulation of GAGs in bone cells and, even if it has not been clearly demonstrated, it could influence OCs activity [15]. In line with results reported in literature, we observed the presence of abnormal electron dense lysosome-like organelles that suggests the pathological GAGs engulfment of MPSIH OCs *in vitro* by transmission electron microscopy (TEM). Additionally, these in *vitro* results were confirmed by the TEM analysis of MPSIH007 bone biopsy collected before GT. Conversely to data reported in literature, we did not observe gross defects in osteoclastogenesis or bone resorptive function when *in vitro* pre-GT MPSIH PBMCs were forced to differentiate into OCs. However, we cannot exclude that *in vitro* culture conditions (cytokines and long time required to obtain osteoclast culture) may overcome the limits of pathological bone environment. With this caveat, we next evaluated the effect of GT on bone cell compartment, we moved to the *in vitro* analysis of MPSIH OCs differentiation and function. OCs obtained from PBMCs of MPSIH patients after GT showed supraphysiological level of IDUA activity both intracellularly and in culture supernatant. The presence of high level of IDUA activity in the supernatant of MPSIH-OCs culture suggests that genetically corrected MPSIH-OCs could provide a sufficient amount of IDUA

enzyme to the bone environment cross-correcting cells belonging to the non-hematopoietic compartment. We successfully validated this hypothesis observing supraphysiological level of IDUA activity in MPSIH-MSCs cultured with post-GT MPSIH-OCs supernatant.

In conclusion, these results contribute to clarify the role of OCs in the delivery of IDUA enzyme to the MSCs-derived cell compartment within the bone and highlight the efficacy of GT in ameliorating bone defects of MPSIH patients. Moreover, the setting of *in vitro* coculture performed in this project could be exploited as 2D platform to investigate bone cells crosstalk in other bone diseases.

In the future, we plan to further investigate the role MSCs/OBs and OCs crosstalk in MPSI bone pathology. In particular, we plan to increase the number of MPSIH bone biopsies analysed pre- and most importantly post-GT to observe the rescue of OCs defects in terms of clearance of lysosomal GAGs. Moreover, we would like to exploit a new powerful tool based on the generation of 3D model to further improve our understanding on the pathophysiological crosstalk of MSCs/OBs/OCs in the MPSIH condition. In particular, we will develop a recently optimized bone-like biomimetic scaffold [16], functionalized by human MSCs/OBs/OCs and by extracellular matrix deposited during culture perfusion in bioreactors, to mimic the osteoblastic niche and study their crosstalk in the presence or absence of an IDUA defect.

## References


1. Sobacchi, C., et al., *Osteopetrosis: genetics, treatment and new insights into osteoclast function.* Nat Rev Endocrinol, 2013. **9**(9): p. 522-36.
2. Campos, D. and M. Monaga, *Mucopolysaccharidosis type I: current knowledge on its pathophysiological mechanisms.* Metab Brain Dis, 2012. **27**(2): p. 121-9.
3. Scimeca, J.C., et al., *Novel mutations in the TCIRG1 gene encoding the a3 subunit of the vacuolar proton pump in patients affected by infantile malignant osteopetrosis.* Hum Mutat, 2003. **21**(2): p. 151-7.
4. Schulz, A.S., et al., *Osteopetrosis. Consensus guidelines for diagnosis, therapy and follow-up*. 2015, ESID and the EBMT WP Inborn Errors.
5. Flores, C., et al., *Nonablative neonatal bone marrow transplantation rapidly reverses severe murine osteopetrosis despite low-level engraftment and lack of selective expansion of the osteoclastic lineage.* J Bone Miner Res, 2010. **25**(9): p. 2069-77.
6. Capo, V., et al., *Expanded circulating hematopoietic stem/progenitor cells as novel cell source for the treatment of TCIRG1 osteopetrosis.* Haematologica, 2020.
7. Wilkinson, A.C., et al., *Long-term ex vivo hematopoietic-stem-cell expansion allows nonconditioned transplantation.* Nature, 2019. **571**(7763): p. 117-121.
8. Steward, C.G., et al., *High peripheral blood progenitor cell counts enable autologous backup before stem cell transplantation for malignant infantile osteopetrosis.* Biol Blood Marrow Transplant, 2005. **11**(2): p. 115-21.
9. Johansson, M.K., et al., *Hematopoietic stem cell-targeted neonatal gene therapy reverses lethally progressive osteopetrosis in oc/oc mice.* Blood, 2007. **109**(12): p. 5178-85.
10. Löfvall, H., et al., *Hematopoietic Stem Cell-Targeted Neonatal Gene Therapy with a Clinically Applicable Lentiviral Vector Corrects Osteopetrosis in.* Hum Gene Ther, 2019. **30**(11): p. 1395-1404.
11. Moscatelli, I., et al., *Lentiviral gene transfer of TCIRG1 into peripheral blood CD34(+) cells restores osteoclast function in infantile malignant osteopetrosis.* Bone, 2013. **57**(1): p. 1-9.

12. Moscatelli, I., et al., *Targeting NSG Mice Engrafting Cells with a Clinically Applicable Lentiviral Vector Corrects Osteoclasts in Infantile Malignant Osteopetrosis.* Hum Gene Ther, 2018. **29**(8): p. 938-949.
13. Scala, S., et al., *Dynamics of genetically engineered hematopoietic stem and progenitor cells after autologous transplantation in humans.* Nature Medicine, 2018. **24**(11): p. 1683-1690.
14. Thudium, C.S., et al., *Regulation and Function of Lentiviral Vector-Mediated TCIRG1 Expression in Osteoclasts from Patients with Infantile Malignant Osteopetrosis: Implications for Gene Therapy.* Calcif Tissue Int, 2016. **99**(6): p. 638-648.
15. Kuehn, S.C., et al., *Impaired bone remodeling and its correction by combination therapy in a mouse model of mucopolysaccharidosis-I.* Hum Mol Genet, 2015. **24**(24): p. 7075-86.
16. Bourgine, P.E., et al., *In vitro biomimetic engineering of a human hematopoietic niche with functional properties.* Proceedings of the National Academy of Sciences, 2018. **115**(25): p. E5688.

**Publications**

1. Capo, V., **Penna, S**., Merelli, I., Barcella, M., Scala, S., Basso-Ricci, L., et al. (2020). Expanded circulating hematopoietic stem/progenitor cells as novel cell source for the treatment of TCIRG1 osteopetrosis. HAEMATOLOGICA, haematol.2019.238261.

2. **Penna, S.**, Capo, V., Palagano, E., Sobacchi, C., & Villa, A. (2019). One disease, many genes: Implications for the treatment of osteopetroses. FRONTIERS IN ENDOCRINOLOGY, 10(FEB), 85.

3. Capo, V., Castiello, M., Fontana, E., **Penna, S.**, Bosticardo, M., Draghici, E., et al. (2018). Efficacy of lentivirus-mediated gene therapy in an Omenn syndrome recombination-activating gene 2 mouse model is not hindered by inflammation and immune dysregulation. JOURNAL OF ALLERGY AND CLINICAL IMMUNOLOGY, 142(3), 928-941.

**Acknowledgments**

First of all, I would like to thank Anna Villa for the precious opportunity to let me attend my PhD programme at SR-Tiget in her research group and for her constant support and mentoring during these fascinating years. Working in her lab enriched both my personal and professional life as researcher.

In addition, I would like to thank Marta Serafini for the supervision of my PhD project from the DIMET side.

I wish to address a thank to Maria Ester Bernardo and her group for our fruitful collaboration and discussion.

A special thank goes to Valentina Capo. She friendly supervised me and she taught me most of the things I know of this work. We closely shared all the funny and troubled days in the lab.

Last but not least, I want to thank all the people that I met during my PhD experience: Carmen, Lucia, Genni, Elena, Ileana, Francesca, Enrica, Rosita, Nicolò, Denise, Martina, Chiara for their brilliant support and for the special time we spent discussing experiment results and enjoying the life in the lab.

# APPENDIX

## One Disease, Many Genes: Implications for the Treatment of Osteopetroses

Sara Penna[1,2†], Valentina Capo[1†], Eleonora Palagano[3,4], Cristina Sobacchi[3,4] and Anna Villa[1,3*]

[1]San Raffaele Telethon Institute for Gene Therapy (SR-Tiget), San Raffaele Hospital, Milan, Italy
[2]Translational and Molecular Medicine (DIMET), University of Milano-Bicocca, Monza, Italy
[3]The National Research Council (CNR) Institute for Genetic and Biomedical Research (IRGB)- CNR-IRGB, Milan Unit, Milan, Italy
[4]Humanitas Research Hospital, Rozzano, Italy

This review was published on *Frontiers in Endocrinology* in 2019 February 19.
DOI: 10.3389/fendo.2019.00085

frontiers in Endocrinology

MINI REVIEW
published: 19 February 2019
doi: 10.3389/fendo.2019.00085

# One Disease, Many Genes: Implications for the Treatment of Osteopetroses

*Sara Penna*[1,2†], *Valentina Capo*[1†], *Eleonora Palagano*[3,4], *Cristina Sobacchi*[3,4] *and Anna Villa*[1,3*]

[1] San Raffaele Telethon Institute for Gene Therapy (SR-Tiget), San Raffaele Hospital, Milan, Italy, [2] Translational and Molecular Medicine (DIMET), University of Milano-Bicocca, Monza, Italy, [3] The National Research Council (CNR) Institute for Genetic and Biomedical Research (IRGB)- CNR-IRGB, Milan Unit, Milan, Italy, [4] Humanitas Research Hospital, Rozzano, Italy

Osteopetrosis is a condition characterized by increased bone mass due to defects in osteoclast function or formation. In the last decades, the molecular dissection of osteopetrosis has unveiled a plethora of molecular players responsible for different forms of the disease, some of which present also primary neurodegeneration that severely limits the therapy. Hematopoietic stem cell transplantation can cure the majority of them when performed in the first months of life, highlighting the relevance of an early molecular diagnosis. However, clinical management of these patients is constrained by the severity of the disease and lack of a bone marrow niche that may delay immune reconstitution. Based on osteopetrosis genetic heterogeneity and disease severity, personalized therapies are required for patients that are not candidate to bone marrow transplantation. This review briefly describes the genetics of osteopetrosis, its clinical heterogeneity, current therapy and innovative approaches undergoing preclinical evaluation.

**Keywords: bone disease, osteopetrosis, osteoclasts, hematopoietic stem cell transplantation, gene therapy**

OPEN ACCESS

***Edited by:***
*Giacomina Brunetti,*
*Università degli Studi di Bari, Italy*

***Reviewed by:***
*Nadia Rucci,*
*University of L'Aquila, Italy*
*Emanuela Galliera,*
*University of Milan, Italy*

***Correspondence:**
*Anna Villa*
*villa.anna@hsr.it*

*†Co-first authorship*

***Specialty section:***
*This article was submitted to Bone Research, a section of the journal Frontiers in Endocrinology*

***Received:*** *14 December 2018*
***Accepted:*** *31 January 2019*
***Published:*** *19 February 2019*

***Citation:***
*Penna S, Capo V, Palagano E, Sobacchi C and Villa A (2019) One Disease, Many Genes: Implications for the Treatment of Osteopetroses. Front. Endocrinol. 10:85. doi: 10.3389/fendo.2019.00085*

## INTRODUCTION

The term osteopetrosis derives from the Greek "osteo," bone, and "petros," stone, to define a genetically heterogenous group of diseases affecting the skeletal tissue, ranging in severity from benign to fatal in early childhood (1). Osteopetrosis is characterized by increased bone mass due to defective resorption activity or differentiation of osteoclasts (2), causing a disequilibrium of bone turnover, deformities, dental abnormalities and impaired mineral homeostasis, and giving rise to structural fragility that causes frequent fractures. Moreover, osteopetrotic patients are characterized by reduction of marrow cavity, affecting hematologic function; related phenotypes are severe anemia, pancytopenia, frequent infections and hepatosplenomegaly (1, 2) and increased frequency of circulating $CD34^{+}$ cells in the peripheral blood (3). The overly dense cranial nerve foramina lead to impairment of neurologic functions with progressive deafness, blindness and nerve palsies (1, 2). Three different forms of osteopetrosis have been described, based on the pattern of inheritance: autosomal recessive osteopetrosis (ARO), autosomal dominant osteopetrosis (ADO) and X-linked osteopetrosis (2, 4). The only cure for osteopetrosis is allogeneic hematopoietic stem cell transplantation (HSCT), that has greatly improved its outcome overtime (5–7). In this review, we describe the different forms of the disease and therapeutic options, highlighting advances in the setting of safer conditioning regimens and alternative therapies to overcome the limited donor availability.

## AUTOSOMAL RECESSIVE OSTEOPETROSIS (ARO)

The autosomal recessive form of osteopetrosis (ARO), also known as infantile malignant osteopetrosis (IMO), has an incidence of 1:250000 live births, with higher rates in specific geographic areas because of geographic isolation, high frequency of parental consanguinity or the presence of a founder effect (8). Unless treated with HSCT, ARO is usually fatal within the first 10 years of life (8). Children present with failure to thrive, skull abnormalities (macrocephaly, frontal bossing, choanal stenosis), hydrocephalus, hypocalcemia due to defective calcium mobilization activity of osteoclasts (1) and abnormal tooth eruption with frequent development of dental caries (9). ARO is caused by mutations in different genes that are implicated in osteoclast function (osteoclast-rich osteopetrosis) or differentiation (osteoclast-poor osteopetrosis) (**Figure 1**).

### Osteoclast-Rich Osteopetrosis

The most frequent form is caused by mutations in the *TCIRG1* (T cell immune regulator 1) gene, accounting for more than 50% of ARO cases. *TCIRG1* encodes for the a3 subunit of V0 complex of the V-ATPase proton pump, mainly expressed by osteoclasts and gastric parietal cells on apical membrane. The V-ATPase pump acidifies the resorption lacuna in the bone for the dissolution of the hydroxyapatite crystals, that form the bone mineral fraction, and the degradation of the matrix (10). The a3 subunit has also been implicated in the interaction between actin cytoskeleton and microtubules, fundamental for the osteoclast ruffled border formation (8, 11). Accordingly, *TCIRG1*-mutated osteoclasts show defective ruffled border and markedly reduced resorptive activity (11, 12). Moreover, the V-ATPase maintains the low pH in the stomach for the dietary $Ca^{2+}$ absorption (13), and, since gastric acidification is also relevant for calcium uptake, this form of osteopetrosis is characterized by rickets or osteomalacia. The second most frequent form of ARO (17% of the cases) is caused by loss of function mutations in the *CLCN7* (chloride voltage-gated channel 7) gene (2, 14). This gene codes a $2Cl^-/H^+$ antiporter regulated by voltage-gating mechanism, expressed on the osteoclast ruffled border and on the membrane of late endosomes and lysosomes (15). This channel cooperates with the V-ATPase in the acid pH maintenance of the resorption lacuna. CLCN7 is involved in vesicle trafficking in early and recycling endosomes by regulating the luminal $Cl^-$ concentration (16). Mutations in the *CLCN7* gene are responsible for a wide spectrum of clinical manifestations. Biallelic mutations cause a very severe form in which bone defects and hematological failure are associated in some patients with primary neurodegeneration, resembling lysosomal storage disease, cerebral atrophy, spasticity, axial hypotonia and peripheral hypertonia (8, 14, 17). Carrier individuals do not show any overt bone phenotype. CLCN7-deficient osteoclasts have been reported to display impaired endolysosomal trafficking (8). In rare intermediate forms of *TCIRG1*- and *CLCN7*-deficient ARO, milder presentation or later onset and slower progression have been recently reported (18–21).

*OSTM1* (osteopetrosis-associated transmembrane protein 1) mutations are reported in 5% of ARO cases (4, 22, 23) and invariably cause osteopetrosis and severe primary neurodegeneration, with a life expectancy lower than 2 years (22, 24–26). OSTM1 has a highly glycosylated N-terminus that has been reported to stabilize CLCN7 protein and to be required, together with its transmembrane region, for CLCN7 $Cl^-/H^+$ transport activity (15). OSTM1 acts also as an E3 ubiquitin ligase for the heterotrimeric G-protein Gαi3 and potentiates WNT canonical signaling by modulating β-catenin/Lef1 interaction (27, 28).

Less than 5% of ARO cases are caused by mutations in the *SNX10* gene, encoding for the sortin nexin 10 protein, one of the major interactors of the V-ATPase. It is involved in the vesicular sorting of the V-ATPase complex from the Golgi network and in its targeting to the ruffled border (8, 29). In the original work, *SNX10*-dependent osteopetrosis was reported to show few and small osteoclasts (30), while in a more recent paper SNX10-deficient osteoclasts were larger and pale at tartrate-resistant acid phosphatase (TRAP) staining (31). Overall, the severity of clinical manifestations is variable (29, 31, 32).

Rare cases of osteoclast-rich osteopetrosis caused by mutations in other genes have also been reported. For example, osteopetrosis caused by carbonic anhydrase II (*CA-II*) deficiency appears in less than one in a million live births and is associated with cerebral calcification and renal tubular acidosis (2, 33). Carbonic anhydrase II enzyme provides protons to the vacuolar proton pump. Since renal defects are more severe than bone abnormalities, *CA-II* deficiency generally is not considered a classic form of ARO (34).

Loss-of-function mutations in the *PLEKHM1* (pleckstrin homology domain–containing family M member 1) gene cause mild osteopetrosis in the *ia* (incisors absent) rat, as well as an intermediate form of human osteopetrosis (35). PLEKHM1 is a cytosolic protein involved in lysosomal trafficking likely acting as an effector of Rab7 (36, 37). Patient-derived *PLEKHM1*-deficient osteoclasts displayed altered morphology and abnormal podosome distribution (35).

Mutations in *FERMT3* (fermitin family member 3) gene have been reported to cause osteopetrosis in association with leukocyte adhesion deficiency type III (LAD III). *FERMT3* gene is expressed in hematopoietic cells and encodes kindlin-3 protein, necessary for integrin signaling and platelet aggregation (38). Patients affected with *FERMT3*-deficiency are characterized by frequent bleeding and recurrent infections (39, 40).

*LRRK1* (leucine-rich repeat kinase 1) gene mutation was found in a single patient affected by osteosclerotic metaphyseal dysplasia, that specifically compromises the methaphyses of long bones, vertebral endplates, costal ends and margin of flat bones (41).

Another mutated gene associated with osteopetrosis is *MITF* (microphtalmia-associated growth factor) that

**Abbreviations:** ADO, autosomal dominant osteopetrosis; ARO, autosomal recessive osteopetrosis; DOS, dysosteosclerosis; DSF, disease-free survival; GT, gene therapy; HLA, human leukocyte antigen; HSCT, hematopoietic stem cell transplantation; HSPC, hematopoietic stem progenitor cells; MSC, mesenchymal stem cell; RIC, reduced intensity conditioning; TRAP, tartrate-resistant acid phosphatase.

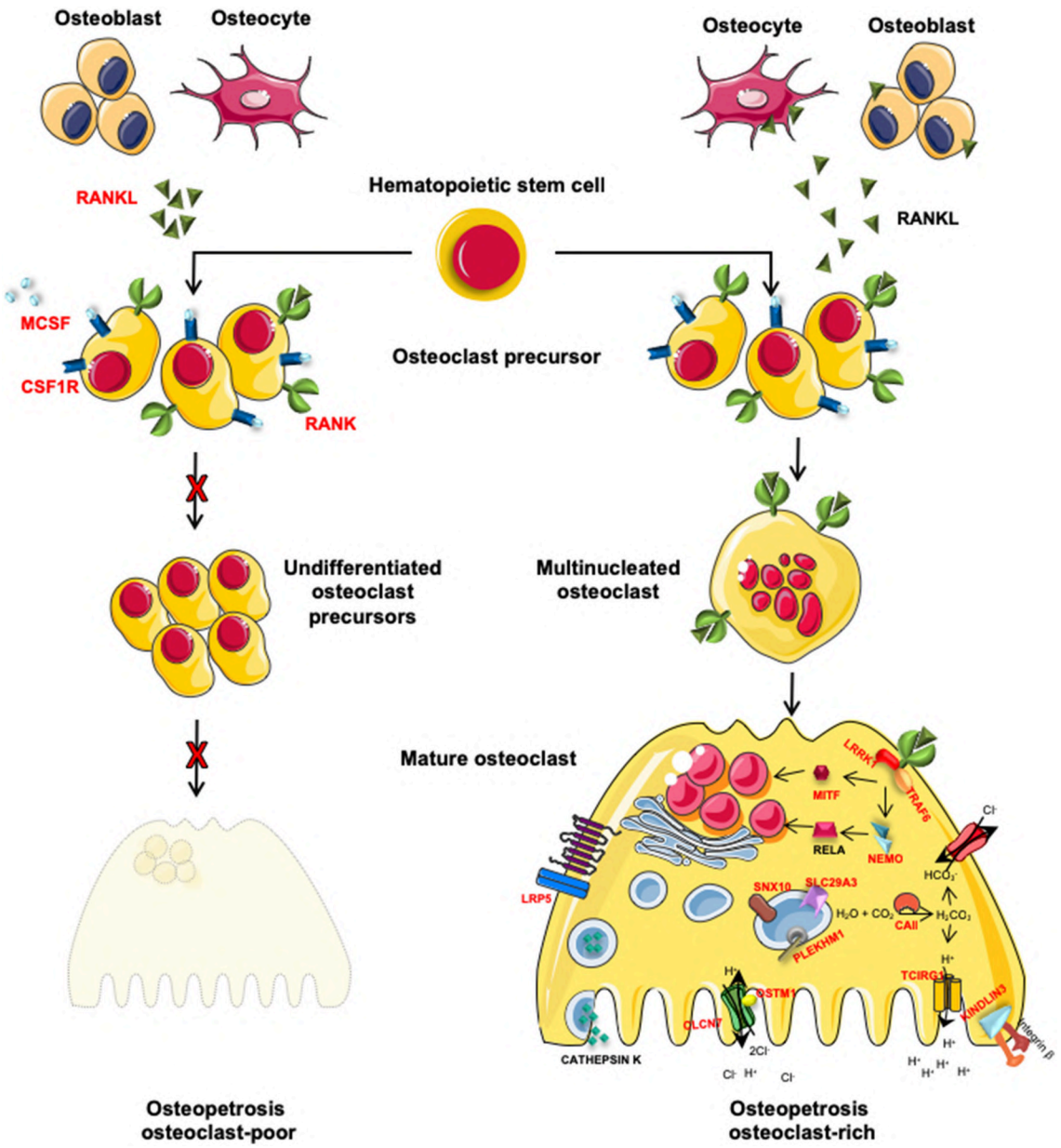


**FIGURE 1 |** Schematic representation of genes involved in osteoclast-poor and osteoclast-rich osteopetrosis. In red are indicated genes involved in the pathogenesis of ARO. MCSF and RANKL, cytokines secreted by osteoblasts and osteocytes, are necessary for the differentiation of osteoclast precursors into mature and resorbing osteoclasts. When these signals are absent (*TNFSF11* gene mutations) or the pathway is interrupted by the lack of cytokine receptors (*TNFRSF11A* and *CSF1R* gene mutations), osteoclast precursors are not able to differentiate into mature osteoclast causing osteoclast-poor forms of osteopetrosis. Alternatively, if osteopetrosis is caused by mutations in genes encoding for protein necessary for bone resorption, the disease is defined as osteoclast-rich osteopetrosis. On the right of the figure, are indicated genes involved in bone resorption activity with different roles: i.e., acidification of resorption lacunae and pH regulation (*TCIRG1, CLCN7, OSTM1,* and *CAII*), vesicular trafficking and sorting of protein complex to the membrane (*SNX10* and *PLEKHM1*), cytoskeletal rearrangement for ruffle border formation (*FERMT3* and *LRRK1).* Other molecules involved in different signal transductions, essential for osteoclast functions (*MITF, LRP5,* and *IKBKG*) are reported.

encodes for a transcription factor acting downstream RANK/RANKL pathway (42). *MITF* deficiency is responsible for COMMAD (coloboma, osteopetrosis, microphthalmia, macrocephaly, albinism, and deafness) syndrome in two unrelated patients, suggesting a role for *MITF* in regulating various processes beside bone development and homeostasis (43).

Finally, a homozygous mutation in *C16orf57* has been described in poikiloderma and neutropenia associated with osteopetrosis (44). This gene encodes for a phosphodiesterase responsible for modification and stabilization of the U6 small nuclear RNA, fundamental element of the spliceosome machinery (45), however, its pathophysiologic function in osteoclast still has to be elucidated.

### Osteoclast-Poor Osteopetrosis

The complete absence of osteoclasts is the key feature of the osteoclast-poor form of osteopetrosis (46). Patients are characterized by absence of TRAP-positive osteoclasts in bone biopsies. The defective osteoclastogenesis is caused by either the lack of RANKL (receptor activator of nuclear kappa B ligand) cytokine (2% of all ARO cases) or of its receptor RANK (4.5% of ARO forms) (47–50). RANKL is encoded by the *TNFSF11* gene and the binding to its receptor RANK, encoded by the *TNFRSF11A* gene, determines the activation of the downstream pathway that drives osteoclast differentiation and activation (51). In bone, RANKL is produced mainly by the stromal compartment in physiological condition, while other cell sources are more important in pathological context (52). Recent evidence suggests that RANKL has also an osteogenic role through an autocrine loop in mesenchymal stem cells (53) and through reverse signaling from the osteoclasts to the osteoblasts (54). In addition, in patients RANKL absence leads to a partial defect in T cell proliferation and cytokine production (50), while RANK-deficiency perturbs B cell memory subset and immunoglobulin production (48, 49).

A rare osteoclast-poor form of osteopetrosis, called dysosteosclerosis (DOS), accompanied by red violet macular atrophy, platyspondyly and metaphyseal osteosclerosis, is caused by mutations of the *SLC29A3* (solute carrier family 29 member 3) gene encoding for a lysosomal nucleoside transporter highly expressed in myeloid cells (21, 55). More recently a novel splice-site mutation in the intron 6 of *TNFRSF11A* has been described in one patient indicating *TNFRSF11A* as additional gene responsible for DOS (56).

A recent report described two affected siblings presenting osteopetrosis associated with severe combined immunodeficiency (SCID) caused by a large deletion on chromosome 11 encompassing *RAG1* and *RAG2* genes and the 5′ region of *TRAF6* (TNF receptor-associated factor 6 gene), the most important adaptor for the RANK/RANKL signaling pathway (57).

Lastly, a heterozygous truncating mutation in the *CSF1R* gene, which encodes for MCSF (macrophage colony-stimulating factor) receptor, was reported in the consanguineous parents of two deceased siblings, showing osteopetrosis and brain malformations (58). This mutation could not be assessed in the probands, however based on this report, this genetic variant could be responsible for the disease in this family (59).

## AUTOSOMAL DOMINANT OSTEOPETROSIS

Autosomal Dominant Osteopetrosis (ADO) has an incidence of 1:20,000 live births with clinical onset typically in adolescence or adulthood (4) and cases diagnosed in pediatric age are reported too (18, 60). It is characterized by diffuse osteosclerosis, primarily involving the axial skeleton, and symmetrical defects of the long bones, with no or little modeling defects. ADO form, also known as benign form, is caused by heterozygous missense mutations of the *CLCN7* gene with dominant negative characteristic, in which the mutant subunit is able to dimerize, functionally impairing the protein (12, 17). Patients affected with ADO present a wide range of symptoms: radiographic alterations, frequent atraumatic fractures, osteonecrosis or osteomyelitis, vision and hearing impairment due to cranial nerve compression and occasional bone marrow failure (4, 8, 61). Although *CLCN7* is widely expressed in the body and the biallelic loss of function causes neurodegeneration in some CLCN7-deficient ARO patients, only sporadic cases of cognitive failure have been reported in ADO patients (4, 12).

## X-LINKED OSTEOPETROSIS

Osteopetrosis caused by mutations of the *IKBKG* (inhibitor of nuclear factor kappa B kinase subunit gamma) gene, located on the X chromosome, occurs as a moderate complication of the OL-EDA-ID syndrome, lymphedema, anhidrotic ectodermal dysplasia and immunodeficiency (hence, the acronym) (62–65). The *IKBKG* gene encodes NEMO, the regulatory subunit of IKK complex, fundamental for the activation of NF-kB transcription factor to induce osteoclastogenesis (62). Consistently, inhibition of NF-kappaB signaling in mouse models of inflammation showed amelioration of osteolysis and inflammation (66). Bone biopsy evaluation in a patient revealed that osteoclasts were present in normal numbers and showed no morphological abnormalities (63). Thus, OL-EDA-ID is classified as an osteoclast-rich osteopetrosis (67).

## CURRENT THERAPIES AND MANAGEMENT OF OSTEOPETROSIS

The majority of osteopetrotic forms are caused by osteoclast dysfunction, while a lower proportion of cases are caused by impaired osteoclastogenesis (8). **Table 1** summarizes the main clinical features in various forms of osteopetrosis. Since osteoclasts derive from the myeloid lineage, HSCT is the recommended treatment. A successful HSCT allows the engraftment of donor-derived osteoclast precursors, which further differentiate and give rise to functional mature osteoclasts, resulting in bone remodeling and haematopoiesis (9). However, HSCT is contraindicated in patients with primary neurodegenerative disease (**Table 1**).

Since secondary neurological defects are not rescued by transplant, genetic diagnosis and HSCT need to be performed as soon as possible (7, 68, 69). To this end, *in utero* HSC transplantation might represent in the future a therapeutic option as demonstrated by successful preclinical studies performed in the *oc/oc* mouse model (70, 71). Multicentre studies reported that patients undergoing HLA-haploidentical HSCT before the age of 10 months, survived with a full donor engraftment. On the contrary, almost all patients receiving HSCT after the age of 10 months underwent graft rejection or autologous reconstitution, even when an haploidentical donor source was used (7). Taken together, these evidences suggest that the fast diagnosis and timing of treatment, play a fundamental role in the long-term efficacy of HSCT (8). The degree of donor

**TABLE 1 |** Main clinical features and indications for treatment in osteopetrosis.

| Gene | Autosomal recessive osteopetrosis | Overall disease severity | Hematological defects | Visual defects | Hypocalcemia | Growth retardation | Primary neurodegeneration | Indication to HSCT |
|---|---|---|---|---|---|---|---|---|
| *TCIRG1* | Osteoclast-rich form | Most often severe | Severe | Mild to severe | Severe | Mild to severe | No | Yes |
| *CICN7* | Osteoclast-rich form | Severe to mild | Mild to severe | Mild to severe | Severe | Mild to severe | Yes | To be evaluated based on the severity of CNS involvement |
| *OSTM1* | Osteoclast-rich form | Severe | Mild to severe | Mild to severe | Moderate | Mild to severe | Yes | No severe CNS involvement |
| *SNX10* | Osteoclast-rich form | Variable | Severe | Severe | Mild | Mild | No | Yes |
| *CAII* | Osteoclast-rich form | Moderate | None | Mild | Mild | Moderate | Cerebral calcification | To be evaluated based on cerebral calcification |
| *PLEKHM1* | Osteoclast-rich form | Mild | None | None | None | None to moderate | No | No mild presentation |
| *FERMT3* | Osteoclast-rich form | Severe | Severe | Mild | Mild | Mild | No | Yes |
| *NEMO* | Osteoclast-rich form | Severe | Severe | None | Mild | Moderate | No | Yes |
| *TNFRSF11A/RANK* | Osteoclast-poor form | Most often severe | Mild | Mild | Mild | Moderate | No | Yes |
| *TNFSF11/RANKL* | Osteoclast-poor form | Intermediate | Mild | Mild | Mild | Severe | No | No |

compatibility is another key point to obtain a high rate of 5-years disease-free survival (DFS) after allogenic transplant. Data collected during the years on transplant outcomes, proved that the early diagnosis, the constant monitoring and prompt intervention for the associate comorbidities, the optimization of the donor source in term of HLA-matching and the choice of reduced intensity conditioning regimens allowed higher efficacy and safety of HSCT (9, 69, 72). The most recent report of transplants performed by Ulm and Paris Transplant Units highlighted the improved outcomes of HSCT with 93% of survival using T cell replete matched donor and 80% of survival using T cell depleted haploidentical donor (7). Unrelated cord blood is not recommended because its use is associated to high risk of primary engraftment failure (73). Fludarabine-based conditioning, performed better than the conventional cyclophosphamide-based one, in terms of higher engraftment and reduced toxicity with a higher 5-years DFS. In a selected cohort of 31 patients transplanted from related or unrelated fully matched donors, reduced intensity conditioning (RIC), based on fludarabine, treosulfan and thiotepa with proximal serotherapy dosing using anti-thymocyte globulin, allowed 100% overall survival (69).

The most frequent post-transplant complication is the engraftment failure caused by a delayed hematological reconstitution, due to limited or nearly absent bone marrow space (7) and graft vs. host disease (GvHD) (69). T-cell replete haploidentical graft with the administration of cyclophosphamide after HSCT has been proposed in patients older than 10 months (74). Frequently, transplanted ARO patients showed liver and pulmonary venous-occlusive disease (VOD) (75). Respiratory problems, such as choanal stenosis with upper airway obstructions, capillary leak syndrome, primary pulmonary infections and primary pulmonary hypertension were also frequent. When feasible, the use of a RIC regimen may reduces significantly the incidence of pulmonary hypertension (9, 69).

In addition, central nervous system complications may occur in terms of hydrocephalus, hypocalcaemic convulsions or deterioration of preexisting symptoms. Lastly a recurrent post-transplant risk was the onset of hypercalcemia, that can be treated by the use of Denosumab (76).

## ALTERNATIVE TREATMENTS AND FUTURE THERAPIES

Despite recent improvement in the HSCT outcome, the availability of HLA-matched donors remains an open issue. For individuals lacking compatible donor, a strategy based on gene therapy (GT) has been proposed. The protocol would exploit the use of genetically modified $CD34^+$ cells, isolated from peripheral blood without the need of pharmacological HSC mobilization (3). The efficacy and the feasibility of GT have been studied in the *oc/oc* murine model, to evaluate neonatal transplantation of genetically corrected HSC in the context of *TCIRG1*-dependent osteopetrosis. Retroviral vectors were able to improve bone resorption and survival of *oc/oc* mice (77). Unfortunately, clinical trials in which immunodeficient patients were treated with this type of vector showed the risk of leukemia (78). In recent years, lentiviral vector GT has proven to provide clinical benefit in

patients affected by a number of diseases, avoiding the leukemic side effects (79, 80). Moreover, transduction of $CD34^+$ cells from the blood of *TCIRG1*-deficient patients with a lentiviral vector achieved the correction of the osteoclast dysfunction *in vitro* (81).

ARO caused by osteoclast extrinsic deficiency, such as *TNFSF11* mutations, requires a different approach. In particular, a replacement therapy has been evaluated at the preclinical level: the product of the *TNFSF11* gene, RANKL cytokine, has been administered pharmacologically to *Tnfsf11* knockout mice, rescuing bone defects and hematopoietic organ architecture (82). Additional strategies could be considered, for example, mesenchymal stem cell (MSC) transplantation to replace the osteoblast precursor population (83); however clinical application still raises doubts and challenges, thus this is far from a mature therapeutic option. The second method exploited the use of biotechnological devices, implanted subcutaneously, to release soluble RANKL and allowing osteoclastogenesis in *Tnfsf11* knockout mice (84). More recently, a promising biomimetic scaffold, seeded with *Tnfsf11* knockout MSC, overexpressing human soluble RANKL after transduction with lentiviral vector has been developed. When implanted subcutaneously, the 3D system was well tolerated and was able to drive the differentiation of TRAP positive cells (85).

Regarding new approaches for the treatment of ADO2, small interfering RNA has been demonstrated to silence specifically the mutated *CLCN7* allele, and to be effective and safe *in vitro* on human cells and *in vivo*, in an ADO2 mouse model (86). Therefore, efforts have been undertaken to move into the clinic (87). Alternatively, the administration of different doses of IFN-γ partially reduced whole-body bone mineral density of ADO2 mice, although further studies for clinical applications are needed (88).

## CONCLUSIONS

Genetic dissection of osteopetrosis has unveiled the complex scenario of molecules involved in the pathogenesis of this disease. Early genetic diagnosis is important to establish treatment and thus prevent worsening of the clinical signs. However, despite new molecular techniques have defined ARO molecular complexity, there is the need to further understand their clinical heterogeneity and design novel and suitable cure to these patients. To this end, significant progress has been made in the treatment of ARO thanks to the improvement of novel conditioning regimens and source of donor HSPC, however additional work remains to be done to overcome the limited availability of donors or lack of a therapy for patients carrying RANKL defects or presenting with neurodegenerative osteopetrosis. On this basis, efforts are currently ongoing to further extend the number of molecular players causative of the disease in parallel with the design of novel clinical strategies to be offered as curative treatment for different forms of osteopetrosis.

## AUTHOR CONTRIBUTIONS

SP, VC, and AV wrote the manuscript. CS and EP critically revised the manuscript and contributed to design the figure.

## FUNDING

The original work was supported by the Italian Telethon Grant C5, the European Community's Seventh Framework Program (FP7/2007-2013, SYBIL Project), PRIN Project (2015F3JHMB_004) and by Programma Nazionale per la Ricerca-Consiglio Nazionale delle Ricerche Aging Project to AV.

## REFERENCES

1. Wu CC, Econs MJ, DiMeglio LA, Insogna KL, Levine MA, Orchard PJ, et al. Diagnosis and management of osteopetrosis: consensus guidelines from the osteopetrosis working group. *J Clin Endocrinol Metab.* (2017) 102:3111–23. doi: 10.1210/jc.2017-01127
2. Palagano E, Menale C, Sobacchi C, Villa A. Genetics of osteopetrosis. *Curr Osteoporos Rep.* (2018) 16:13–25. doi: 10.1007/s11914-018-0415-2
3. Steward CG, Blair A, Moppett J, Clarke E, Virgo P, Lankester A, et al. High peripheral blood progenitor cell counts enable autologous backup before stem cell transplantation for malignant infantile osteopetrosis. *Biol Blood Marrow Transplant.* (2005) 11:115–21. doi: 10.1016/j.bbmt.2004.11.001
4. Teti A, Econs MJ. Osteopetroses, emphasizing potential approaches to treatment. *Bone* (2017) 102:50–9. doi: 10.1016/j.bone.2017.02.002
5. Ballet JJ, Griscelli C, Coutris C, Milhaud G, Maroteaux P. Bone marrow transplantation in osteopetrosis. *Lancet* (1977) 310:1137. doi: 10.1016/S0140-6736(77)90592-X
6. Coccia PF, Krivit W, Cervenka J, Clawson C, Kersey JH, Kim TH, et al. Successful bone-marrow transplantation for infantile malignant osteopetrosis. *N Engl J Med.* (1980) 302:701–8. doi: 10.1056/NEJM198003273021301
7. Schulz AS, Moshous D, Steward CG, Villa A, Sobacchi C. *Osteopetrosis. Consensus Guidelines for Diagnosis, Therapy and Follow-Up* (2015). Available online at: https://Esid.Org/.2015.654
8. Sobacchi C, Schulz A, Coxon FP, Villa A, Helfrich MH. Osteopetrosis: genetics, treatment and new insights into osteoclast function. *Nat Rev Endocrinol.* (2013) 9:522–36. doi: 10.1038/nrendo.2013.137
9. Natsheh J, Drozdinsky G, Simanovsky N, Lamdan R, Erlich O, Gorelik N, et al. Improved outcomes of hematopoietic stem cell transplantation in patients with infantile malignant osteopetrosis using fludarabine-based conditioning. *Pediatric Blood Cancer* (2015) 63:535–40. doi: 10.1002/pbc.25801
10. Frattini A, Orchard PJ, Sobacchi C, Giliani S, Abinun M, Mattsson JP, et al. Defects in TCIRG1 subunit of the vacuolar proton pump are responsible for a subset of human autosomal recessive osteopetrosis. *Nat Genet.* (2000) 25:343–6. doi: 10.1038/77131
11. Nakamura I, Takahashi N, Udagawa N, Moriyama Y, Kurokawa T, Jimi E, et al. Lack of vacuolar proton ATPase association with the cytoskeleton in osteoclasts of osteosclerotic (Oc/Oc) mice. *FEBS Lett.* (1997) 401:207–12. doi: 10.1016/S0014-5793(96)01454-8
12. Del Fattore A, Peruzzi B, Rucci N, Recchia I, Cappariello A, Longo M, et al. Clinical, genetic, and cellular analysis of 49 osteopetrotic patients: implications for diagnosis and treatment. *J Med Genet.* (2006) 43:315–25. doi: 10.1136/jmg.2005.036673
13. Schinke T, Schilling AF, Baranowsky A, Seitz S, Marshall RP, Linn T, et al. Impaired gastric acidification negatively affects calcium homeostasis and bone mass. *Nat Med.* (2009) 15:674–81. doi: 10.1038/nm.1963

14. Kornak U, Kasper D, Bösl MR, Kaiser E, Schweizer M, Schulz A, et al. Loss of the ClC-7 chloride channel leads to osteopetrosis in mice and man. *Cell* (2001) 104:205–15. doi: 10.1016/S0092-8674(01)00206-9
15. Leisle L, Ludwig CF, Wagner FA, Jentsch TJ, Stauber T. ClC-7 is a slowly voltage-gated 2Cl-/1H+-exchanger and requires Ostm1 for transport activity. *EMBO J.* (2011) 30:2140–52. doi: 10.1038/emboj.2011.137
16. Novarino G, Weinert S, Rickheit G, Jentsch TJ. Endosomal chloride-proton exchange rather than chloride conductance is crucial for renal endocytosis. *Science* (2010) 328:1398–402. doi: 10.1126/science.1188070
17. Pang Q, Chi Y, Zhao Z, Xing X, Li M, Wang O, et al. Novel mutations of CLCN7 cause autosomal dominant osteopetrosis Type II (ADO-II) and intermediate autosomal recessive osteopetrosis (IARO) in Chinese patients. *Osteoporos Int.* (2016) 27:1047–55. doi: 10.1007/s00198-015-3320-x
18. Pangrazio A, Pusch M, Caldana E, Frattini A, Lanino E, Tamhankar PM, et al. Molecular and clinical heterogeneity in CLCN7-dependent osteopetrosis: report of 20 novel mutations. *Hum Mutat.* (2010) 31:1071–80. doi: 10.1002/humu.21167
19. Palagano E, Blair HC, Pangrazio A, Tourkova I, Strina D, Angius A, et al. Buried in the middle but guilty: intronic mutations in the TCIRG1 gene cause human autosomal recessive osteopetrosis. *J Bone Miner Res.* (2015) 30:1814–21. doi: 10.1002/jbmr.2517
20. Sobacchi C, Pangrazio A, Lopez AG, Gomez DP, Caldana ME, Susani L, et al. As little as needed: the extraordinary case of a mild recessive osteopetrosis owing to a novel splicing hypomorphic mutation in the TCIRG1 gene. *J Bone Miner Res.* (2014) 29:1646–50. doi: 10.1002/jbmr.2203
21. Howaldt A, Nampoothiri S, Quell LM, Ozden A, Fischer-Zirnsak B, Collet C, et al. Sclerosing bone dysplasias with hallmarks of dysosteosclerosis in four patients carrying mutations in SLC29A3 and TCIRG1. *Bone* (2018) 120:495–503. doi: 10.1016/j.bone.2018.12.002
22. Chalhoub N, Benachenhou N, Rajapurohitam V, Pata M, Ferron M, Frattini A, et al. Grey-lethal mutation induces severe malignant autosomal recessive osteopetrosis in mouse and human. *Nat Med.* (2003) 9:399–406. doi: 10.1038/nm842
23. Lange PF, Wartosch L, Jentsch TJ, Fuhrmann JC. ClC-7 requires Ostm1 as a β-subunit to support bone resorption and lysosomal function. *Nature* (2006) 440:220–3. doi: 10.1038/nature04535
24. Pangrazio A, Poliani PL, Megarbane A, Lefranc G, Lanino E, Di Rocco M, et al. Mutations in OSTM1 (Grey Lethal) define a particularly severe form of autosomal recessive osteopetrosis with neural involvement. *J Bone Miner Res.* (2006) 21:1098–105. doi: 10.1359/jbmr.060403
25. Ott CE, Fischer B, Schröter P, Richter R, Gupta N, Verma N, et al. Severe neuronopathic autosomal recessive osteopetrosis due to homozygous deletions affecting OSTM1. *Bone* (2013) 55:292–7. doi: 10.1016/j.bone.2013.04.007
26. Overholt KM, Rose MJ, Joshi S, Herman GE, Bajwa R, Abu-Arja R, et al. Hematopoietic cell transplantation for a child with OSTM1 osteopetrosis. *Blood Adv.* (2017) 1:279–81. doi: 10.1182/bloodadvances.2016002345
27. Fischer T, De Vries L, Meerloo T, Farquhar MG. Promotion of G Alpha I3 subunit down-regulation by GIPN, a putative E3 ubiquitin ligase that interacts with RGS-GAIP. *Proc Natl Acad Sci USA.* (2003) 100:8270–5. doi: 10.1073/pnas.1432965100
28. Feigin ME, Malbon CC. OSTM1 regulates β-Catenin/Lef1 interaction and is required for Wnt/β-catenin signaling. *Cell Signal.* (2008) 20:949–57. doi: 10.1016/j.cellsig.2008.01.009
29. Pangrazio A, Fasth A, Sbardellati A, Orchard PJ, Kasow KA, Raza J, et al. SNX10 mutations define a subgroup of human autosomal recessive osteopetrosis with variable clinical severity. *J Bone Miner Res.* (2013) 28:1041–9. doi: 10.1002/jbmr.1849
30. Aker M, Rouvinski A, Hashavia S, Ta-Shma A, Shaag A, Zenvirt S, et al. An SNX10 mutation causes malignant osteopetrosis of infancy. *J Med Genet.* (2012) 49:221–6. doi: 10.1136/jmedgenet-2011-100520
31. Stattin EL, Henning P, Klar J, McDermott E, Stecksen-Blicks C, Sandström PE, et al. SNX10 gene mutation leading to osteopetrosis with dysfunctional osteoclasts. *Sci Rep.* (2017) 7:1–16. doi: 10.1038/s41598-017-02533-2
32. Mégarbané A, Pangrazio A, Villa A, Chouery E, Maarawi J, Sabbagh S, et al. Homozygous stop mutation in the SNX10 gene in a consanguineous Iraqi boy with osteopetrosis and corpus callosum hypoplasia. *Eur J Med Genet.* (2013) 56:32–5. doi: 10.1016/j.ejmg.2012.10.010
33. Alsharidi A, Al-Hamed M, Alsuwaida A. Carbonic anhydrase II deficiency: report of a novel mutation. *CEN Case Reports* (2016) 5:108–12. doi: 10.1007/s13730-015-0205-y
34. Stark Z, Savarirayan R. Osteopetrosis. *Orphanet J Rare Dis.* (2009) 4:5. doi: 10.1186/1750-1172-4-5
35. Van Wesenbeeck L, Odgren PR, Coxon FP, Frattini A, Moens P, Perdu B, et al. Involvement of PLEKHM1 in osteoclastic vesicular transport and osteopetrosis in incisors absent rats and humans. *J Cell Invest.* (2007) 117:919–30. doi: 10.1172/JCI30328
36. Fujiwara T, Ye S, Castro-Gomes T, Winchell CG, Andrews NW, Voth DE, et al. plekhm1/def8/rab7 complex regulates lysosome positioning and bone homeostasis. *JCI Insight* (2016) 1:e86330. doi: 10.1172/jci.insight.86330
37. Marwaha R, Arya SB, Jagga D, Kaur H, Tuli A, Sharma M. The Rab7 effector PLE KHM1 binds Arl8b to promote cargo traffic to lysosomes. *J Cell Biol.* (2017) 216:1051–70. doi: 10.1083/jcb.201607085
38. Moser M, Nieswandt B, Ussar S, Pozgajova M, Fässler R. Kindlin-3 is essential for integrin activation and platelet aggregation. *Nat. Med.* (2008) 14:325–30. doi: 10.1038/nm1722.
39. McDowall A, Svensson L, Stanley P, Patzak I, Chakravarty P, Howarth K, et al. Two mutations in the KINDLIN3 gene of a new leukocyte adhesion deficiency III patient reveal distinct effects on leukocyte function *in vitro*. *Blood* (2010) 115:4834–42. doi: 10.1182/blood-2009-08-238709
40. Palagano E, Slatter MA, Uva P, Menale C, Villa A, Abinun M, et al. Hematopoietic stem cell transplantation corrects osteopetrosis in a child carrying a novel homozygous mutation in the FERMT3 gene. *Bone* (2017) 97:126–9. doi: 10.1016/j.bone.2017.01.012
41. Iida A, Xing W, Docx MK, Nakashima T, Wang Z, Kimizuka M, et al. Identi Fi cation of Biallelic LRRK1 mutations in osteosclerotic metaphyseal dysplasia and evidence for locus heterogeneity. *J Med Genet*. (2016) 53:568–74. doi: 10.1136/jmedgenet-2016-103756
42. Lu SY, Li M, Lin YL. Mitf regulates osteoclastogenesis by modulating NFATc1 activity. *Exp Cell Res.* (2014) 328:32–43. doi: 10.1016/j.yexcr.2014.08.018
43. George A, Zand DJ, Hufnagel RB, Sharma R, Sergeev YV, Legare JM, et al. Biallelic mutations in MITF cause coloboma, osteopetrosis, microphthalmia, macrocephaly, albinism, and deafness. *Am J Human Genet.* (2016) 99:1388–94. doi: 10.1016/j.ajhg.2016.11.004
44. Colombo EA, Bazan JF, Negri G, Gervasini C, Elcioglu NH, Yucelten D, et al. Novel C16orf57 mutations in patients with poikiloderma with neutropenia: bioinformatic analysis of the protein and predicted effects of all reported mutations. *Orphanet J Rare Dis.* (2012) 7:7. doi: 10.1186/1750-1172-7-7
45. Mroczek S, Krwawicz J, Kutner J, Lazniewski M, Kucinski I, Ginalski K, et al. C16orf57, a gene mutated in poikiloderma with neutropenia, encodes a putative phosphodiesterase responsible for the U6 SnRNA 3′ end modification. *Genes Dev.* (2012) 26:1911–25. doi: 10.1101/gad.193169.112
46. Villa A, Guerrini MM, Cassani B, Pangrazio A, Sobacchi C. Infantile malignant, autosomal recessive osteopetrosis: the rich and the poor. *Calcif Tissue Int.* (2009) 84:1–12. doi: 10.1007/s00223-008-9196-4
47. Lo Iacono N, Pangrazio A, Abinun M, Bredius R, Zecca M, Blair HC, et al. RANKL cytokine: from pioneer of the osteoimmunology era to cure for a rare disease. *Clin Dev Immunol.* (2013) 2013:412768. doi: 10.1155/2013/412768
48. Guerrini MM, Sobacchi C, Cassani B, Abinun M, Kilic SS, Pangrazio A, et al. *Human Osteoclast-Poor Osteopetrosis with Hypogammaglobulinemia Due to TNFRSF11A (RANK) Mutations*. *Am J Hum Genet.* (2008) 83:64–76. doi: 10.1016/j.ajhg.2008.06.015
49. Pangrazio A, Cassani B, Guerrini MM, Crockett JC, Marrella V, Zammataro L, et al. RANK-dependent autosomal recessive osteopetrosis: characterization of five new cases with novel mutations. *J Bone Miner Res.* (2012) 27:342–51. doi: 10.1002/jbmr.559
50. Sobacchi C, Frattini A, Guerrini MM, Abinun M, Pangrazio A, Susani L, et al. Osteoclast-poor human osteopetrosis due to mutations in the

gene encoding RANKL. *Nat Genet.* (2007) 39:960–2. doi: 10.1038/ng2076
51. Leibbrandt A, Penninger JM. RANK/RANKL: regulators of immune responses and bone physiology. *Ann N Y Acad Sci.* (2008) 1143:123–50. doi: 10.1196/annals.1443.016
52. Liu W, Zhang X. Receptor activator of nuclear factor-κB ligand (RANKL)/RANK/osteoprotegerin system in bone and other tissues (Review). *Mol Med Rep.* (2015) 11:3212–8. doi: 10.2119/molmed.2015.00022
53. Schena F, Menale C, Caci E, Diomede L, Palagano E, Recordati C, et al. Murine Rankl–/– mesenchymal stromal cells display an osteogenic differentiation defect improved by a RANKL-expressing lentiviral vector. *Stem Cells* (2017) 35:1365–77. doi: 10.1002/stem.2574
54. Ikebuchi Y, Aoki S, Honma M, Hayashi M, Sugamori Y, Khan M, et al. Coupling of bone resorption and formation by RANKL reverse signalling. *Nature* (2018) 561:195–200. doi: 10.1038/s41586-018-0482-7
55. Campeau PM, Lu JT, Sule G, Jiang MM, Bae Y, Madan S, et al. Whole-exome sequencing identifies mutations in the nucleoside transporter gene SLC29A3 in dysosteosclerosis, a form of osteopetrosis. *Human Mol Genet.* (2012) 21:4904–9. doi: 10.1093/hmg/dds326
56. Guo L, Elcioglu NH, Karalar OK, Topkar MO, Wang Z, Sakamoto Y, et al. Dysosteosclerosis is also caused by TNFRSF11A mutation. *J Hum Genet.* (2018) 769–74. doi: 10.1038/s10038-018-0447-6
57. Weisz Hubshman M, Basel-Vanagaite L, Krauss A, Konen O, Levy Y, Garty BZ, et al. Homozygous deletion of RAG1, RAG2 and 5′ region TRAF6 causes severe immune suppression and atypical osteopetrosis. *Clin Genet.* (2017) 91:902–7. doi: 10.1111/cge.12916
58. Monies D, Maddirevula S, Kurdi W, Alanazy MH, Alkhalidi H, Al-Owain M, et al. Autozygosity reveals recessive mutations and novel mechanisms in dominant genes: implications in variant interpretation. *Genet Med.* (2017) 19:1144–50. doi: 10.1038/gim.2017.22
59. Dai XM, Ryan GR, Hapel AJ, Dominguez MG, Russell RG, Kapp S, et al. Targeted disruption of the mouse colony-stimulating factor 1 receptor gene results in osteopetrosis, mononuclear phagocyte deficiency, increased primitive progenitor cell frequencies, and reproductive defects. *Blood* (2002) 99:111–20. doi: 10.1182/blood.V99.1.111
60. Frattini A, Pangrazio A, Susani L, Sobacchi C, Mirolo M, Abinun M, et al. Chloride channel ClCN7 mutations are responsible for severe recessive, dominant, and intermediate osteopetrosis. *J Bone Miner Res.* (2009) 18:1740–7. doi: 10.1359/jbmr.2003.18.10.1740
61. Waguespack SG, Hui SL, Dimeglio LA, Econs MJ. Autosomal dominant osteopetrosis : clinical severity and natural history of 94 subjects with a chloride channel 7 gene mutation. *J Clin Endocrinol Metab.* (2007) 92:771–8. doi: 10.1210/jc.2006-1986
62. Döffinger R, Smahi A, Bessia C, Geissmann F, Feinberg J, Durandy A, et al. X-linked anhidrotic ectodermal dysplasia with immunodeficiency is caused by impaired NF-κB signaling. *Nat. Genet.* (2001) 27:277–85. doi: 10.1038/85837
63. Dupuis-Girod S, Corradini N, Hadj-Rabia S, Fournet JC, Faivre L, Le Deist F, et al. Osteopetrosis, lymphedema, anhidrotic ectodermal dysplasia, and immunodeficiency in a boy and incontinentia pigmenti in his mother. *Pediatrics* (2002) 109:e97. doi: 10.1542/peds.109.6.e97
64. Roberts CM, Angus JE, Leach IH, McDermott EM, Walker DA, Ravenscroft JC. A novel NEMO gene mutation causing osteopetrosis, lymphoedema, hypohidrotic ectodermal dysplasia and immunodeficiency (OL-HED-ID). *Eur J Pediatr.* (2010) 169:1403–7. doi: 10.1007/s00431-010-1206-7
65. Carlberg VM, Lofgren SM, Mann JA, Austin JP, Nolt D, Shereck EB, et al. Hypohidrotic ectodermal dysplasia, osteopetrosis, lymphedema, and immunodeficiency in an infant with multiple opportunistic infections. *Pediatr Dermatol.* (2013) 31:716–21. doi: 10.1111/pde.12103
66. Abu-Amer Y, Darwech I, Otero J. Role of the NF-κB axis in immune modulation of osteoclasts and bone loss. *Autoimmunity* (2008) 41:204–11. doi: 10.1080/08916930701694543
67. Steward CG. Hematopoietic stem cell transplantation for osteopetrosis. *Pediatr Clin North Am.* (2010) 57:171–80. doi: 10.1016/j.pcl.2009.11.006
68. Behfar M, Dehghani SS, Hosseini AS, Jalali A, Hamidieh AA, Ghavamzadeh A. Non-total body irradiation myeloablative conditioning with intravenous busulfan and cyclophosphamide in hematopoietic stem cell transplantation for malignant infantile osteopetrosis. *Pediatr Transplant.* (2015) 19:422–7. doi: 10.1111/petr.12476
69. Shadur B, Zaidman I, NaserEddin A, Lokshin E, Hussein F, Oron HC, et al. Successful hematopoietic stem cell transplantation for osteopetrosis using reduced intensity conditioning. *Pediatric Blood Cancer* (2018) 2017:e27010. doi: 10.1002/pbc.27010
70. Frattini A, Blair HC, Sacco MG, Cerisoli F, Faggioli F, Catò EM, et al. Rescue of ATPa3-deficient murine malignant osteopetrosis by hematopoietic stem cell transplantation *in utero*. *Proc Natl Acad Sci USA.* (2005) 102:14629–34. doi: 10.1073/pnas.0507637102
71. Tondelli B, Blair HC, Guerrini M, Patrene KD, Cassani B, Vezzoni P, et al. Fetal liver cells transplanted *in utero* rescue the osteopetrotic phenotype in the Oc/Oc mouse. *Am J Pathol.* (2009) 174:727–35. doi: 10.2353/ajpath.2009.080688
72. Orchard PJ, Fasth AL, Le Rademacher J, He W, Boelens JJ, Horwitz EM, et al. Hematopoietic stem cell transplantation for infantile osteopetrosis. *Blood* (2015) 126:270–6. doi: 10.1182/blood-2015-01-625541
73. Chiesa R, Ruggeri A, Paviglianiti A, Zecca M, Gónzalez-Vicent M, Bordon V, et al. Outcomes after unrelated umbilical cord blood transplantation for children with osteopetrosis. *Biol Blood Marrow Transplant.* (2016) 22:1997–2002. doi: 10.1016/j.bbmt.2016.07.015
74. Fuchs EJ. Human leukocyte antigen-haploidentical stem cell transplantation using T-cell-replete bone marrow grafts. *Curr Opin Hematol.* (2012) 19:440–7. doi: 10.1097/MOH.0b013e32835822dc
75. Corbacioglu S, Kernan N, Lehmann L, Brochstein J, Revta C, Grupp S, et al. Defibrotide for the treatment of hepatic veno-occlusive disease in children after hematopoietic stem cell transplantation. *Expert Rev Hematol.* (2012) 5:291–302. doi: 10.1586/ehm.12.18
76. Shroff R, Beringer O, Rao K, Hofbauer LC, Schulz A. Denosumab for post-transplantation hypercalcemia in osteopetrosis. *New Engl J Med.* (2012) 367:1766–7. doi: 10.1056/NEJMc1206193
77. Johansson MK, de Vries TJ, Schoenmaker T, Ehinger M, Brun AC, Fasth A, et al. Hematopoietic stem cell – targeted neonatal gene therapy reverses lethally progressive osteopetrosis in Oc / Oc mice. *Blood* (2007) 109:5178–85. doi: 10.1182/blood-2006-12-061382
78. Naldini L. *Ex vivo* gene transfer and correction for cell-based therapies. *Nat Rev Genet.* (2011) 12:301–15. doi: 10.1038/nrg2985
79. Sessa M, Lorioli L, Fumagalli F, Acquati S, Redaelli D, Baldoli C, et al. Lentiviral haemopoietic stem-cell gene therapy in early-onset metachromatic leukodystrophy: an ad-hoc analysis of a non-randomised, open-label, phase 1/2 trial. *Lancet* (2016) 388:476–87. doi: 10.1016/S0140-6736(16)30374-9
80. Thrasher AJ, Williams DA. Evolving gene therapy in primary immunodeficiency. *Mol Ther.* (2017) 25:1132–41. doi: 10.1016/j.ymthe.2017.03.018
81. Moscatelli I, Löfvall H, Schneider Thudium C, Rothe M, Montano C, Kertész Z, et al. Targeting NSG mice engrafting cells with a clinically applicable lentiviral vector corrects osteoclasts in infantile malignant osteopetrosis. *Hum. Gene Ther.* (2017) 29:938–49. doi: 10.1089/hum.2017.053
82. Lo Iacono N, Blair HC, Poliani PL, Marrella V, Ficara F, Cassani B, et al. Osteopetrosis rescue upon RANKL administration to Rankl-/-Mice: a new therapy for human RANKL-dependent ARO. *J Bone Miner Res.* (2012) 27:2501–10. doi: 10.1002/jbmr.1712
83. Bianco P, Robey PG. (2004). Skeletal stem cells. *Handbook Stem Cells.* 2:415–24. doi: 10.1016/B978-012436643-5/50129-2
84. Cappariello A, Paone R, Maurizi A, Capulli M, Rucci N, Muraca M, et al. Biotechnological approach for systemic delivery of membrane receptor activator of NF-κB ligand (RANKL) active domain into the circulation. *Biomaterials* (2015) 46:58–69. doi: 10.1016/j.biomaterials.2014.12.033
85. Menale C, Campodoni E, Palagano E, Mantero S, Erreni M, Inforzato A, et al. MSC-seeded biomimetic scaffolds as a factory of soluble RANKL in rankl-deficient osteopetrosis. *Stem Cells Transl Med.* (2018) 8:22–34. doi: 10.1002/sctm.18-0085

86. Capulli M, Maurizi A, Ventura L, Rucci N, Teti A. Effective small interfering RNA therapy to treat CLCN7-dependent autosomal dominant osteopetrosis Type 2. *Mol Ther.* (2015) 4:e248. doi: 10.1038/mtna.2015.21
87. Maurizi A, Capulli M, Patel R, Curle A, Rucci N, Teti A. RNA interference therapy for autosomal dominant osteopetrosis type 2. towards the preclinical development. *Bone* (2018) 110:343–54. doi: 10.1016/j.bone.2018.02.031
88. Alam I, Gray AK, Acton D, Gerard-O'Riley RL, Reilly AM, Econs MJ. Interferon gamma, but not calcitriol improves the osteopetrotic phenotypes in ADO2 mice. *J Bone Miner Res.* (2015) 30:2005–13. doi: 10.1002/jbmr.2545

**Conflict of Interest Statement:** The authors declare that the research was conducted in the absence of any commercial or financial relationships that could be construed as a potential conflict of interest.